Universitat Autònoma de Barcelona

A Thesis for the

Master in Telecommunication Engineering

DRO Design for Ku, X and Ka band

by

Joan Ramirez Garcia

Supervisor: Pedro de Paco Sánchez

Departament de Telecomunicació i Enginyeria de Sistemes

Escola Tècnica Superior d'Enginyeria (ETSE)
Universitat Autònoma de Barcelona (UAB)

January 20222

UAB

Abstract

This thesis researches the use of the dielectric resonator in order to achieve the receiver specifications for the Copernicus Imager Microwave Radiometer. Apart from the introduction and the conclusions, the thesis consists of four well differentiated parts. The first part introduces the theoretical basis about the oscillators, which emphasizes the benefits of using the dielectric resonator. The second part analyzes the resonator's resonant frequency in different scenarios. Moreover, two tuning techniques are explained. The first of them provides a wide frequency tuning range, around 500 MHz, whereas the second technique provides a fine tuning, around a few of MHz. The third part of this thesis analyzes the active device as the essential device to obtain the oscillation condition, it is mandatory to obtain the enough gain to accomplish the Barkhausen criterion. Finally, the thesis is closed showing some simulations and, thus, evaluating all the theoretical basis. Additionally, all three oscillator are compared to observe the similarities between them.

Resumen

Esta tesi estudia el uso del resonador dielectrico con el fin de cubrir las especificaciones que el receptor de CIMR (Copernicus Imager Microwave Radiometer) demanda. Además de la introducción y las conclusiones, la tesis consiste en cuatro partes bien diferenciadas. La primera parte introduce la base teórica de los osciladores, la cual enfatiza en los beneficios de usar un resonador dieléctrico. La segunda parte analiza la frecuencia de resonancia del resonador en diferentes escenarios. Además, dos técnicas de tuning son mencionadas. La primera de ellas proporciona un gran rango de tuning en frecuencia, entorno a los 500 MHz, mientras que la segunda técnica proporciona un ajuste más fino, entorno unos pocos MHz. La tercera parte de la tesi analiza el dispositivo activo como elemento esencial para cumplir la condición de oscilación, es obligatorio obtener la suficiente ganancia para cumplir el criterio de Barkhausen. Por último, la tesis concluye mostrando las simulaciones, y de esta forma, evaluando la teórica de los osciladores. Además, los tres osciladores son comparados con la finalidad de encontrar similitudes entre ellos.

Resum

Aquesta tesi estudia l'ús del ressonador dielèctric per tal de cobrir les especificacions que el receptor de CIMR (Copernicus Imager Microwave Radiometer) demanda. A més de la introducció i les conclusions, la tesi consisteix en quatre parts ben diferenciades. La primera part introdueix la base teòrica dels oscil·ladors, la qual emfatitza en els beneficis d'usar un ressonador dielèctric. La segona part analitza la freqüència de ressonància del ressonador en diferents escenaris. A més, dues tècniques de tuning són esmentades. La primera d'elles proporciona un gran rang de tuning en freqüència, entorn dels 500 MHz, mentre que la segona tècnica proporciona un ajust més fi, entorn uns pocs MHz. La tercera part de la tesi analitza el dispositiu actiu com a element essencial per complir la condició d'oscil·lació, és obligatori obtenir el suficient guany per complir el criteri de Barkhausen. Per últim, la tesi conclou mostrant les simulacions, i d'aquesta manera, avaluant la teòrica dels oscil·ladors. A més, els tres oscil·ladors són comparats amb la finalitat de trobar similituds entre ells.

Acknowledgments

I would like to thank to Alberto Alonso for his support during this thesis.

I also would like to thank to Sener Aeroespacial and the colleagues for their guidance and design tips.

Finally, I want to express my gratitude to my family and my sweetie, they are the pillar of my life.

Contents

List of Figures

List of Tables

Chapter 1

Introduction

1.1 The CIMR mission

The CIMR (Copernicus Imaging Microwave Radiometer) mission is a high priority candidate satellite mission within the European Copernicus Expansion program. The satellite is designed to observe the ocean and sea ice as well as other geophysical parameters. Key parameters under observation are: Sea Ice Concentration (SIC), Sea Ice Extent (SIE), Sea Surface Temperature (SST), Thin Sea Ice, Sea Ice Drift, Ice type, Total Snow Area, Snow Water Equivalent, Ice Surface Temperature (IST), Sea Surface Salinity (SSS), wind speed over ocean, Soil Moisture, Land Surface Temperature, cloud liquid water over ocean, precipitation over ocean, terrestrial surface water extern [3].

The CIMR system consists of up to three satellites dedicated to day-and-night monitoring of land, ice and oceans. Measurements will be co-located and near-contemporaneous with other satellites like Metop SG, AMSR and SMOS. CIMR orbit is quasi-polar, near circular and sun-synchronous. The instrument rotates continuously around the satellite nadir axis scanning the Earth surface and the reflector pointing direction is selected to look at the Earth. The antenna system watches the Earth scene with a nearly constant incidence angle of about 55.5^{o} [4].

Each CIMR satellite has a wide-swath conically-scanning multi-frequency reflector and microwave radiometers provided by OHB Italia and operating at L, C, X, Ku and Ka band enabling radiometric measurements with a high level of accuracy. SENER Aeroespacial is responsible

for the design of the radiometers at X, Ku and Ka-band.
CIMR will be designed for a 7 years nominal lifetime with a sub-daily Arctic and Antarctic area coverage, it will be compatible with Vega-C and Ariane 6-2 launchers and will be fitted by a controlled reentry system.

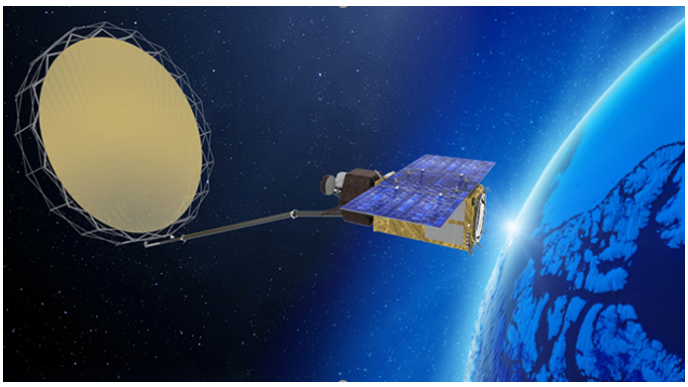

Figure 1.1: CIMR instrument and 8-m deployable reflector (Thales Alenia Space Italy)

The choice of CIMR frequency bands is based on the following criteria:

- Frequency sensitivity to geophysical parameters of interest
- Historical perspective (continuity of measurement for climate record)
- Technical feasibility

Figure 1.2 shows the sensitivity of microwave emissivity (brightness temperature) of open sea-water for a variety of geophysical parameters [5]. This figure justifies the CIMR channels in order to maximize the information available in the 1.4-37GHz frequency range.
The radiometers in CIMR are Total Power Radiometers. The main characteristics of each radiometric channel in CIMR instrument are reported in Figure 1.3.

A general block diagram proposed by SENER Aeroespacial for X, Ku and Ka band radiometers is shown in Figure 1.4. The Internal Calibration Assembly (ICA) includes a switch for internal calibration purposes. The Receiver Front (RXFE) is a superheterodyne receiver which downconverts the RF channel to IF for filtering and amplification. The same LO is used for H and V channels; synchronization is required in order to retrieve the Full Stokes parameters [6].

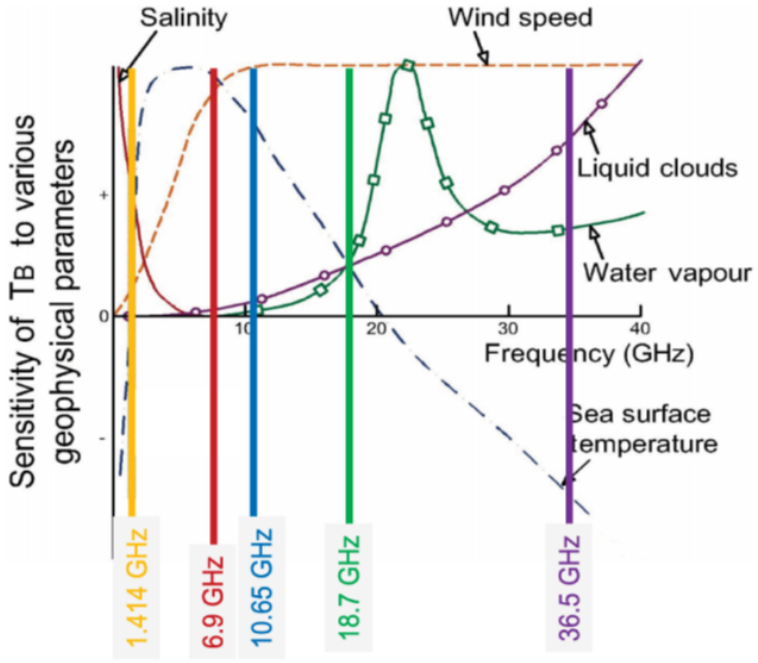

Figure 1.2: Brigthness temperature sensitivity for open seawater vs. CIMR frequencies for key geophysical parameters

Parameter	**Units**	**L-band**	**C-band**	**X-band**	**Ku-band**	**Ka-band**
Center Frequency	GHz	1.4135	6.925	10.65	18.7	36.5
Polarization	N/A	H and V with provision for Full Stokes				
Max. BW	MHz	25	300	100	200	300
Center freq. stability	MHz	<0.015	<15	<15	<15	<15
Swath width	km	>1900				
Footprint size	km	<60	<15	<15	<5.5	<4
Observation Zenith Angle	deg	55.0+/-1.5				
NEΔT at 150K (1sigma)	K	<0.3	<0.2	<0.3	<0.4	<0.7
Dynamic range	K	From 2.7 up to 340				

Figure 1.3: CIMR instrument main specification

Some filtering is used for RFI rejection. The digitization and data collection of H and V signals is done in another subsystem (not under SENER responsibility).

The LOs for RxFE are free-running oscillators (no external reference locking) based on Voltage Controlled Dielectric Resonator oscillator (VC-DRO) and a section including LO multiplier, filtering, amplification, Automatic Level Control loop (ALC), and output power control. The VCO is voltage electronically controlled with a varactor which allows a fine tuning (BoL setting) and a compensation of temperature variations. It is a SENER qualified design that will be explained and retuned along this document..

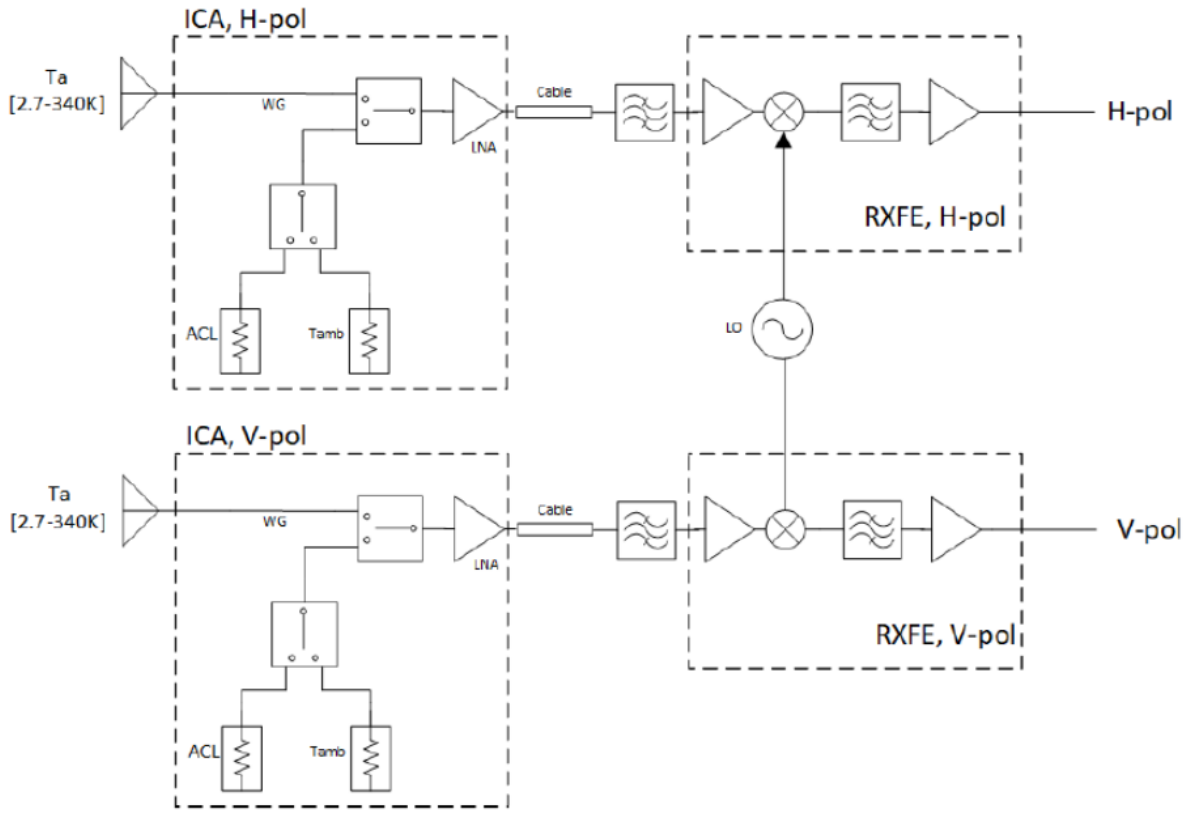

Figure 1.4: Radiometer and Calibration Assembly for CIMR

1.2 Motivation of the work

Nowadays, oscillators are the key device for some communication systems. For example, the CIMR mission system's performance directly depends on the oscillator properties. The Receiver Front (RXFE) mounts a superheterodyne downconverter where the carrier frequency is provided by the oscillator.

The oscillator is defined by a large quantity of properties that will specify the system's performance. For microwave frequencies, there are too much types of resonators and, each of them will provide a set of properties that will enhance the system's quality. Specifications as phase noise, dimension or material are the most important to take into account.

Dielectric resonator is a good choice for space missions since they are characterized for being small, having a good quality factor and being stable against thermal modifications. However, the dielectric resonator tend to be manufactured in custom dimensions since they are very sensitive to dimensions or material composition. Thus, these resonators can not be produced in big scale and multiple iterations with suppliers are usually needed for frequency tuning.

Additionally, the oscillator's output power is also a critical parameter since the oscillator is in charge of running the downconverter but, a power excess inside the oscillator's loop could become into a devices saturation.

Thinking on the CIMR mission, Sener company bets on designing two DROs (Main and Redundant) working in cold redundancy (only one of them is ON at the same time) for each of the frequency bands, whose carrier frequencies are the following:

- Ku band converter at 7.63 GHz
- X band converter at 8.63 GHz
- Ka band converter at 12.41 GHz

Moreover, as it is desired to avoid the supplier iterative process during the project's phase B, some tuning techniques will be presented. The metallic screw allows a wide frequency tuning while the varactor diode will provide a fine tuning.

1.3 Aim of the thesis

For this thesis, the aim is covering the 3 DROs for the CIMR mission. As the oscillators are demanded to be precise, an strict design procedure needs to be followed. Briefly, the main thesis points are the following:

1. The resonator choice is an extremely rigorous procedure since the resonator's delivery period is around 4 months. Thus, EM software, as Ansys HFSS, provides an approximation of the resonator properties.

2. The resonator will be enclosed inside a metallic cavity. Thus, it will be difficult to modify the resonator dimensions in case of frequency tuning. Some external tuning techniques will be studied for perfectly making it resonates at the desired frequency.

3. Following the oscillation theory, an active device also belongs to the oscillator loop. The active device (amplifier) needs to be biased according to the design specifications. Moreover, there is a theoretical basis behind the active device.

4. Evaluating the final design and deciding if the oscillator accomplishes the desired specifications.

Therefore, the aim of this thesis is covering the full oscillator design. From the resonator selection to evaluating if the proposed design covers the CIMR mission specifications.

1.4 Thesis structure

This thesis focuses on the design of three different dielectric resonator oscillators for the CIMR mission frequencies following the parallel feedback configuration.

In Chapter 2, fundamentals of oscillators are covered. The basic oscillation criterion and the devices which allow to obtain it are briefly explained.

In Chapter 3, resonator's properties are explained. The dielectric resonator is decomposed and analyzed by separate parts. The use of EM simulator is fundamental for extracting some conclusions. Moreover, two different frequency tuning techniques are introduced. Both of them provide controlling the resonator externally but, each of them have its own properties.

In Chapter 4, the active device specifications are mentioned. It contains information about the biasing network and the important parameters for these devices. The design of the active device core is explained for the three CIMR oscillators.

In Chapter 5, the resonator EM simulations are detailed. Using the Ansys HFSS software, each of the resonators is modelled and validated. Additionally, from the obtained results, a budget balance is done to check the validation of the design.

In chapter 6, the thesis objectives are evaluated, also the future work is included.

Chapter 2

Oscillators

2.1 Introduction

An Oscillator is an electronic circuit that produces an oscillating electronic signal, often a sine wave, that converts direct current (DC) from a power supply to an alternating current (AC) signal [1]. Oscillators are the basic microwave energy source for some microwave systems as radars or navigation systems.

Typically, an oscillator can be characterized by an active device (transistor) and a passive resonant element, which determines the main tone's frequency. In Figure 2.1, a generic oscillator configuration is given by a linear feedback network as follows

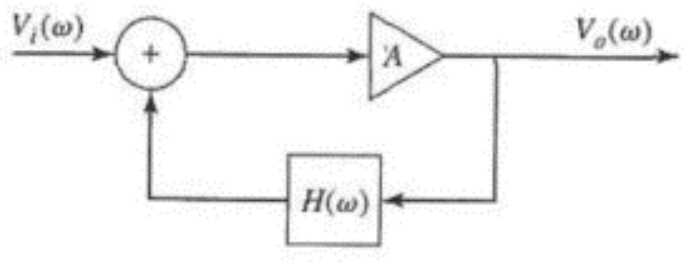

Figure 2.1: Generic oscillator scheme

In Figure 2.1, $V_i(\omega)$ is the system's input, which is amplified by a certain gain $A(\omega)$, and $H(\omega)$ is the transfer function of the feedback and, $V_o(\omega)$ is the output.

Following the oscillators theory, the early condition for an oscillator input is the noise condition, which means that there is no need of feeding.

Back to Figure 2.1, the system's output can be mathematically expressed as

$$A(\omega)[V_i(\omega) + H(\omega)V_o(\omega)] = V_o(\omega) \tag{2.1}$$

Which results to describe the output system as

$$V_o(\omega) = \frac{A(\omega)}{1 - A(\omega)H(\omega)}V_i(\omega) \tag{2.2}$$

From 3.2, it can be observed that if $A(\omega)$ and $H(\omega)$ are equal to one at a certain frequency, the denominator becomes to zero, and a non-zero output power will be obtained for that frequency. That result is also known as the $Barkhausen$ criterion, and it is one of the main rules that governs the oscillator design.

The same mathematical development can be translated in terms of microwaves. In Figure 2.2, the oscillator scheme is represented by the reflection coefficients (incident and reflected signals).

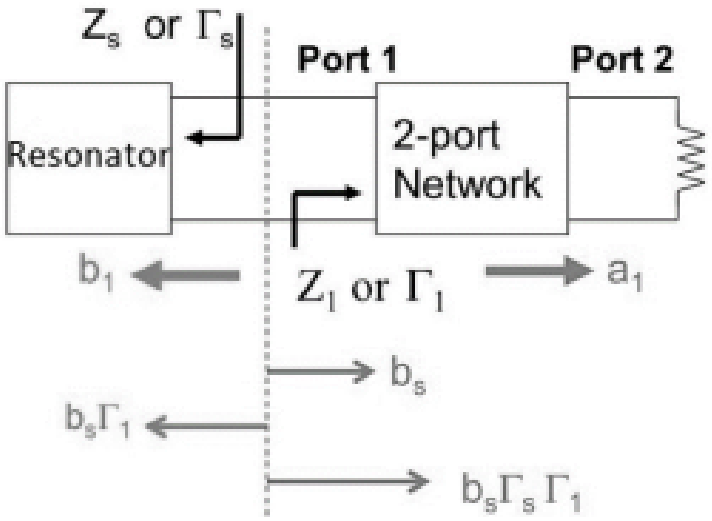

Figure 2.2: Oscillator scheme (microwaves)

$$\frac{b_1}{b_s} = \frac{\Gamma_1}{1 - \Gamma_1\Gamma_s} \tag{2.3}$$

Attending to 2.3, there are some similarities by the way both expressions are represented. So, it is unequivocal that if Γ_1 and Γ_s are equal to one, the denominator is zero. In microwaves, the

condition where there is non-zero incident and reflected power at a specific frequency is known as oscillation or unstability condition.

The negative resistance methodology is an oscillator design method which looks for accomplishing that scenario to get a resonance. Negative resistance method will be shortly explained during this document [7].

At that point, the whole provided explanation can be only applied for linear condition, where the feedback is always the same. However, the second bold point here is that oscillators are nonlinear systems. Thus, oscillators do not consist on steady poles, and those poles can vary as a function of time.

On the early phase, both poles must be real positive part-complex conjugate to increase the oscillation's magnitude. As in Figure 2.3.a, the noise is amplified in time domain. In fact, it is correct to think that the power will be amplified infinitely but, the active device will reach a equilibrium at some point since the active device starts compressing. At the farthest, the device will reach saturation as the equilibrium point..

Once the early phase has been acquired, the desired oscillation condition can be only obtained when both poles are conjugated and located just over the imaginary axis, being a zero real part. As in Figure 2.3.b, the oscillation condition it is determined by a stable magnitude in time terms.

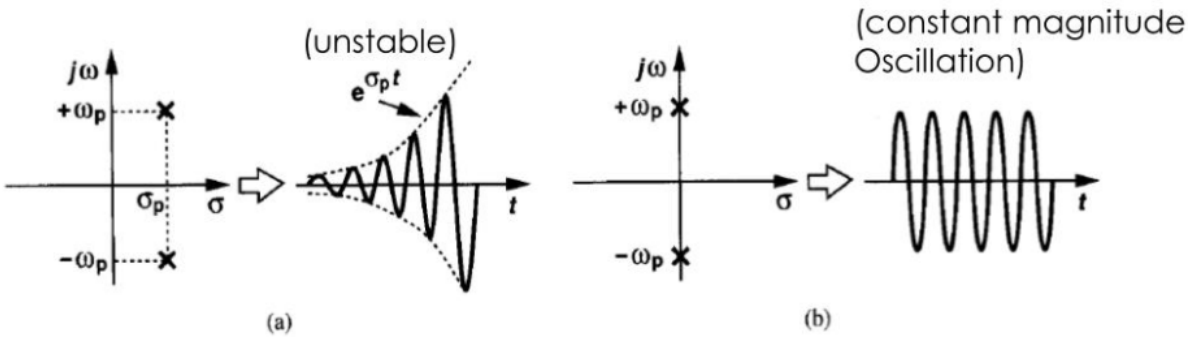

Figure 2.3: Poles representation: (a) Start-up condition; (b) Oscillation condition [1]

Then, the oscillation condition will be only achieved when the 2.3 denominator roots are complex conjugated pair with zero real part, which can be resumed easily by the following two expressions

$$|A(\omega)H(\omega)|_{@\omega_o} = 1 \tag{2.4}$$

$$phase(A(\omega)H(\omega))|_{@\omega_o} = 0 \tag{2.5}$$

In other words:

- Condition 2.4: The feedback loop gain must be always over 1 at the beginning. In terms of decibels, the loop gain must be always 0dB. During compression of the active device the gain equality will be achieved.
- Condition 2.5: The electrical phase around the loop must be 360 degree or 2π.

If one of the previous conditions are not satisfied, the oscillation condition will not be achieved. In conclusion, in contrast to what typically a designer looks for active devices, an oscillator wants to be at unstability condition. Additionally, the steady oscillation can be only reached when there is a specific gain and phase condition around the loop..

2.2 Negative Resistor Method

As aforementioned, there is a general method for designing oscillators, which is known as the Negative Resistor method. In this section, a theoretical demonstration shows how that negative resistance can be obtained and its ability to describe the oscillation scenario.
The negative resistance method is fundamental for oscillators design since it provides a very approximated oscillation frequency and quantifies the oscillator ability to provide a signal at the desired frequency. The main fact for using this method is the nonlinear behavior that the active device follows. Nevertheless, conditions 2.5 and 2.6 are still the key conditions that the oscillator must accomplish to resonate.
As in Figure 2.4, the basic oscillator scheme can be defined as a resonator (the selective device in the linear feedback scenario), an unstable active network and a matching network. The resonator generates the oscillation frequency as long as the unstable active device, which resistance

value is negative, accomplishes the oscillation scenario in its ports. Additionally, the matching network ensures that the Barkhausen condition is met.

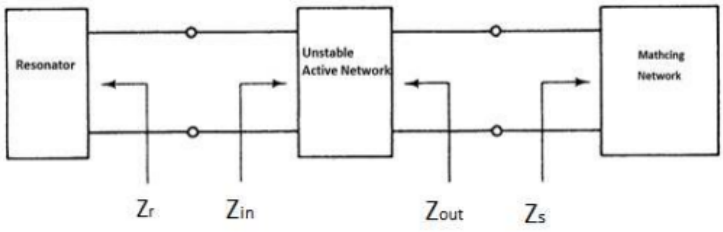

Figure 2.4: basic oscillator scheme [2]

As previously mentioned, the oscillating condition must be obtained between the resonator and the active device ports. So, back to eqn(2.3), denominator must be zero at the oscillation frequency to observe a non-zero reflected and incident power. Then, $\Gamma_r\Gamma_{in}$ must be equal to 1. Before starting with the negative resistance proof, there is still a detail that cannot be neglected. In fact, its reasonable to initially state that reflection coefficient for the active device will be higher than 1 since the product between the resonator's reflection coefficient ($\Gamma_r < 1$) and the active's device reflection coefficient (Γ_{in}) needs to be 1.

In this point, the negative resistor procedure is going to be explained. Firstly, let's start with the coefficient reflection formula (2.7), which it is mandatory to be higher than 1 for oscillation

$$|\Gamma_{in}| = |\frac{Z_{in} - Z_o}{Z_{in} + Z_o}| \geq 1 \tag{2.6}$$

where Z_o is the characteristic impedance for a transmission line.

Eqn(2.6) can be shortened considering that Z_{in} is a complex number

$$R_{in}^2 - 2R_{in}Z_o + Z_o^2 + Z_{in}^2 \geq R_{in}^2 + 2R_{in}Z_o + Z_o^2 + Z_{in}^2 \tag{2.7}$$

Eqn(2.7) reduces to

$$0 \geq R_{in}Z_o \tag{2.8}$$

Finally, considering that Z_o is a real positive value for a lossless transmission line

$$R_{in} \leq 0 \tag{2.9}$$

Below this point, oscillation condition is applied for the oscillator and the active device

$$\Gamma_r\Gamma_{in} = 1 \tag{2.10}$$

$$\frac{Z_r - Z_o}{Z_r + Z_o}\frac{Z_{in} - Z_o}{Z_{in} + Z_o} = 1 \tag{2.11}$$

Expression 2.11 leads to

$$Z_r Z_{in} - Z_{in} Z_o - Z_o Z_r + Z_o^2 = Z_r Z_{in} + Z_{in} Z_o + Z_o Z_r + Z_o^2 \tag{2.12}$$

$$2Z_o(Z_r + Z_{in}) = 0 \tag{2.13}$$

As Z_o cannot be null

$$Z_r + Z_{in} = 0 \tag{2.14}$$

Where 2.15 and 2.16 are the impedance conditions for the oscillation scenario

$$R_{in} + R_r = 0 \tag{2.15}$$

$$X_{in} + X_r = 0 \tag{2.16}$$

The above procedure is just considering one port but, shown in Figure 2.4, the oscillator is a two port system.

In fact, when the oscillation condition occurs between resonator and active device, the same conditions are translated between active device and matching network interface. Then, $\Gamma_{out}\Gamma_s$ is 1

$$\Gamma_r \Gamma_{in} = \Gamma_{out}\Gamma_s = 1 \tag{2.17}$$

where 2.17 indicates equality of conditions over both ports.

Below at 2.18 and 2.19, the same procedure as 2.7 to 2.14 can be applied, obtaining finally that

$$R_{in} + R_r = 0 \tag{2.18}$$

$$X_{in} + X_r = 0 \tag{2.19}$$

Exactly the same result as the one for the one port case.

2.2.1 Resonator

As mentioned in section 2.1, the resonator is the most critical part in an oscillator system. The rapid advancement of technology had unlocked some types of resonators that provides interesting properties. Low noise, high Q material, low size, high temperature stability and low cost

are the main characteristics to value in an oscillator design.
This thesis integrates a ceramic material dielectric resonator that allows resonances at RF frequencies (over 3 GHz). Moreover, dielectric resonators have a set of primary characteristics that make them a relevant option for resonators:

- High Q factor: Approximately the inverse of the loss tangent, the high Q factor allows the designer to obtain abrupt resonances.
- Temperature coefficient: Includes the thermal expansion of the dielectric resonator and the package.
- Dielectric constant (ϵ_r): Typically defined by a high dielectric constant, it allows obtaining resonators at very high frequencies.

Chapter 3 describes the initial definition of the resonator dimensions and how the EM solver simulates a fine tuning to obtain the desired results. Furthermore, two tuning methodologies are explained in order to obtain the desired oscillation frequency.

2.2.2 Active Device

As mentioned in Section 2.2, the active device is another element of the oscillator network. The active device is the one in charge of providing the negative resistance to obtain the oscillation conditions. In other words, and attending to eqn(2.4), a transistor provides a certain loop gain around the whole feedback network.
Thus, there are some characteristics that the designer must value during the active device selection:

- Does the active device operate at design frequencies? The transistor must cover its frequencies to accomplish the oscillation criterion. Moreover, the device migth be potentially unstable for a wide range of frequencies, which is totally undesired.
- Which is the active device noise figure? Well, it depends on where the oscillator will be placed. As mentioned in section 1, phase noise is not a critical parameter since it is

mounted on a radiometer.

- Does the transistor's output power need some emphasis? Once again, its characteristic depends on where the oscillator is mounted. For this thesis, there are some additional stages after DRO to regulate the output power. Anyway, as it is explained in section 4, there is a PI attenuator that regulates the DRO output power.

For being an active element, there is no doubt that unstability is the most critical point. As mentioned above, there is mandatory to provoke an unstable scenario between ports (negative resistor) but, the active element cannot be unstable.
The active device stability refers to an amplifier's immunity to causing spurious oscillations. The outside band oscillations can arouse some gain loss in systems and, in oscillator cases, the oscillation frequency could become into that spurious frequency.
Rollet's stability factor (K) is the most recognized tool for network stabilization. When selecting an amplifier from datasheets, it is important to observe what frequency bands the selected amplifier could cause a spurious oscillation. So, the K factor indicates where the designer could have problems [8].

$$K = \frac{1 - |S_{11}|^2 - |S_{22}|^2 + |\Delta|^2}{2|S_{21}S_{12}|} \tag{2.20}$$

$$\Delta = S_{11}S_{22} - S_{12}S_{21} \tag{2.21}$$

As eqn(2.20) indicates, the K factor directly depends on the Scattering parameters.
Rollet's factor values three different scenarios determined as:

- Unconditionally stable ($K > 1$): Refers to a network that can see any possible impedance inside Gamma=1 circle on the Smith Chart. In other words, the system is assessing positive real part impedances. Remember from Section 2.2 that the negative resistance is the main condition to accomplish for oscillation.

- Conditionally unstable (potentially unstable) ($K < 1$): Despite the unconditionally stable condition, the conditionally unstable shows that an impedance could be settled outside the unitary gamma circle. So, that condition never has to be valued, there is some gap of information about the true state of the active device.

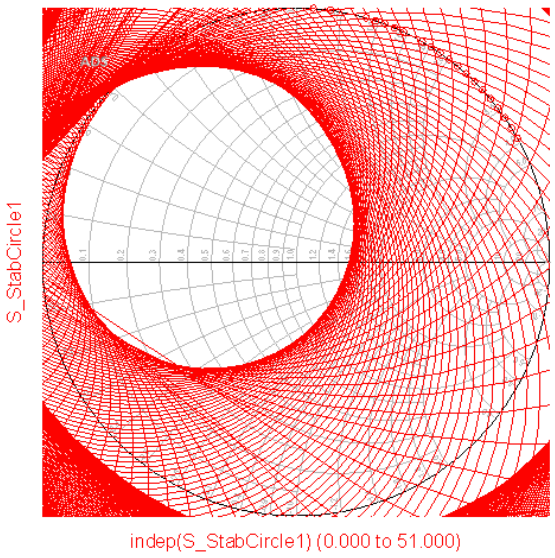

Figure 2.5: Unstability through Smith Chart

For amplifiers stabilization, not the K factor has the whole merit. In fact, there are other factors that quantifies the margin of unstability. The Mu1 and Mu2 show the margin of unstability and give information about where the unstable condition could be found, either input or output interface, also through the Smith Chart [9]. However, K factor is not the factor which defines if the active device is stable or unstable. In fact, if both Mu values are over 1, active device will be stable, which is a necessary and sufficient condition.
In conclusion, it is mandatory ensuring that the Mu factors are at least one for a wide range of frequencies (from DC until the transition frequency (f_T)). Additionally, Mu factor are great tools for locating where, either input or output, the unstability is appearing.

2.2.2.1 Transistor choice

The amplifier provides an accomplishment of the oscillation conditions and, some characteristics as gain or noise are important.
For this thesis, a SiGe bipolar transistor Space Qualified will be evaluated. According to supplier's datasheet, the transistor provides a high reliability as the component is assembled in hermetically sealed package. Moreover, the transistor is characterized by a high gain and ultra low noise. Thus, this component look like the ideal ones for an oscillator.

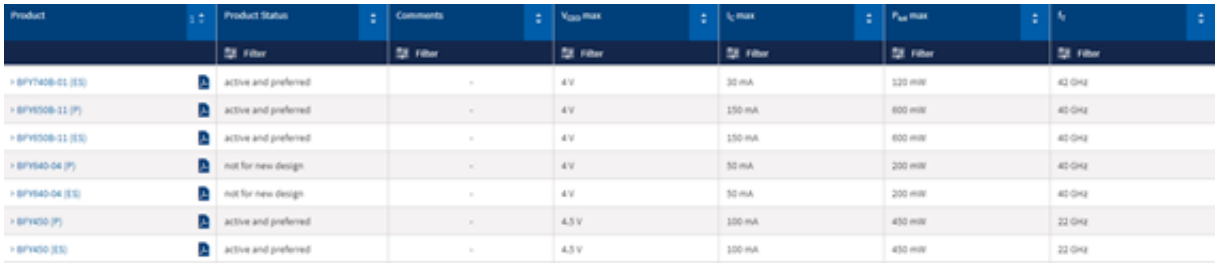

Product	Product Status	Comments	V_{CEO} max	I_C max	P_{tot} max	f_T
	Filter	Filter	Filter	Filter	Filter	Filter
BFY740B-01 (ES)	active and preferred	-	4 V	30 mA	120 mW	42 GHz
BFY650B-11 (P)	active and preferred	-	4 V	150 mA	600 mW	40 GHz
BFY650B-11 (ES)	active and preferred	-	4 V	150 mA	600 mW	40 GHz
BFY640-04 (P)	not for new design	-	4 V	50 mA	200 mW	40 GHz
BFY640-04 (ES)	not for new design	-	4 V	50 mA	200 mW	40 GHz
BFY450 (P)	active and preferred	-	4.5 V	100 mA	450 mW	22 GHz
BFY450 (ES)	active and preferred	-	4.5 V	100 mA	450 mW	22 GHz

Figure 2.6: SiGe bipolar transistor Space Qualified available options

Attending to Figure 2.6, each of the transistors has two options: (ES) for ESA space level for Flight modules (FM) and, (P) for professional level used in Engineering Modules (EM). By columns; there is the V_{CE} column that indicates the maximum collector-emitter voltage, the I_c column shows the maximum collector current and, the f_T column indicates the transition frequency, where transistor's current gain will be 1 (0 dB).

So, the transistor choice will depend firstly on the transition frequency. In this case, it is desired to have the biggest f_T.

The next step is asking the supplier about the ADS Large signal model for each desired transistor. Large signal models are composed by a circuit which replicates the transistor behavior. These models are usually used for defining the biasing network and simulate the entire oscillator loop.

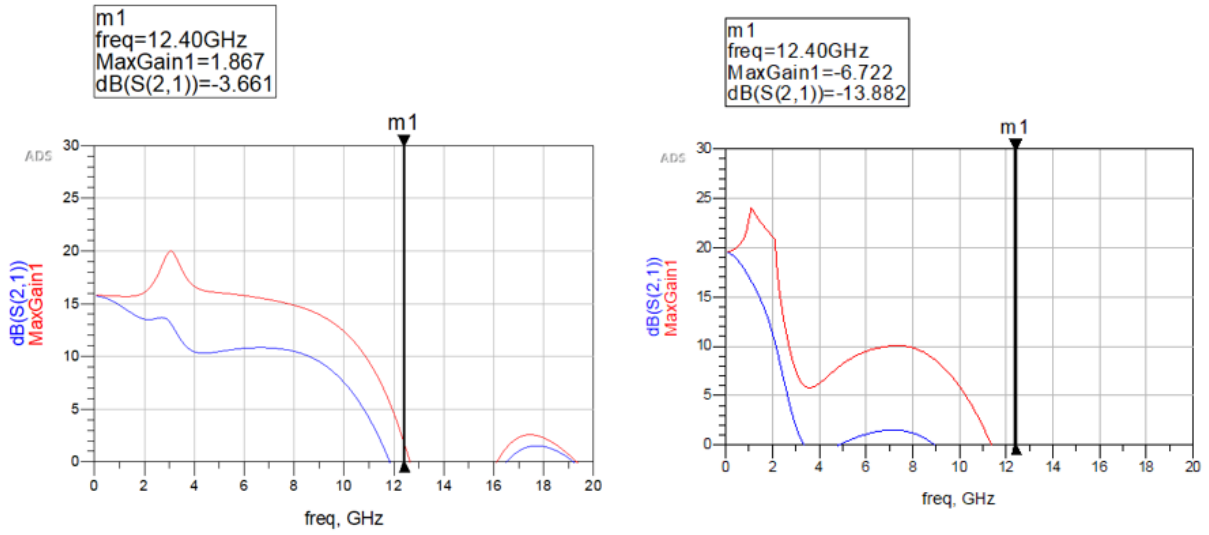

Figure 2.7: SiGe bipolar transistor Space Qualified high signal simulation: (a) option 1; (b) option 2

Finally, the PN selected cannot be disclosed in this document due to intellectual properties but will be shown during the thesis defense.

2.2.3 Matching network

As mentioned in Section 2.1, the active device performs the gain loop criterion plus the negative resistor for the oscillation condition. However, there is still the phase criterion that it is mandatory to be accomplished. In that case, it is a good practice locating multiple phase pads to select the right path.
During this thesis, three kind of phase pads are explained: the 15-degree pad, the 30-degree pad and, the 45-degree pad. Additionally, as the project is running three different designs, there is a total of 9 phase pads.

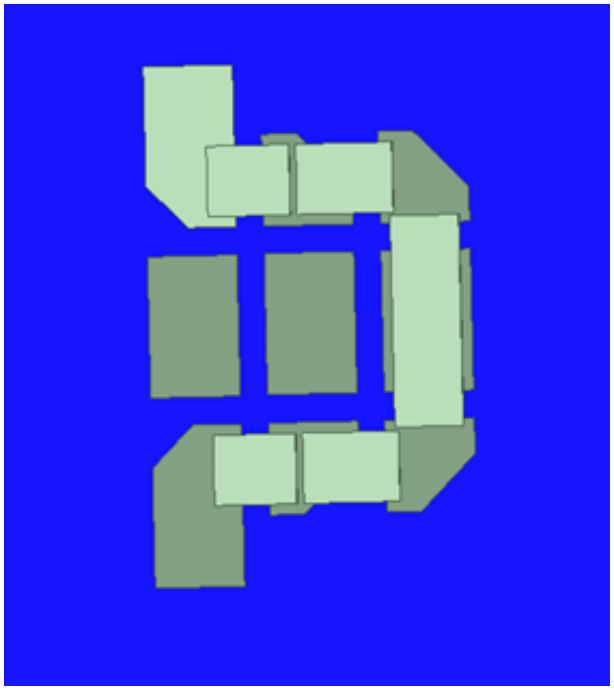

Figure 2.8: Phase pads

As Figure 2.8 shows, the phase pad consists of a path where the phase step can be selected in function of which pads are connected through a metallic sheet. Recommended by the manufacturer, the minimum distance between pads is 0.2 mm so, the design optimization will start with that distance.

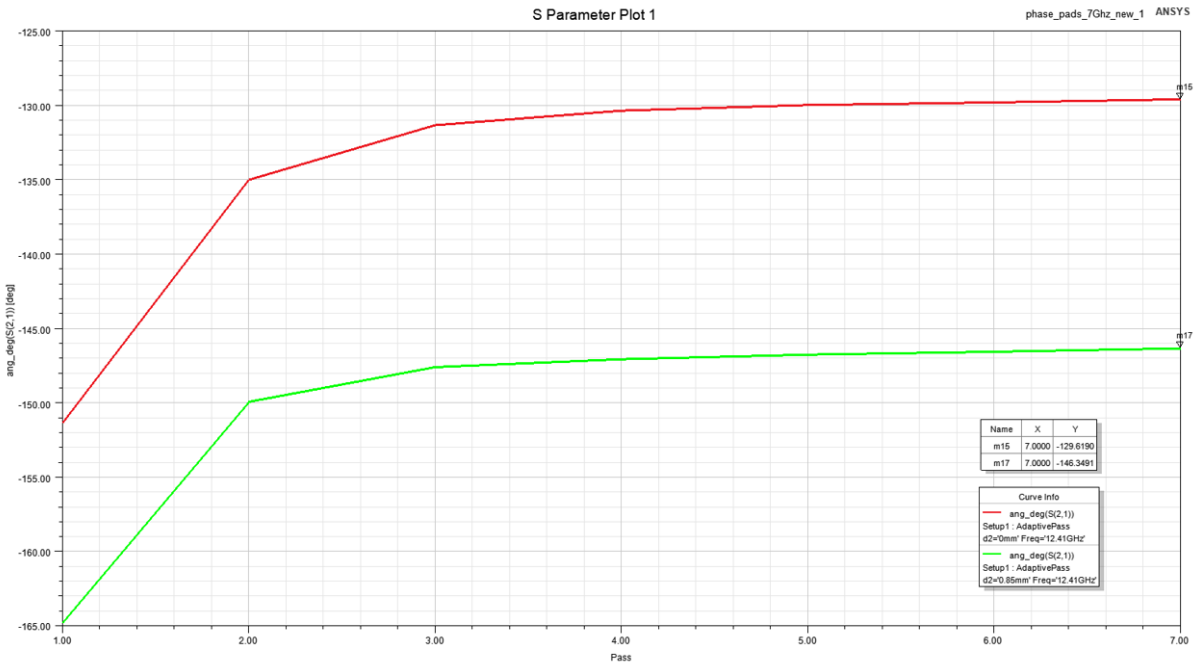

Figure 2.9: Phase pad simulation

For example, attending to Figure 2.9, there is the simulation for the 12.41 GHz phase pads. As indicated, the red line, which is the start-up case, there is an arbitrary phase. Then, the green line indicates that growing the path by 0.85 mm, a phase difference of 15-degree can be acquired. As a brief note, the design provided for this thesis considers a phase shift around 600-degree for the fine tuning. So, it is desired to locate these phase pads around the whole oscillator loop according to the three different sizes for each of the designs.

2.3 Design Procedure for DROs

As explained during this chapter, the main aim is accomplishing the oscillation criterion to obtain the desired oscillation frequency. In fact, there are two design configurations for DROs: series feedback and parallel feedback DROs.

The series feedback DRO acts as a reflection mode. In that configuration, the resonator works as an open circuit for the resonance frequency, thus, reflecting the power into the unstable active device. Series DROs are not the best resonator's coupling configuration so, high gain transistors are needed [10].

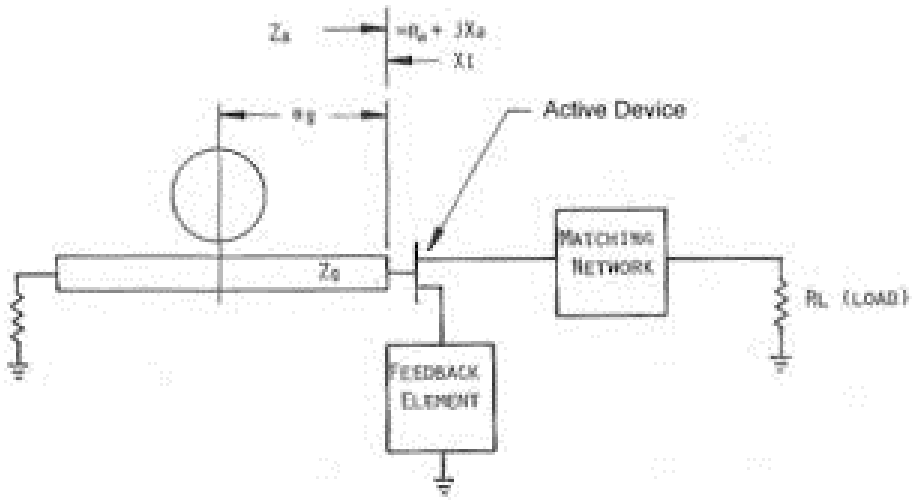

Figure 2.10: Series DRO configuration

As shown in Section 2.2.2.1, the available transistors for space missions tends to low gain for high frequencies. On that manner, there is need to have better coupling than the one the series feedback provides. The parallel feedback DRO allows a better coupling, in this way, the amplifier chosen for this project can meet the oscillation criterion.

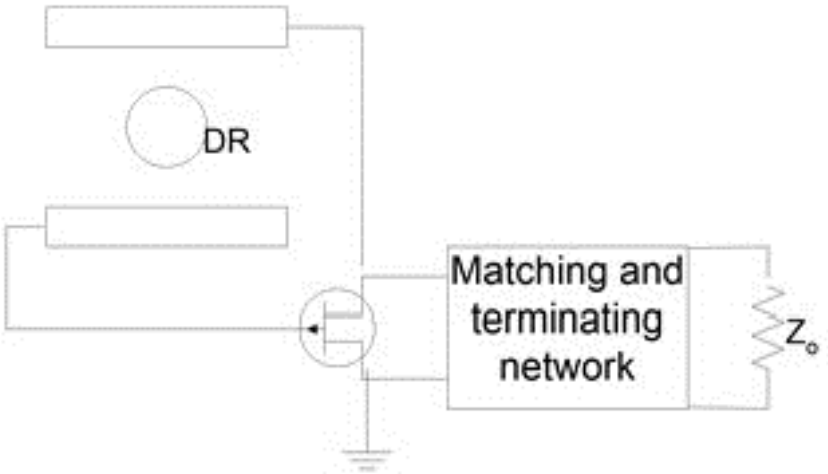

Figure 2.11: Parallel DRO configuration

As depicted in Figure 2.11, the resonator is wrapped by a couple of coupling lines. Thus, the resonator is directly choosing the resonance frequency. As mentioned previously, the parallel configuration allows a better coupling and, the output power specification will be better in

comparison with the series configuration. On the other hand, the parallel configuration generally has worst tuning possibilities [11]. Therefore, the parallel configuration will be used for the three designed oscillators.

As a summary, there is a set of steps that needs to be followed in order to obtain a well-designed DRO:

1. Select the desired resonant frequency and choose which of the available suppliers can satisfy the requeriments.
2. Once the material has been selected, puck dimensions need to be modeled, plus the tuning techniques that will adjust the desired frequency.
3. Select the active device, ensure that it can accomplish the loop gain criterion and ensure that it is stable.
4. Close the oscillator loop, designing the correct phase pad.

Chapter 3

Dielectric Resonator

3.1 Introduction

As showed in Chapter 2, the resonator is the critical component in an oscillator design. Resonator is the key element which selects at which frequency the oscillator is going to work. There are many types of resonators depending on shape, material, or configuration, so the previous selection process is a very important step to do. In general, there are four mainly specifications to consider which define the resonator depending on the application:

- Quality factor: Improve the oscillator stability, being a shield against phase noise.
- Resonant frequency: Not all the materials allow designs for high frequencies, directly dependent on configuration and the dielectric constant.
- Thermal coefficient: Determines the resonator behavior against temperature changes.
- Size: The resonator must fit inside a metal cavity considering that multiple tuning methodologies will be applied.

Additionally, the coupling factor, determined by both the loaded and unloaded quality factor, is an important value. Coupling ensures a low phase noise [12].
For this thesis, a ceramic dielectric resonator will be used. As it is explained during this chapter, the ceramic resonator provides a high quality factor, a reasonable size and, also a good coupling.

3.2 Dielectric Resonator

A dielectric resonator is a type of resonator which is characterized by a large dielectric constant. As the rest of resonators, the dielectric resonator exhibits an arbitrary frequency depending on its shape and dimensions.
As mentioned in Chapter 2, a dielectric resonator tends to accomplish the whole set of specification that a designer needs in a resonator:

- The quality factor is defined as the ratio between the energy stored within the resonator to the dissipated in the air per cycle.

$$Q = \omega \frac{average.energy.stored}{energy.loss/second} \tag{3.1}$$

  Also, the Q factor is equals to the inverse of tangent losses

$$Q = \frac{1}{tg(\delta)} = \frac{\epsilon^{'}}{\epsilon^{''}} \tag{3.2}$$

  Being $\epsilon^{'}$ the dielectric constant and $\epsilon^{''}$ the dielectric losses.
  Thus, it is desired to obtain a high Q resonator to protect the oscillator against the phase noise and be more selective in terms of frequency. Typically, a Q (unloaded) over 10000 is considered a good resonator.

- Temperature is also a critical parameter. In the oscillator case, it is mandatory obtaining the most stable possible and, temperature could be a big issue. Fortunately, some materials can include a temperature coefficient that allows a temperature compensation, decreasing in high magnitude the frequency shift caused by the temperature variation.

$$\tau_f = \frac{\Delta f}{f} \cdot \frac{1}{\Delta T} \tag{3.3}$$

  As the temperature coefficient expression indicates, a positive temperature coefficient can cover a few MHz of frequency shifted by the temperature variation.
  The temperature coefficient combines the thermal expansion of the resonator and the cavity in which the resonator is located in.

- The dielectric constant of the resonator will drive its dimensions. The bigger the dielectric constant is, the smaller the resonator will be. Thus, a high dielectric constant resonator helps to minimize the resonator's area but, the Q factor tends to diminish.

  Using Figure 3.1 as summary, the dielectric constant will define the range of frequencies

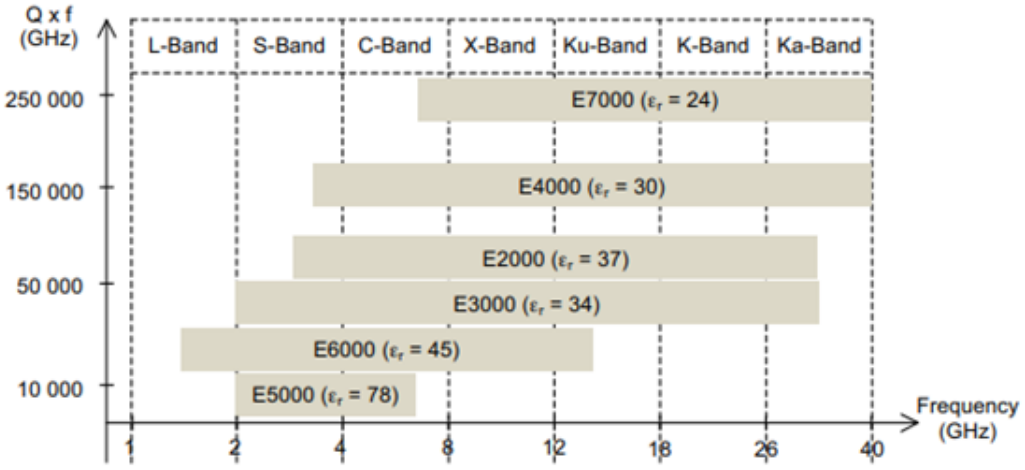

Figure 3.1: Resonator materials: Q vs frequency

that the resonator can work, its physical dimensions and, the Q factor. For example, the resonator E5000 ($\epsilon_r = 78$) will be the smaller one. Otherwise, the frequency response will not be much selective and the optimum frequency range of use will be smaller. On the other hand, the resonator E7000 ($\epsilon_r = 24$) will be the biggest one, being at the same time the most selective in frequency and the one with the biggest range of frequencies. Moreover, it can be checked that the Figure 3.1 uses the Qxf value to indicates the losses as they are linear with frequency.

3.3 Resonator EM analysis

During this section, the theoretical basis behind the resonator behavior is going to be detailed. Moreover, it is necessary to clarify that the presented model in this section is not definitive, some tuning techniques will add elements to the design.

As explained in Section 3.2, dielectric resonators "pucks" are mainly characterized by a high dielectric constant material. It is known that when the material dielectric constant is much

higher than the air one, the resonator's walls act as an open boundary, which behavior could remember to the classical antenna one. In fact, there is a kind of dielectric resonator which it is used as an antenna, dielectric resonator antenna (DRA) [13]. The unique difference between DRAs and resonator is the way they are feed, being the DRA feed from the bottom of the dielectric piece.

Thus, these similarities with a classical antenna can help to better understand the resonator fields shape. For the fields analysis, the Tranverse Electric mode (TE_{01}) will be used, being that the most used in many microwave applications.

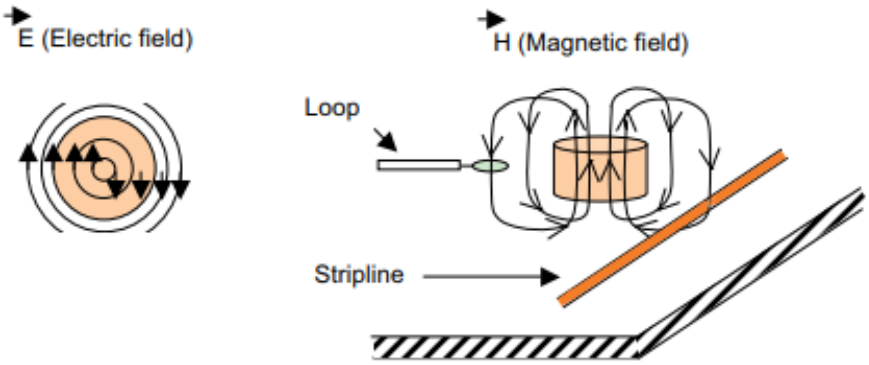

Figure 3.2: Puck fields: (a) Electric Field; (b) Magnetic field

Electrical and magnetic field around dielectric resonator are shown in Figure 3.2. As previously mentioned, the cylindrical puck has a recognizable donut shape for the magnetic field. Then, resonator can be coupled easily to microstrip lines just tuning the distance between them.

3.3.1 Puck

The puck dimensioning is critical since it is the key parameter that will allow fine selecting the oscillation frequency. For a cylindrical resonator, the dimensioning can be done just by changing the diameter and height of the resonator.

Typically, there is a theoretical approximation eqn(3.4) for dimensioning as a starting point. However, that equation will never be a certain one, the metallic cavity which contains the resonator will also have its frequencies, and will affect the general one computed using this

equation [14].

$$f_{GHz} = \frac{34}{a\sqrt{\epsilon_r}}(\frac{a}{L} + 3.45) \tag{3.4}$$

Where a is the radius of the puck, L is the height. Both parameters must be indicated in millimeters and, the obtained frequency has GHz as unit.

In parallel, the supplier indicates that its resonators are better modeled with the following expression:

$$f = \frac{233}{\sqrt{\epsilon_r}V^{\frac{1}{3}}} \tag{3.5}$$

Being determined only by the resonator's volume.

As a design rule, it is known that the dielectric resonator must accomplish a height around the 40% the diameter. Basically, breaking that rule, new modes could be excited [2].

3.3.2 Spacer

The spacer is a piece of low dielectric constant which adds some space between the resonator and the cavity sidewalls. Mainly, the critical distance is located at the resonator's bottom, being the separation distance only defined by the PCB's height.

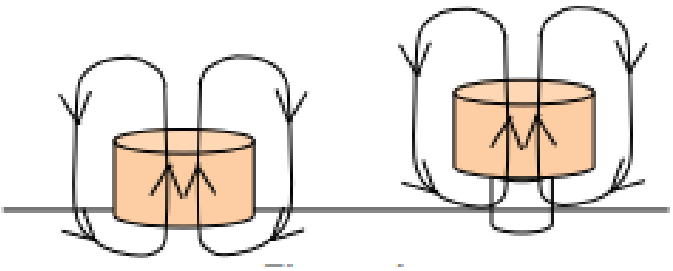

Figure 3.3: Spacer effect

As shown in Figure 3.3, being the resonator located near the metallic cavity, some part of the magnetic field is lost, thus, the resonant frequency will be changed and a worse Q factor will be obtained.

Additionally, the spacer addition provides some other benefits in a resonator. In fact, a better coupling could be achieved taking profit of the space between puck and PCB, which results in a better Q factor.

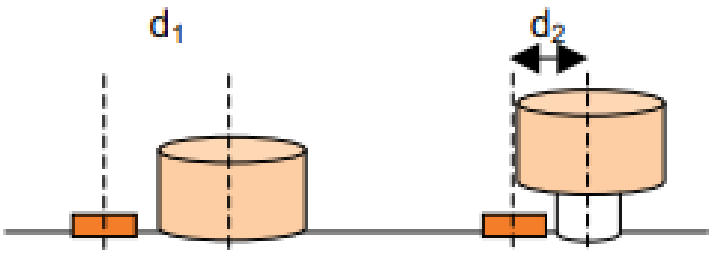

Figure 3.4: Spacer benefit

As Figure 3.4 indicates, spacer allows the resonator to overhang the microstrip line. Then, a new design parameter appears, which is the distance between the puck center and the coupled line.

Finally, Figure 3.5 shows the cross-section view of the simulation setup on the early design step. As mentioned before, some other parts will be added later to perform a fine frequency tuning.

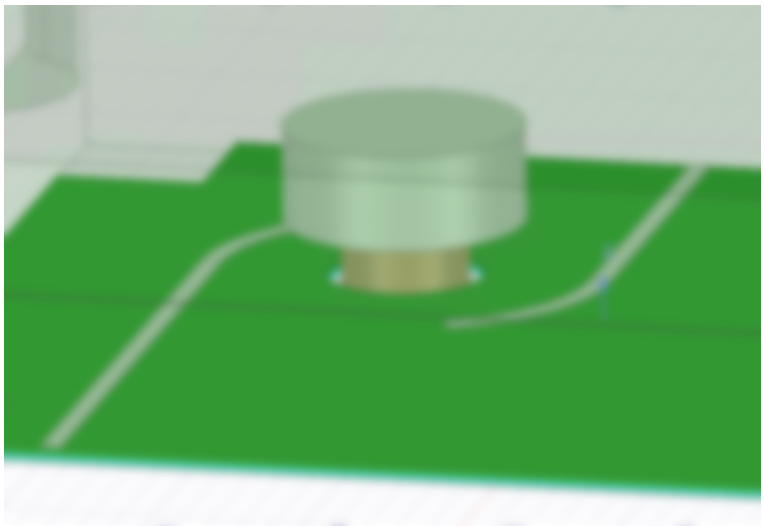

Figure 3.5: Cross-section screenshot

3.4 Puck Dimensioning

There are some dimensioning parameters to be taken into account to choose the correct puck dimensions. Firstly, the behavior of puck diameter and height will be analyzed.

In this section, the goal is to design a 7.63 GHz resonator for Ku band converter. Thus, let's

start checking how the supplier indicates the first dimensioning approximation.

Firstly, the supplier indicates that for a $\epsilon_r = 29.5$ dielectric resonator, the puck diameter follows the Figure 3.5 diameter range

Frequency (MHz)	Diameter range (mm)		
$2110 \leq F \leq 33250$	$D_{min} = \frac{52800}{F}$	$D_{typ} = \frac{59600}{F}$	$D_{max} = \frac{66500}{F}$
	$2 \leq D \leq 25$		

Figure 3.6: Supplier's diameter range

Where through the typical diameter expression, it can be obtained that the first approximation for the diameter is 7.81 mm. Thus, for the oscillator height, expression eqn(3.4) will be applied, which height results to be 3.1 mm.

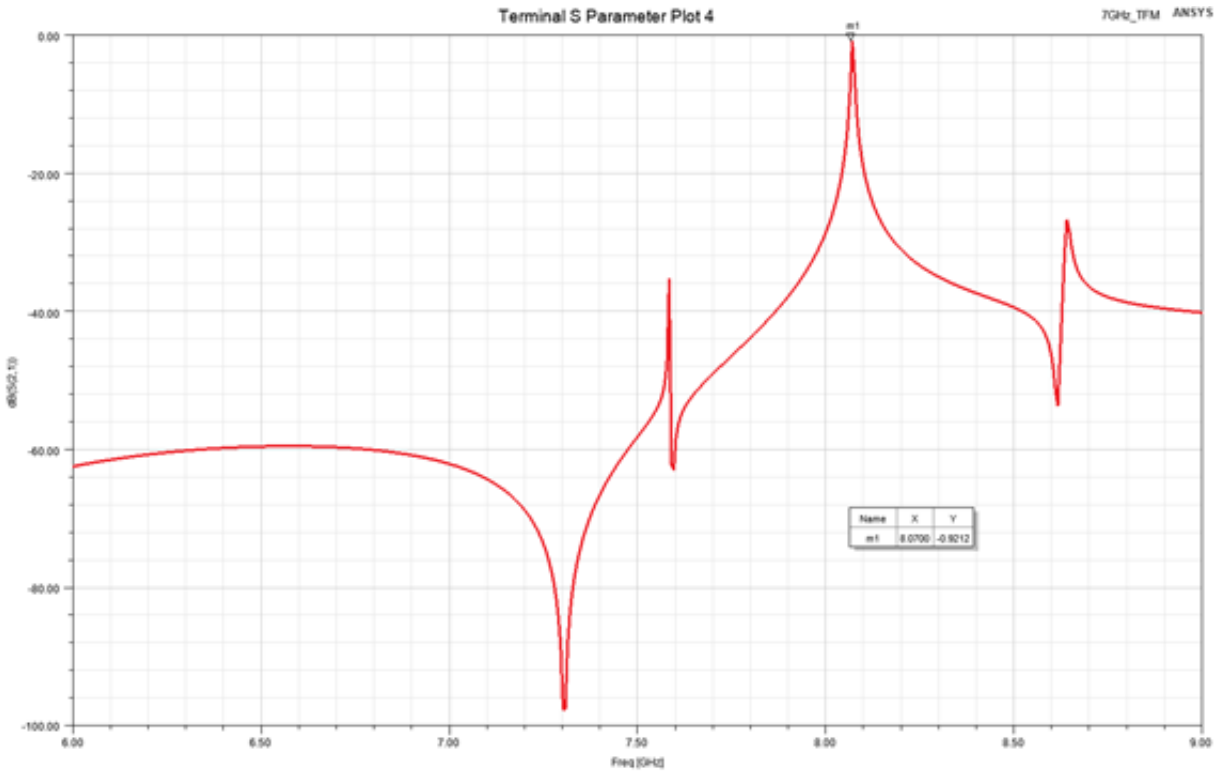

Figure 3.7: Puck HFSS simulation

As mentioned previously, Figure 3.7 shows that the obtained resonance frequency is 400 MHz over the desired one. All that behavior is done by the metallic cavity and how the resonator is being coupled. It can be seen that there are two additional resonances that may be caused by

the metallic cavity. At this point, some puck physical parameters will be varied to obtain the desired resonant frequency.

Firstly, let's start making some tuning over the puck diameter. At first instance, it is reasonable that as the diameter decreases, the resonance frequency will increase but, coupling will be worse.

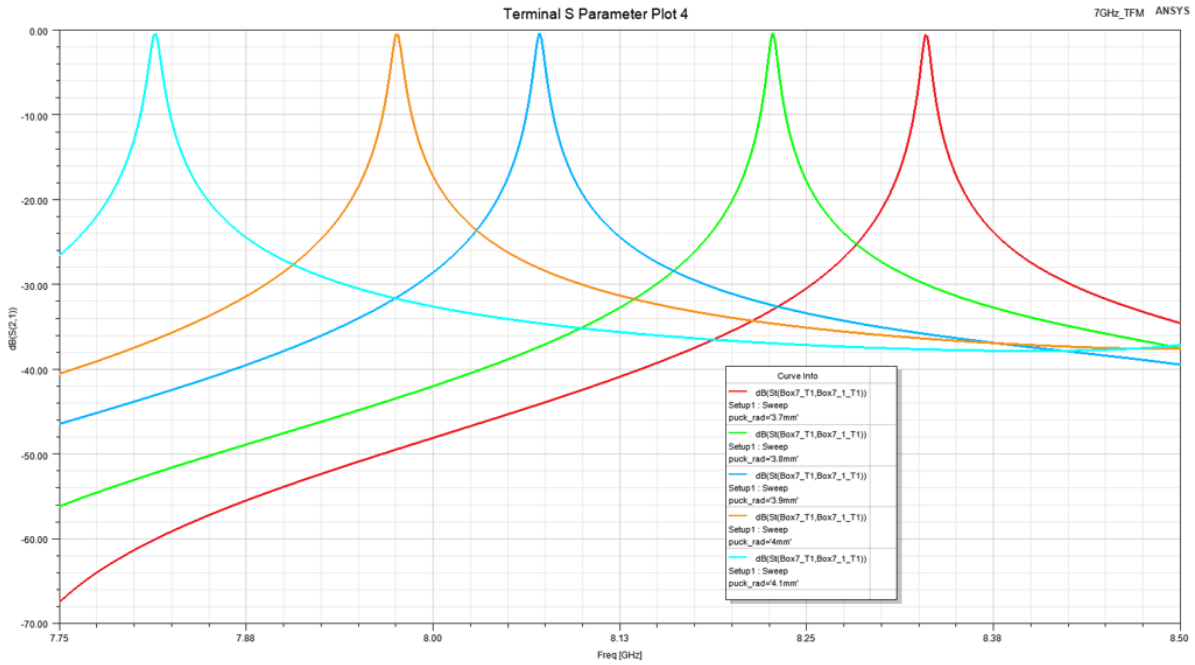

Figure 3.8: Puck diameter Tuning

As Figure 3.8 indicates, the above statement is perfectly accomplished. Starting from the right, as the resonator has a smaller diameter, the main resonance frequency is located for a higher frequency. On the contrary, starting from the left, the resonator with the biggest diameter has the lowest resonance frequency.

The impact of the diameter variation is detailed in Table 3.1, where it follows the previous mentioned behavior and, the Q factor increases as the puck diameter decreases. Moreover, all that conclusion can be assumed in a visual way just by looking at Figure 3.9, where the resultant curve clearly justifies a negative trend as diameter diminishes.

Once the diameter effect has been defined, let's see how the resonant frequency reacts against a height variation. In that case, it is reasonable that a height variation could follow a similar behavior in comparison to the diameter case.

Diameter (mm)	Resonant frequency (GHz)	Loaded Q
7.4	8.32	1388
7.6	8.22	1469
7.8	8.07	1261
8	7.97	1190
8.2	7.81	1100

Table 3.1: Diameter vs resonant frequency vs Loaded Q

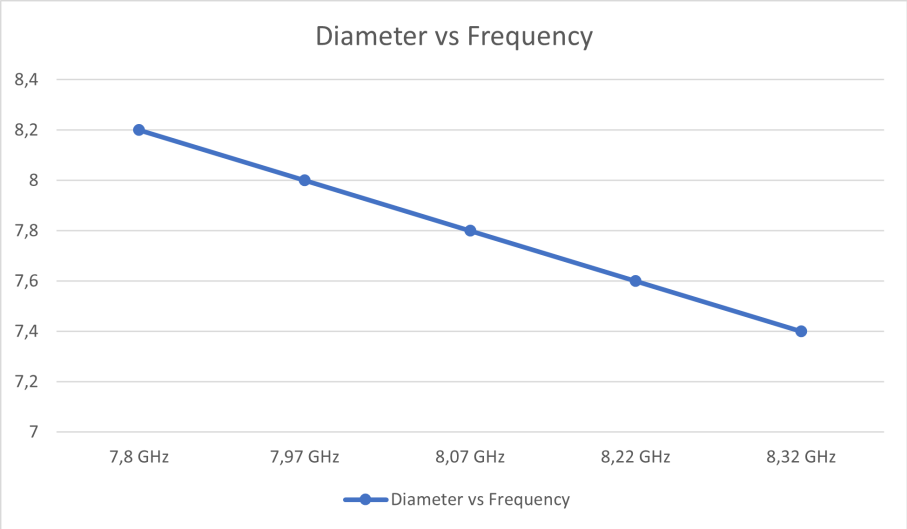

Figure 3.9: Diameter vs frequency

As mentioned, the puck height acquires a similar behavior to diameter tuning. In Figure 3.10, from left to right, the tallest puck has the widest resonant frequency. On the other hand, the smallest puck obtains a higher resonant frequency.
As shown for the diameter case, the height behavior can be understood properly through Table 3.1.

From Table 3.2, it can be checked that the height vs frequency behavior follows the same pattern as diameter vs frequency. Also occurs with the Q factor, where it decreases as the puck becomes smaller. Moreover, in Figure 3.11, also a negative trend has been obtained.
In conclusion, some physical dimensions and how they affect the resonant frequency were presented. On the following section, some tuning procedure will be described, in this project, the

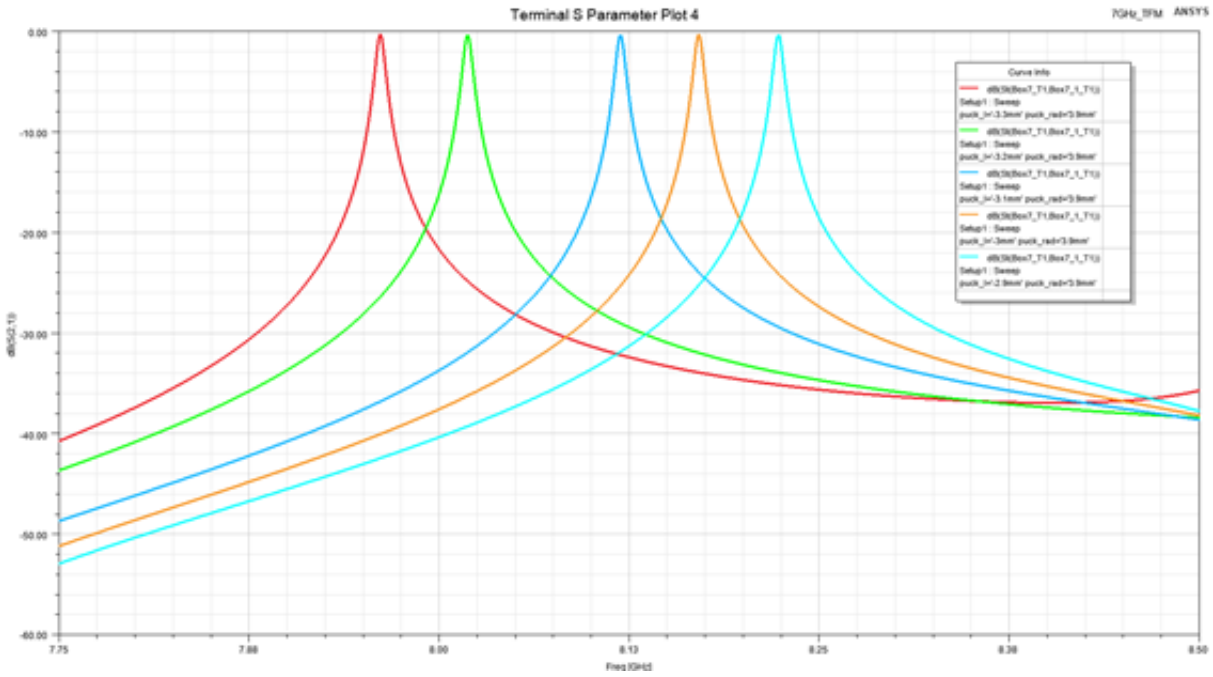

Figure 3.10: Puck height Tuning

Height (mm)	Resonant frequency (GHz)	Loaded Q
2.9	8.22	1284
3	8.17	1276
3.1	8.11	1268
3.2	8.01	1252
3.3	7.96	1243

Table 3.2: Height vs resonant frequency vs loaded Q

tuning is done by using a metallic screw and a hyper-abrupt varactor diode.

3.5 Tuning techniques for DROs

DROs designs are very complex since resonators are customs pieces and delivery time tends to be critical in these kinds of systems. For this thesis, the delivery time was 12 weeks so, the resonator selection needs to be as accurate as possible. For this reason, the puck dimensions need to be precise and a certain margin is mandatory for shifting the resonant frequency without

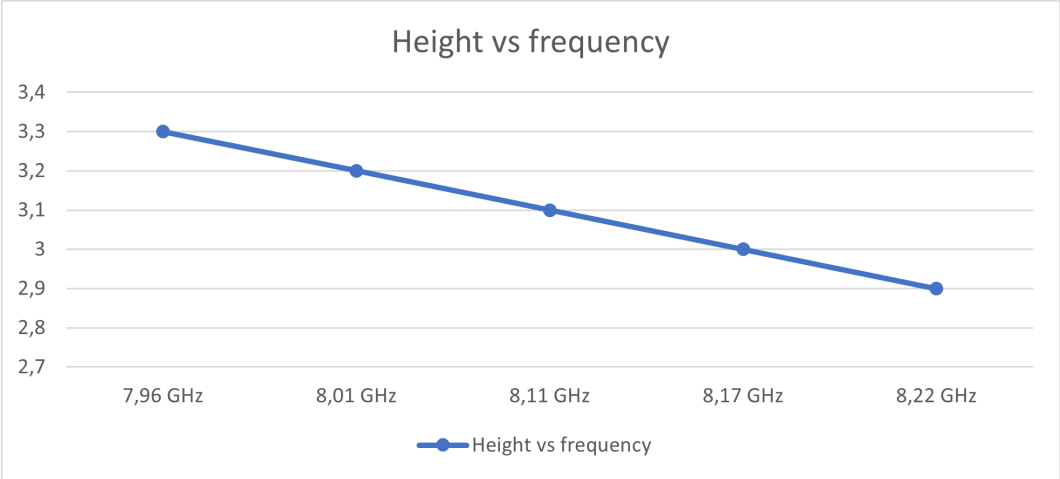

Figure 3.11: Height vs frequency

modifying its characteristics.

As mentioned in the previous section, some external components will be added to modify the resonator response. For this thesis, two tuning techniques are applied: the metallic screw and the coupled varactor diode.

Below this point, both techniques functionality are explained and a benefits/drawbacks balance values the necessity for each of these.

3.5.1 Metallic screw

The metallic screw technique is based on the perturbation theory for EM fields [2]. Basically, it is known that the cavity which encloses the resonator defines an operational range of frequencies. Thus, resonant frequency changes if fields are receiving some variations in volume.

Metallic screw, as its name indicates, is a metallic disk that varies its distance respect to the resonator's top. The metallic screw is oriented in the Z-axis with resonator and allows some frequency shifting. In fact, metallic screw is the ideal technique to obtain a big frequency shifting, which it will ensure that the desired resonant frequency will be tuned to [15].

As shown in Figure 3.12, the metallic screw adjusts its position until the desired oscillation frequency is acquired. As mentioned in Section 3.3, magnetic field is in charge of the coupling within puck and microstrip lines and, due to the TE mode, the magnetic field is predominant in

Figure 3.12: Resonator plus metallic screw

the space over puck. Basically, as the metallic screw approximates to the puck, the magnetic field is confined in a smaller volume. Thus, it becomes into a magnetic field variation, which finally becomes in a frequency shifting.

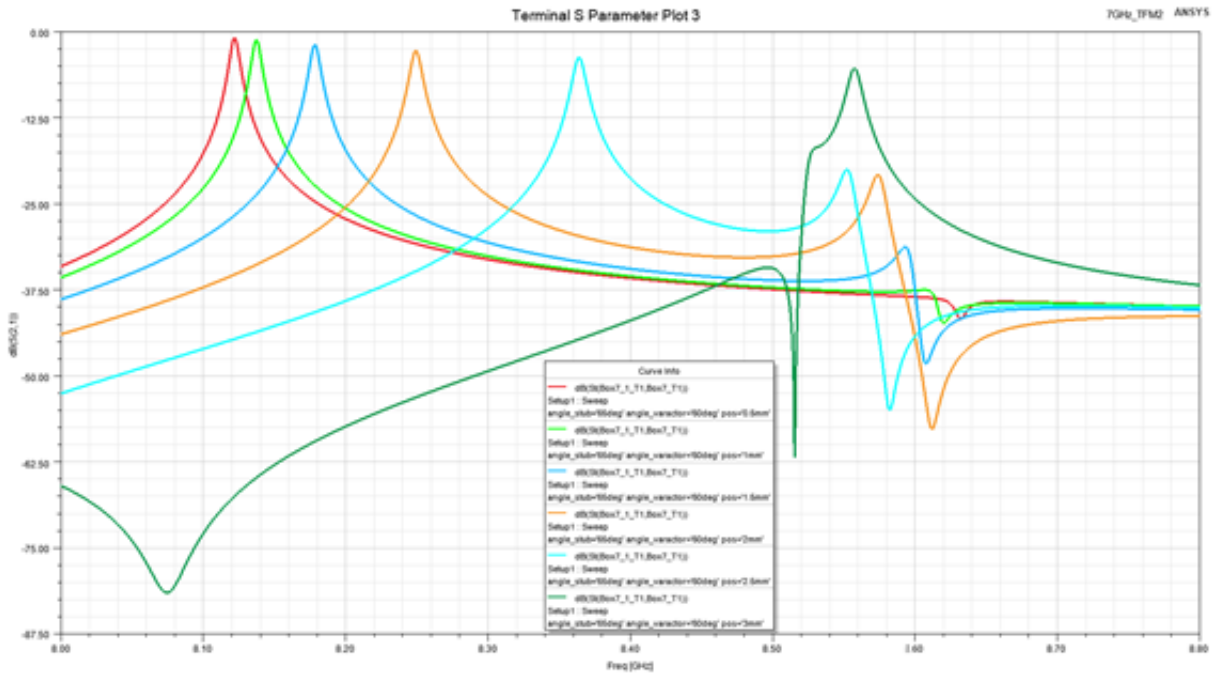

Figure 3.13: Frequency tuning (metallic screw)

For the metallic screw tuning case, as distance between screw and puck is reduced, higher is

the obtained resonant frequency (Figure 3.13). On the contrary, as the distance between them is maximized, the resonant frequency is in a lower frequency band. As explained with the puck parameters, a more visual analysis helps to correctly understand which pattern the metallic screw follows.

Distance puck-screw (mm)	Resonant frequency (GHz)	S21 (dB)
0.5	8.55	-5.33
1	8.36	-3.74
1.5	8.24	-2.79
2	8.17	-1.91
2.5	8.13	-1.22
3	8.12	-0.90

Table 3.3: Distance puck-screw tuning

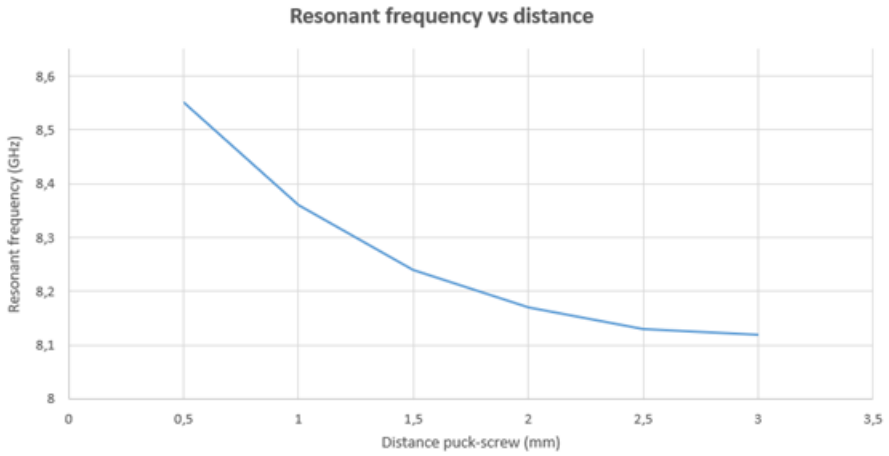

Figure 3.14: Resonant frequency vs distance

As Figure 3.14 indicates, the resonant frequency increases as the screw approximates the resonator, thus, metallic screw allows a wide range of frequency tuning, which is around 500 MHz. Furthermore, a larger frequency shift, provides more losses in the passive element of the oscillation loop. In Figure 3.15, the minimum distance indicates a -5.3 dB losses, whereas the maximum distance has -0.9 dB. Additionally, it is not a good guide working with a large screw because non-desired perturbations tend to appear, as green curve on Figure 3.13 shows.

For this thesis, there is a designing threshold defined around the position of the screw. In this

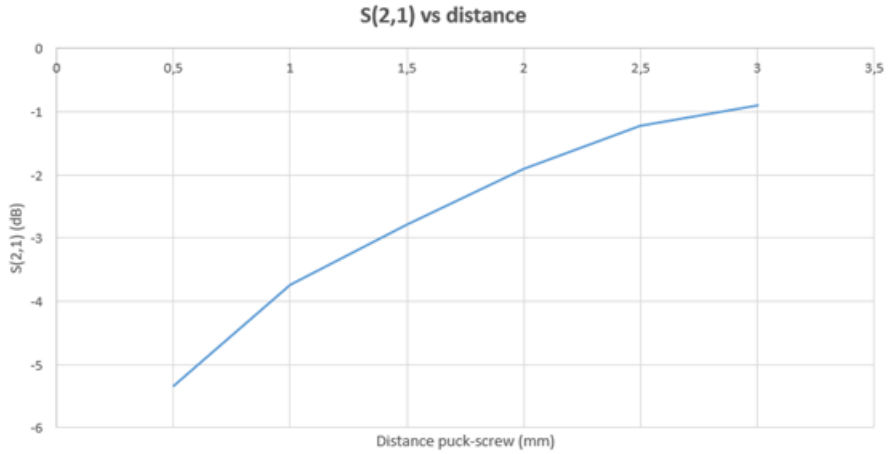

Figure 3.15: Resonant frequency vs S(2,1)(dB)

case, design follows an optimum screw position of 2/3 the whole distance of separation. In other words, there is 1/3 of distance between resonator and metallic screw. Thus, some additional tuning could be done during the measurement phase.

As conclusion for the metallic screw, it allows resonator shifting its frequency approximately over 500 MHz but, it is mandatory to contemplate the resonator losses increasement as the frequency is shifted.

Metallic screw technique can be considered a “mechanical” technique but, there is another frequency shifting techniques that will allow the finest selection of the resonant frequency.

3.5.2 Varactor Diode

Varactor diodes are frequently used for controlling the resonant frequency against temperature. These kinds of designs are called Voltage Controlled Oscillator (VCO). In this thesis, varactor diode has a tuning behavior, where coupled to puck, a finest tuning can be obtained [16].

A varactor diode is a device which varies its capacitance as some voltage is applied. The larger the voltage applied, the lower the effective capacitance. In this thesis, the varactor diode is directly connected with a microstrip path. The piece of microstrip acts as a coupled inductance, thus, the resonator becomes into a LC resonator plus a coupled inductance. Therefore, once the varactor capacitance changes, a few of frequency shifting over the resonant frequency will be achieved.

Before starting with the results obtained through simulations, it is convenient to model the varactor as suppliers tend not to show all the varactor's information in their datasheets.
Firstly, consider that the varactor curves equal Junction Capacitance + Package Capacitance, where the package capacitance is, hopefully, small and constant.

$$C_T(V_R) = C_j(V_R) + C_{pkg} \tag{3.6}$$

The junction capacitance can be modeled as follows:

$$C_j(V_R) = \frac{C_j(V_x)}{(\frac{V_R+\phi}{V_x+\phi})^\gamma} \tag{3.7}$$

where $C_j(V_R)$ is junction capacitance at voltage V_R, $C_j(V_x)$ is junction capacitance at voltage V_x, being V_x an arbitrary reference voltage (typically 0V), ϕ is built-in voltage and, γ the slope exponent, being $\gamma = 0.5$ for abrupt junction and $\gamma > 0.5$ for hyper-abrupt junction.
If V_x, the arbitrary reference, is 0, the equation is left as

$$C_j(V_R) = \frac{C_j(V_x)}{(1 + \frac{V_R}{\phi})^\gamma} \tag{3.8}$$

With built-in potential values being around 0.7 V for Si-based (like the varactor option 1) varactors and 1.2 V for GaAs.
As mentioned, some varactor datasheets show neither curves nor plots, instead, they give you some of these parameters. From them, it is possible approximately model their functions. Additionally, as the maximum that the oscillator receives from voltage regulator is 5V, varactor capacitance will be valued from 0V to 5V.
The first varactor to be modeled is the option 1. It has a $\gamma = 1.25$ and a 2V/12V voltage ratio of 4.2. As Figure 3.16 indicates, the obtained ratio is a bit far from the datasheet, it is difficult to exactly model which is the package capacitance. Moreover, there is only that parameter to model it, thus, it is difficult to exactly represent its behavior.
Then, it is reasonable, through the obtained modelling, that the option 1 varactor has a capacitance range from 2.96 pF to 0.51 pF, 2.45 pF of tuning.
On the other hand, the option 2 varactor is a great option since its datasheet provides more useful values, so it can be modeled in a better way.
As Figure 3.17 shows, the option 2 goes from 4.2 pF to 1.05 pF, which is a range of 3.15 pF.

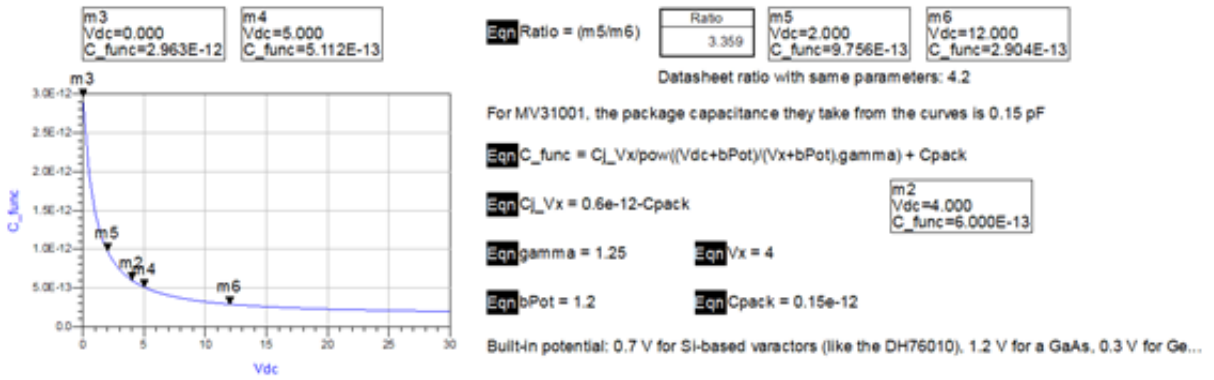

Figure 3.16: Option 1 Modelling

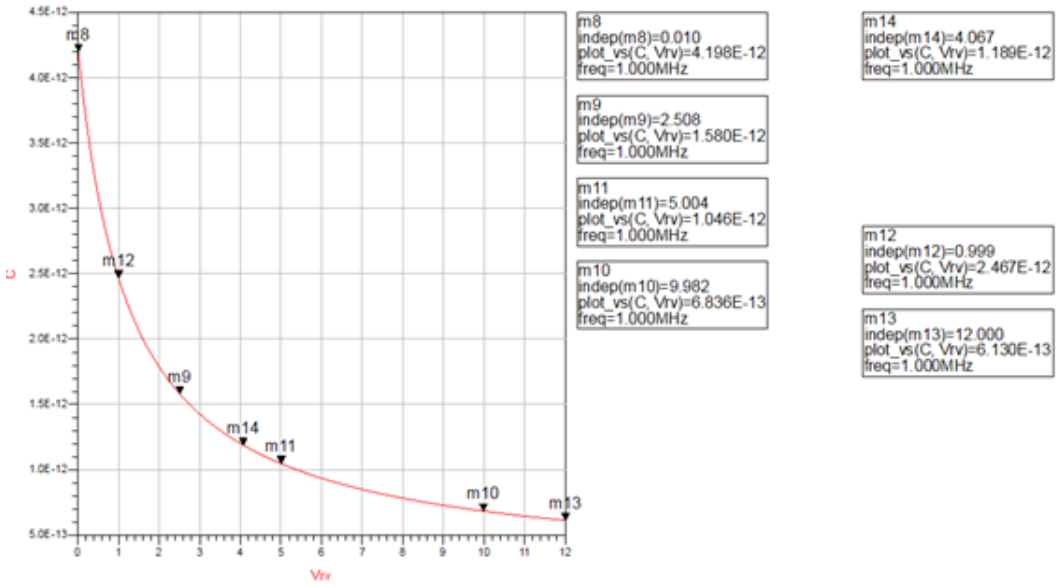

Figure 3.17: Option 2 Modelling

In this case, the project will mount the option 2 varactor since it provides a wider range of capacitance and, at first instance, more range can be translated as a wider frequency tuning range. Therefore, an optimized coupled line will be mounted between resonator coupled lines to induce a greater impact over the resonant frequency as Figure 3.18 depicts.

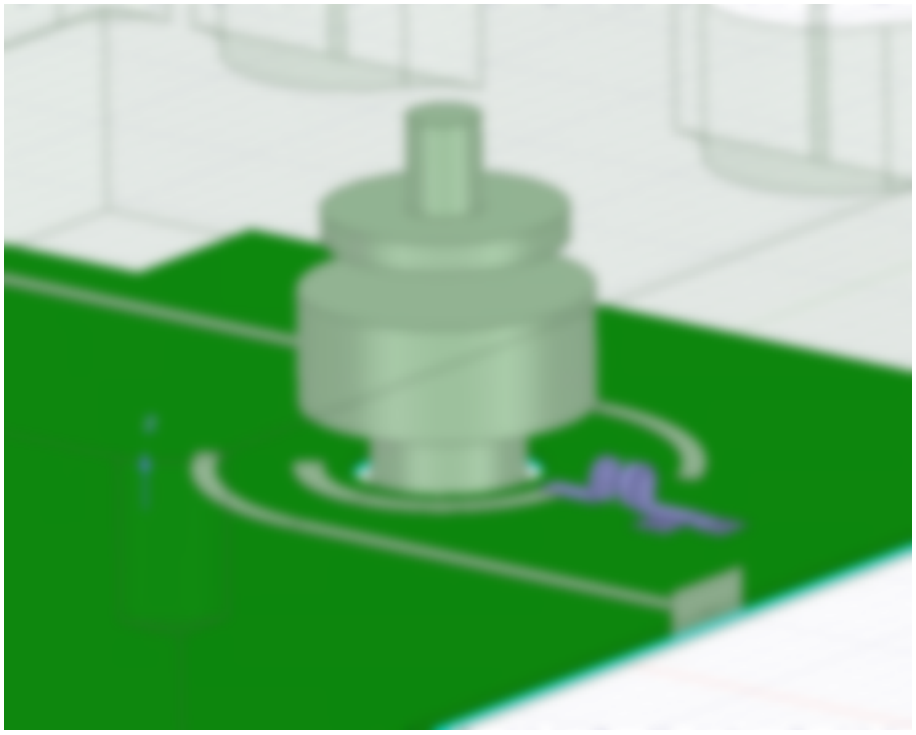

Figure 3.18: Resonator plus varactor

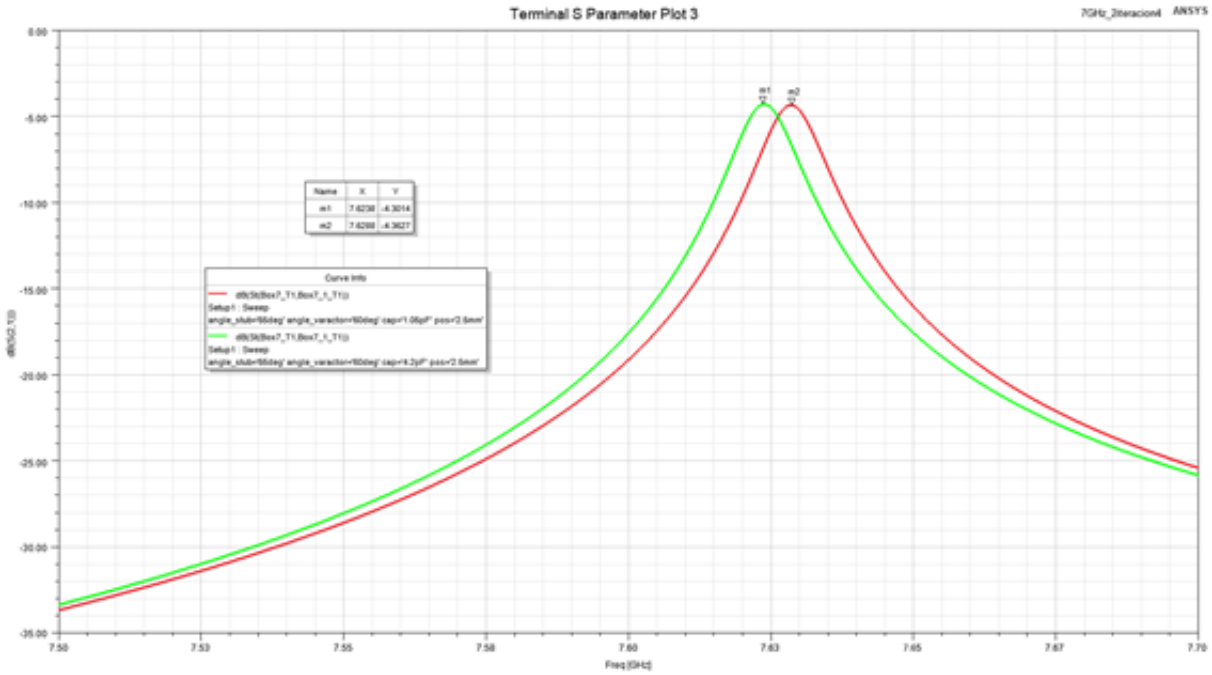

Figure 3.19: Varactor tuning simulation

As Figure 3.19 shows, varactor's tuning is around a few of MHz. In this case, the shifting is 5 MHz, which is a nice range to obtain the exact frequency required. Moreover, despite of

HFSS does not simulates active devices, results follow the expected behavior. As capacitance increases, the oscillation becomes into a lower frequency value. In other words, as more voltage is provided to varactor, the higher the frequency becomes.

In conclusion, metallic screw will provide a wider frequency shifting, around 500 MHz, and varactor diode will be used for fine tuning, being ahead of a 5 MHz tuning, which is all the needed to exactly accomplish the desired resonance frequency.

Chapter 4

Active Device

4.1 Biasing network design (SiGe bipolar transistor Space Qualified for X band)

As explained in Section 2.2.2, SiGe bipolar transistor Space Qualified is the final choice for active device selection. Suppliers usually send some data to work with with:

- Large signal model: Is a non-linear model that includes the effects on the current voltages in the circuit. The model value small variations over the response, which result can be very approximated to real application. Large signal model is used for designing the bias point.

- Small signal model: Is a linear model that is determined at a determined DC operating point. For this model, signal is unaffected by the non-linear effects. Small signal model is used for stabilization and matching.

Therefore, firstly it is mandatory choosing the biasing point through using the large signal model. For this work, it is desired to obtain the maximum gain, as some gain issues could be found and phase noise is not a critical point.
From the amplifier's datasheet, the active device has a maximum value of $V_{ce} = 4V$ and $I_c = 30mA$ as operating point. Furthermore, as this is a space application, some deratings

have to be applied to ensure that the maximum bias point is not surpassed [17].

Table 6-35: Derating of parameters for Transistors family-group code 12-10 and 12-13

Parameters	Load ratio or limit
Collector-emitter voltage (V_{CE})	75 %
Collector-base voltage (V_{CB})	75 %
Emitter-base voltage (V_{EB})	75 %
Collector current (I_C)	75 %
Base current (I_B), if specified	75 %
Power dissipation (P_D)	65 % or limited by the derating on operating temperature.
Junction temperature (T_j)	110 °C or $T_{j\,max}$ - 40 °C (whichever is lower) for Si and SiGe bipolar transistors. 115 °C or $T_{j\,max}$ - 25°C (whichever is lower) for GaAs and InP bipolar transistors.

Figure 4.1: Transistor derating

As Figure 4.1 indicates, it is mandatory to apply a 75% derating to collector-emitter voltage (V_{ce}) and collector current (I_c). Some extra margin is left since when oscillating current consumption will increase. At this point, a bias network topology needs to be selected. It is known that common emitter collector feedback configuration is one of the most used configurations for amplifiers.

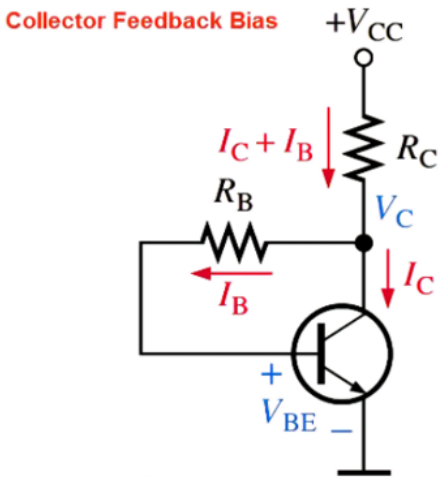

Figure 4.2: Collector feedback configuration

Collector feedback bias network provides a good response against Ic variations caused by the

temperature range, being the variation on base current inverse to variation on collector current. Moreover, this topology has a slightly dependence with transistor's current gain (β)

$$I_c = \beta \cdot I_b \tag{4.1}$$

Thus, resistor value for base and current can be obtained as follows

$$R_c = \frac{V_{cc} - V_{ce}}{I_c(1 + \frac{1}{\beta})} \tag{4.2}$$

$$R_b = \frac{V_{ce} - V_{be}}{I_b} = \beta \frac{V_{ce} - V_{be}}{I_c} \tag{4.3}$$

Attending to eqn(4.2) and eqn(4.3), resistor values for collector and base have a slightly dependence on gain current changes and, as previously mentioned, collector feedback configuration is robust against temperature changes.

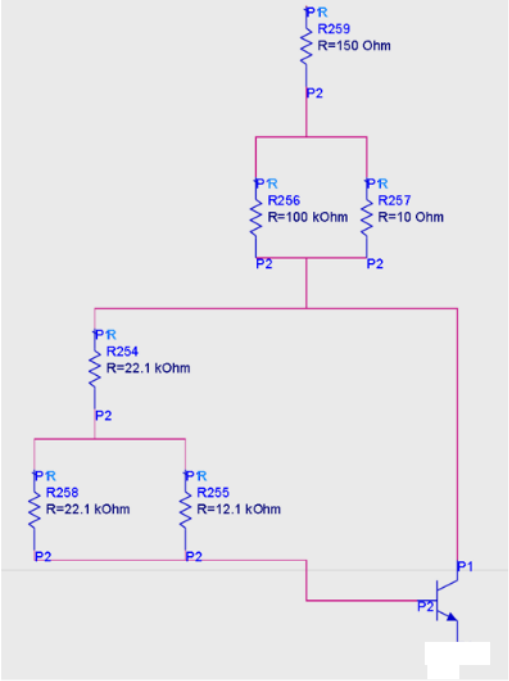

Figure 4.3: Bias network schematic

As Figure 4.3 shows, biasing network is composed by 6 resistors, three of them for collector and the others for base resistor. The benefits of using this resistor distribution network are obtaining a robust bias network and distribute the stress among all of them. In other words, once oscillator is in a prototype, changes in bias point can be easily done, just substituting resistor by other

values. With this strategy we can overcome variations of beta among the different transistors that will be used..

Until this point, we do not care about gain or matching, and the only aim is to achieve the desired bias point, and large model is essential for this task. Now, next step is stabilizing the active device using small signal model, which is a S-Param data defined at a specific biasing point, the one we have previously configured.

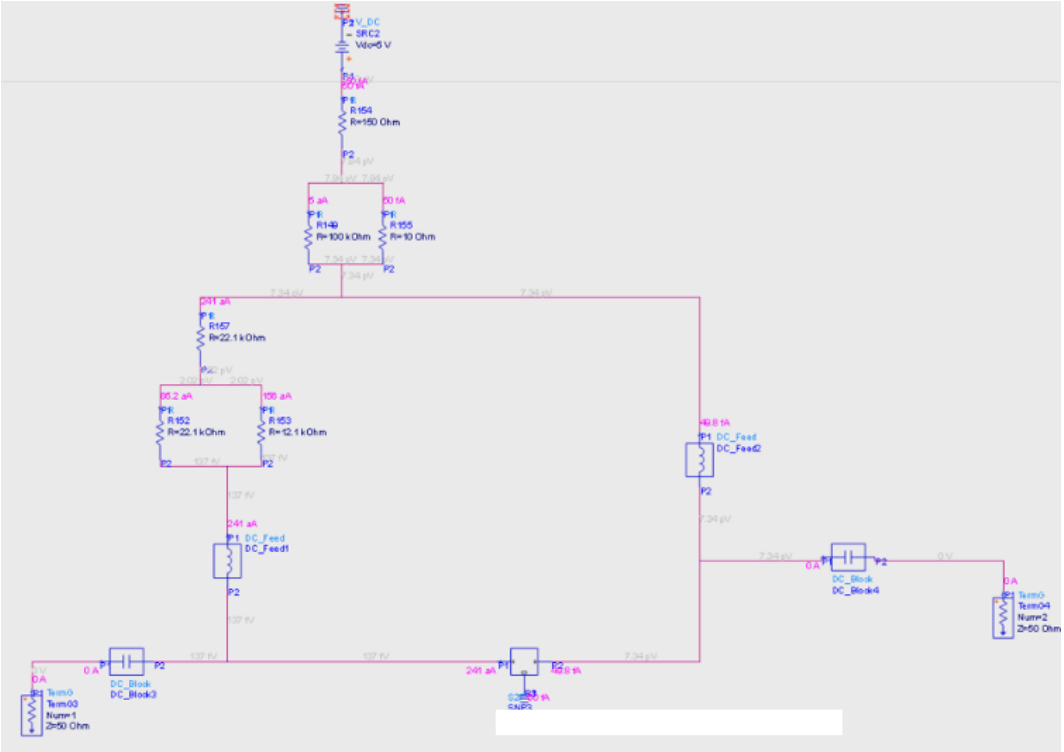

Figure 4.4: Small signal schematic

The scheme for small signal model (Figure 4.4) changes in comparison to large signal one (Figure 4.3). Now, as linear parameters are considered, Terminals are needed for simulation. Additionally, DC block and DC feed ideal components are included to correctly simulate the circuit. This is the functionality for each of these components:

- DC Block: Block any flow of DC signal, just allowing RF signals to access.
- DC Feed: Protect the biasing network against any RF signal, thus, none of DC bias network components can be influenced by RF flow.

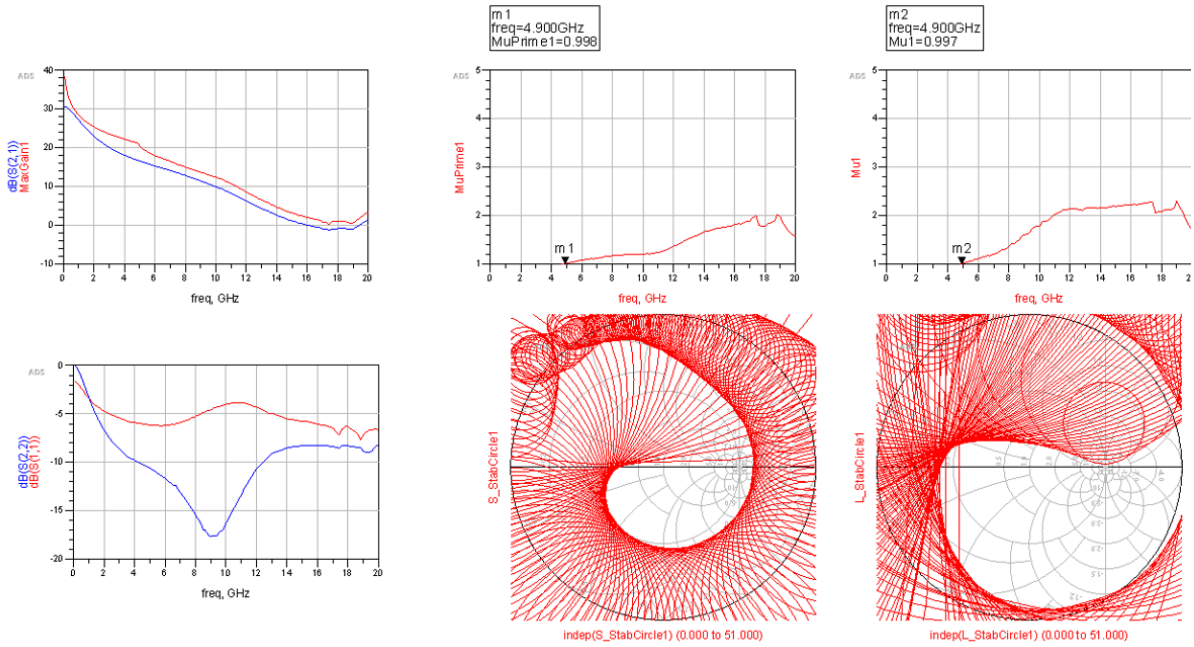

Figure 4.5: Small signal simulation results

Figure 4.5 shows a brief summary about amplifier's simulations. Starting from left, the active device has a linear behavior on gain, approving that it is a good choice for this project. Below gain chart, Load and Source matching curves are presented, which show that SiGe bipolar transistor Space Qualified has a good matching at its output (collector). The two following columns represents Mu and MuPrime on Cartesian and stability circles on Smith charts. Both agree that amplifier is conditionally unstable from DC to 5 GHz, thus, some stabilization is mandatory for this range.

Next step is to substitute the whole set of ideal components into its equivalents. In this case, DC block can be easily substituted by a low capacitance value. On the other hand, DC feed can be understood as bias Tee, where RF flow sees an open circuit in DC port.

As Figure 4.6 indicates, the simulation perfectly fits a bias Tee at the desired frequency. In this case, there is an open circuit for 8.668 GHz and, it can be appreciated that Port 3 is the DC network port. A basic bias Tee can be designed using a butterfly structure.

There is a simple theoretical basis behind the Figure 4.7 design. In this case, the transmission line length between Port 3 (DC port) and the other ports is $\lambda/4$ for resonant frequency. Ad-

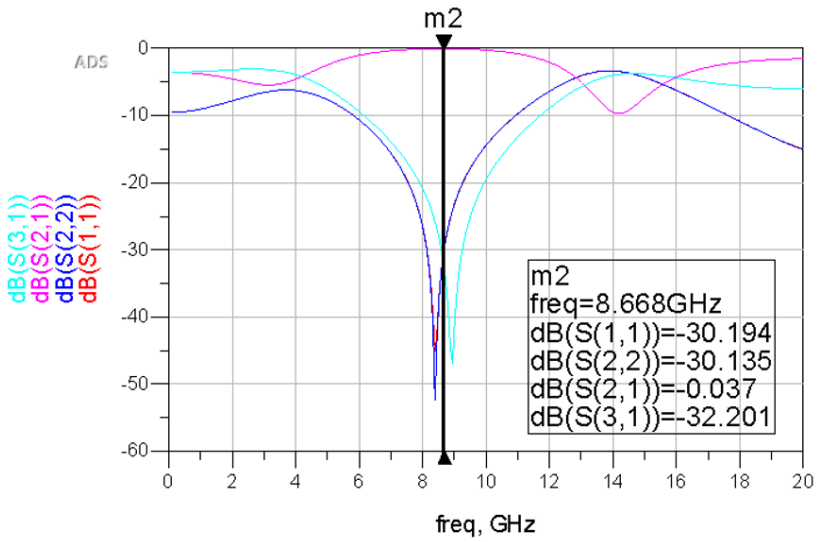

Figure 4.6: Bias Tee simulation

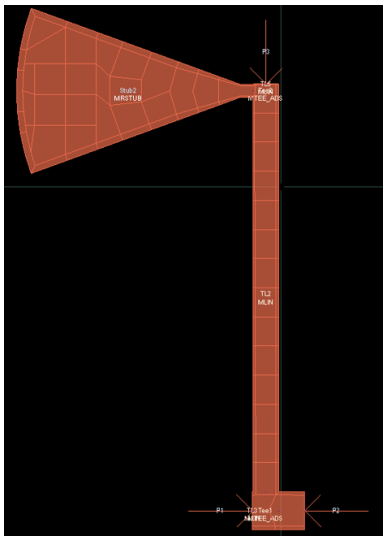

Figure 4.7: Bias Tee

ditionally, for reducing total dimensions, a butterfly acts as an open-circuit at the frequency of interest. Therefore, at bias-T P3, butterfly acts as a short circuit, being an open circuit for RF at the RF transmission line point.. As drawbacks, this structure acts as bias Tee for an extremely limited range of frequencies but, a double butterfly structure could be used to improve its bandwidth, if needed.

Once the bias Tee has been designed, it can be included in ADS (Figure 4.8). In this case, two Tees are needed, as design is following a collector feedback configuration. Additionally, it can

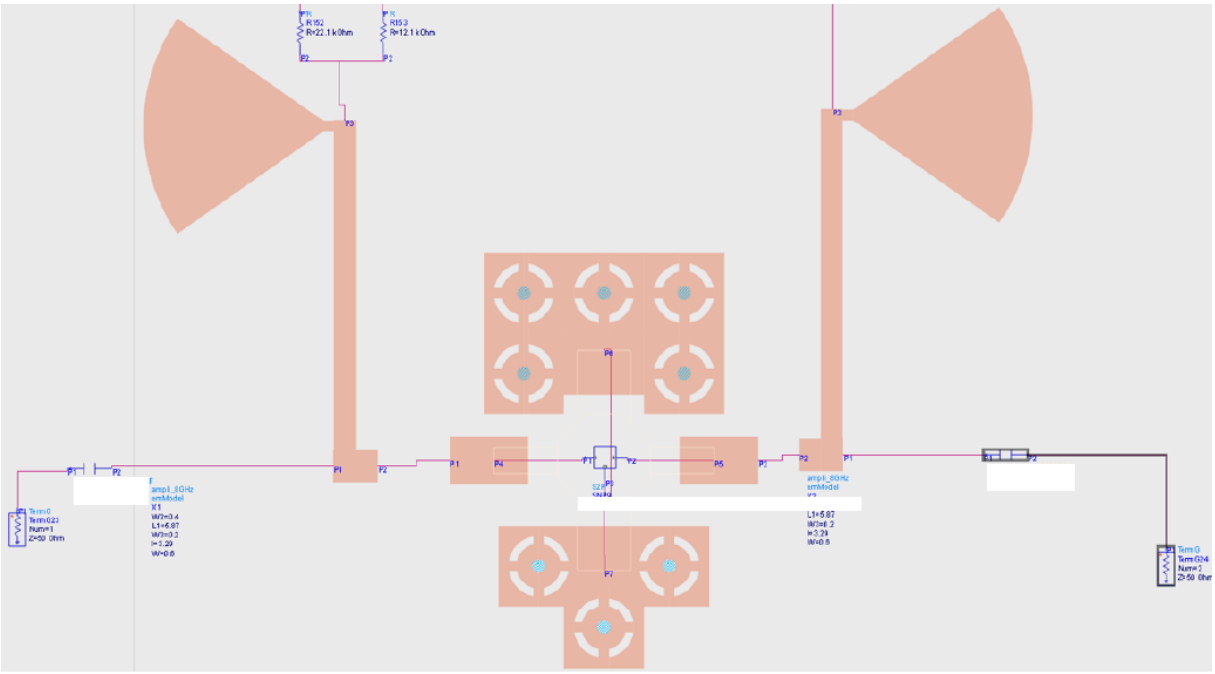

Figure 4.8: Small signal model plus bias Tee and SiGe bipolar transistor Space Qualified footprint

be appreciated that the active device emitter is connected to a set of via holes. These via holes correspond to the amplifier's footprint, in other words, this is the correct way of connecting emitter to ground. The amplifier's footprint is special since it is mounted in a 4 ports footprint, being two of them emitter ports.

From Figure 4.9, it seems that the active device characteristics have improved. As recently mentioned, matching still has a good level (load port), gain also has a good value for accomplishing the loop gain criterion and, stabilization has improved. Now, transistor is conditionally unstable from DC to 2GHz. In fact, this improvement could be caused by changing active's device emitter connection to ground. In Figure 4.4, the transistor was simply connected to an ideal ground element, otherwise, Figure 4.9 has a more realistic connection to ground, by the inductive behavior provided using via holes and, the use of Momentum in ADS, which it is a 2.5 dimension simulation tool.

Then, Figure 4.8 can be the starting point for stabilizing the amplifier. The easiest way to achieve stabilization could be just adding some losses at base and collector ports but, it is a

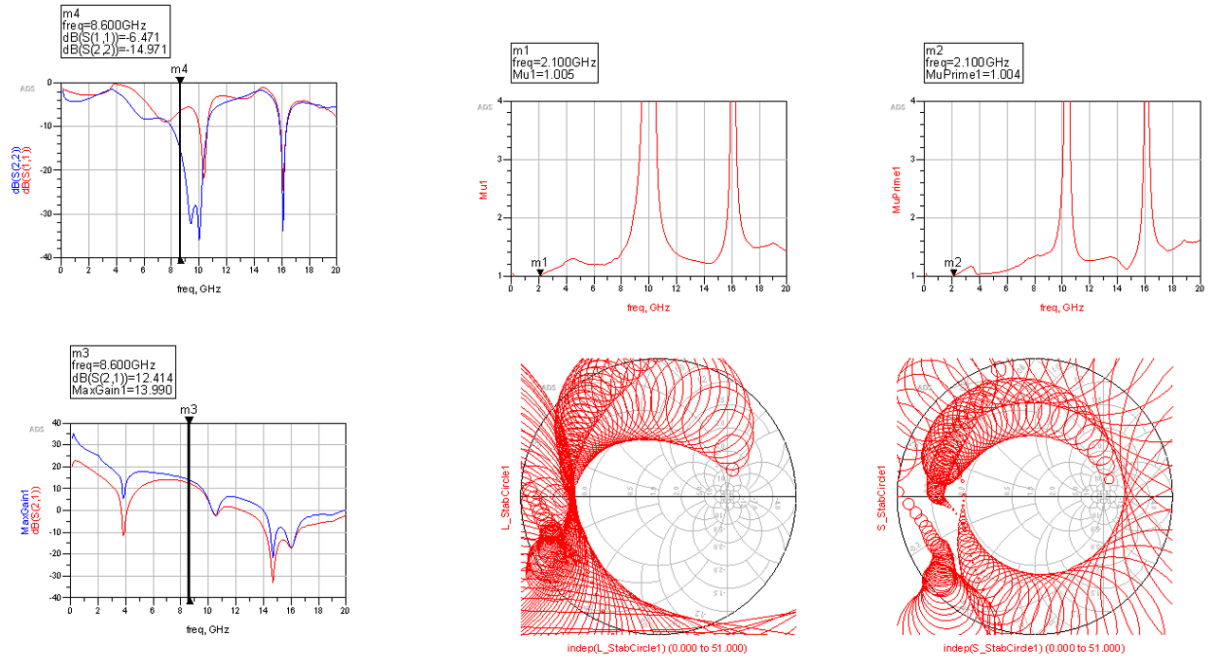

Figure 4.9: Figure 4.8 simulation results

good practice to firstly modify the DC bias network. At this point, the SiGe bipolar transistor design has a DC bias network, which it can not impact over stabilization, and a custom impedance inverter. The trick here is that bias Tee was designed for 50Ω in all ports and, the DC bias ports have another different resistance value.

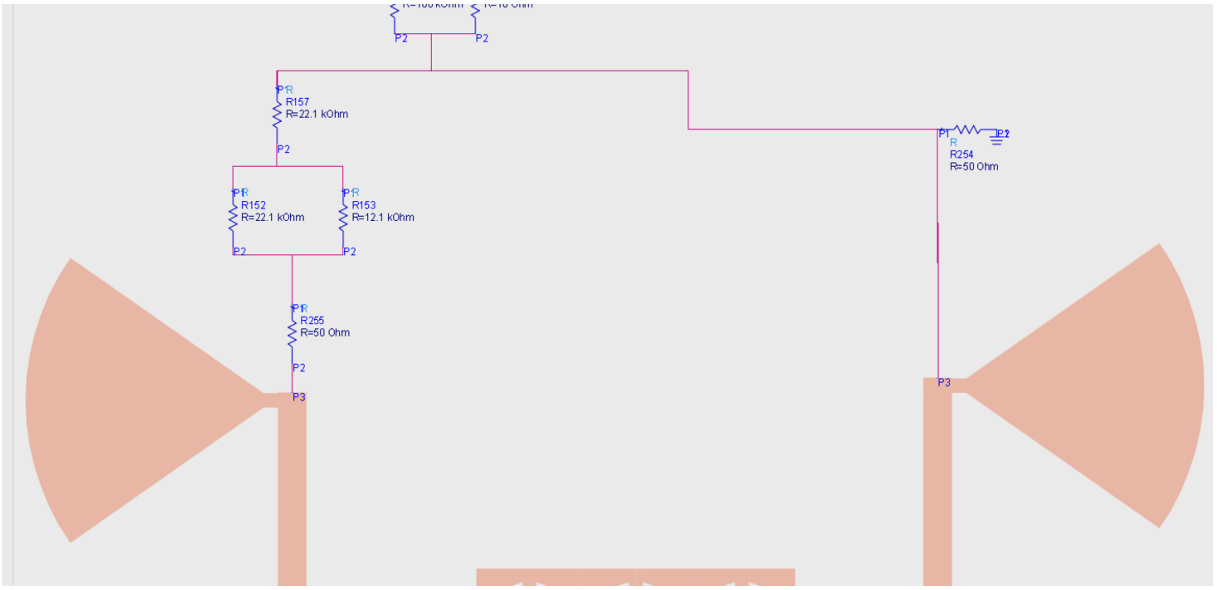

Figure 4.10: Core's stabilization

As Figure 4.10 indicates, this couple of 50Ω resistors is the solution for improving stabilization. Starting from left, as it is connected to base, no modification in bias point can be produced. In fact, at base, there is a 30K resistor in series with the recently added resistor so, its effect can be negligible. On the other hand, the 50Ω resistor located at collector needs to be in parallel configuration for not changing the bias point.

Making some reconfiguration at biasing network, designer can avoid some gain losses or adding large quantities of noise at active device ports, which it could be a negative scenario. Moreover, following the Figure 4.10 modification, bias point cannot be shifted so, only stabilization is being modified.

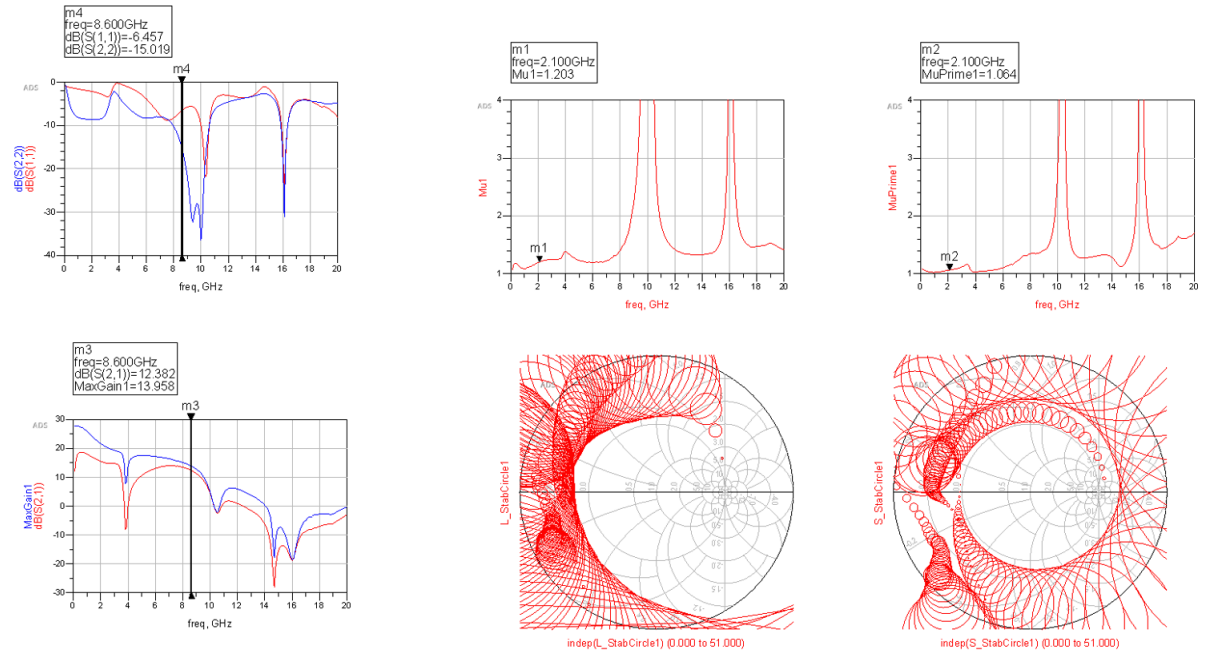

Figure 4.11: SiGe bipolar transistor results after stabilization

Finally, the transistor has been stabilized (Figure 4.11). In cartesian charts, both Mu and MuPrime values are over 1 for the whole range of frequencies, from DC to 20 GHz. Thus, knowing that Mu factors are over 1, it can be said that the transistor is now an unconditionally stable active device.

The amplifier's gain can be upgraded just matching it. As Figure 4.11 indicates, S(2,2) is almost matched, thus, matching can be easily obtained for the output. On the other hand, input port tends to have a bad matching value. In any case, matching is probably the easiest step during

this chapter.

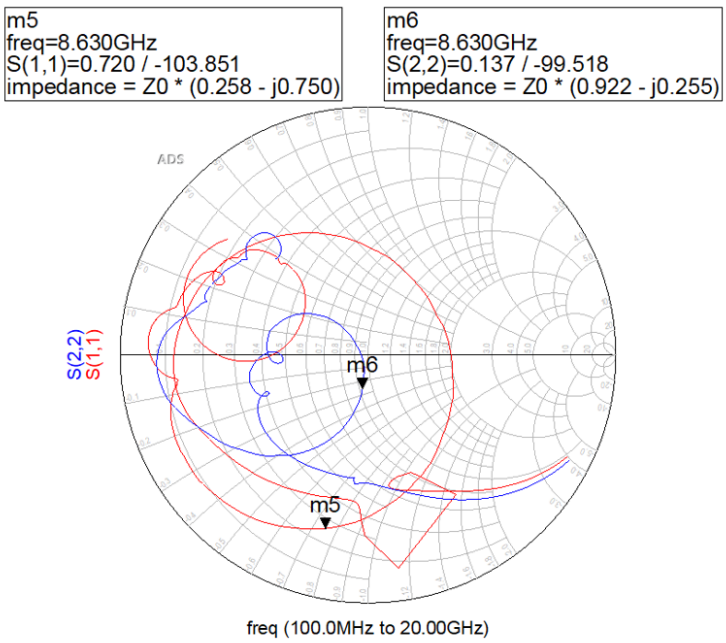

Figure 4.12: SiGe bipolar transistor early Smith Chart

Firstly, it is mandatory to mention that Smith Chart is the key tool for matching. As Figure 4.12 indicates, Smith Chart provides a more visual tool for knowing what component could help for getting the center of the Smith Chart. As mentioned above, output port (blue line) is practically at center of the chart, whereas input port (red line) is far.
In this case, due to the high frequencies related to the design, a stub will be used instead of lumped components.

ADS software has a very potential tool for easily design matching networks. Once again, Smith chart is the key tool for observing the impedance movements around it.

SiGe bipolar transistor Space Qualified for X band has its own particularities. Moreover, it can be appreciated that the transistor has swept, base is now located on the right side, since collector is on the left. Below this point, there is a brief description about functionality for each of the numbers (Figure 4.14):

1. There is a series RC used for cleaning some of the residual DC flow that could arrive

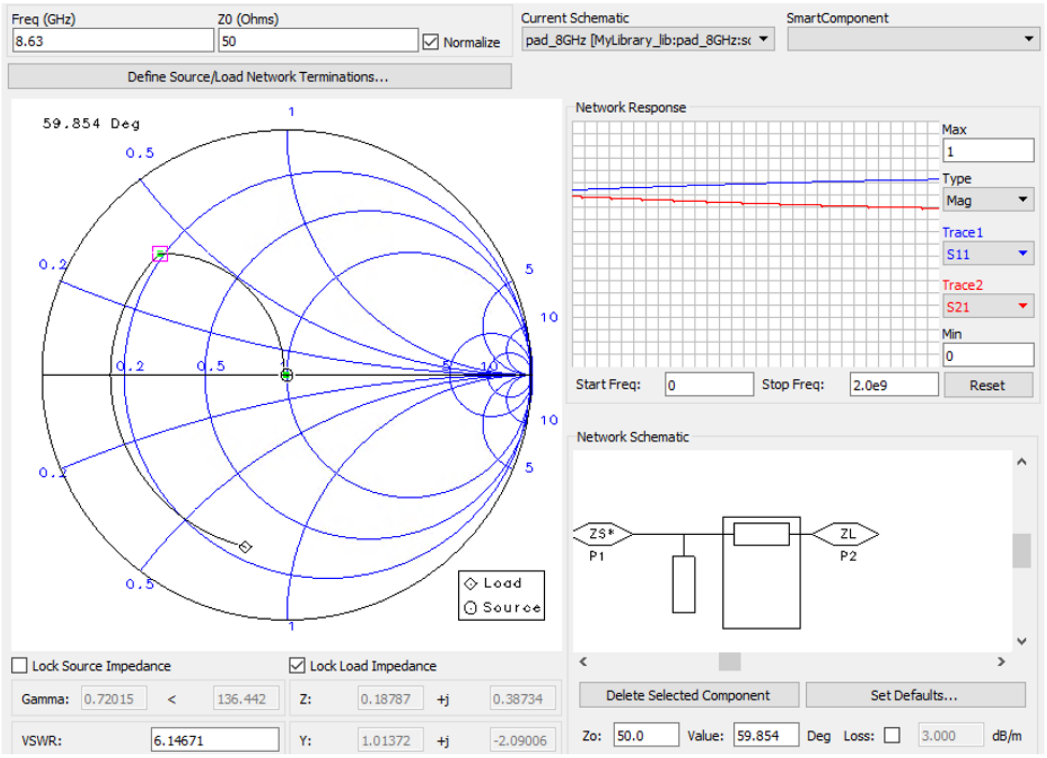

Figure 4.13: ADS Smith Chart tool

from the feeding point. In fact, it is desired feeding the transistor with a stable DC flow. The reality is that there are external factors, as EMC interferences, that produces irregular peaks, it could affect in a negative way.

2. As the active device uses a collector feedback configuration, base port needs to be protected as much as possible. For the same reason as 1, a set of capacitances are mounted just after the RF butterfly for ensuring that no residual DC signal arrives to RF main line. As higher is the capacitance value, more down in frequency the capacitor is protecting.

3. The same as point 2 is in collector port but, as it is less important for bias point, just a capacitor is in a short-circuited series RC.

In conclusion, the amplifier core for X band can be considered as closed (Figure 4.14). Looking for the transistor specifications for X band (Figure 4.16), a gain of 14.27 dB has been obtained. Additionally, the transistor still is unconditionally stable since there are no changes on biasing network, last step is just adding some extra matching outside the core.

Figure 4.14: SiGe bipolar transistor Space Qualified for X band (no matching)

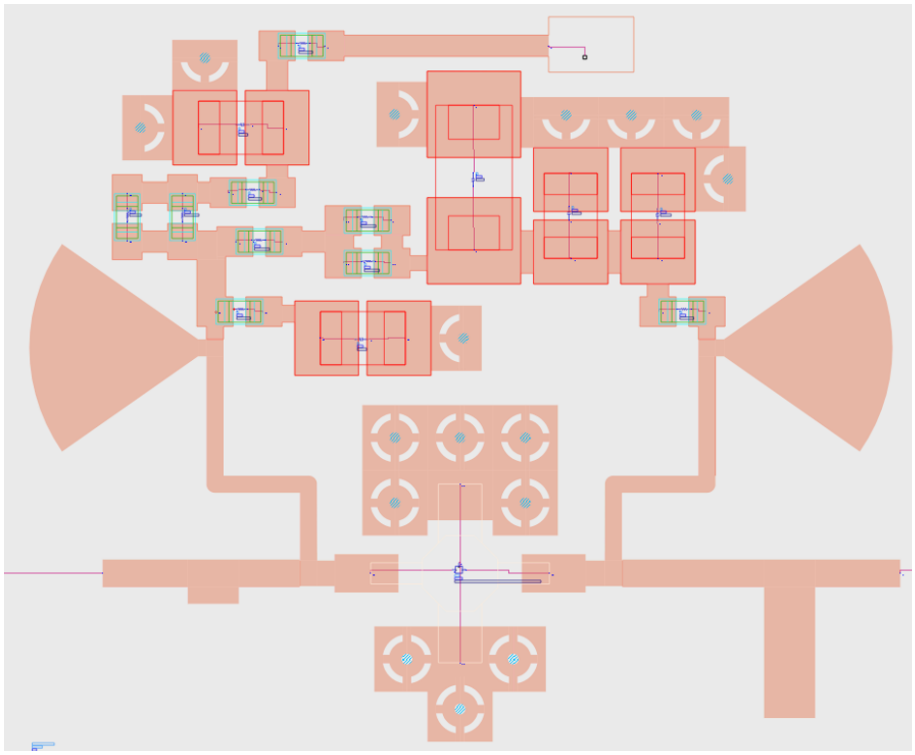

Figure 4.15: Matched SiGe bipolar transistor for X band

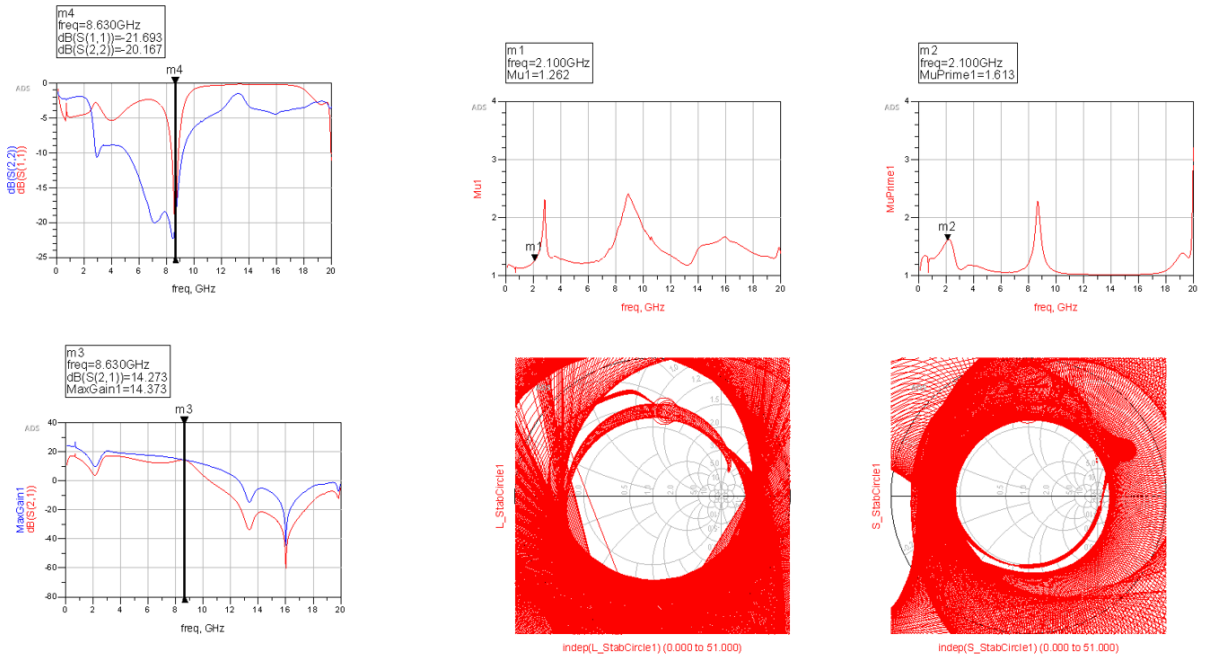

Figure 4.16: SiGe bipolar transistor simulations for X band

4.2 Amplifier for Ku band

The amplifier's core does not need modification for Ku band due to similarities between frequency band, in fact, there a 1 GHz gap between them. However, there are some steps which are custom for each of the designs.

Firstly, as bias Tee has an extremely low operation bandwidth, a new one has to be designed.

In this case, the Bias Tee follows a different shape since the transistor's footprint needs some space (Figure 4.17). Attending to results (Figure 4.18), Bias Tee perfectly resonates at the desired frequency. Therefore, at first instance, the transistor X band core can be reused for Ku band design.

Once Ku bias Tee has been added, the whole Ku band core can be simulated since, as mentioned above, the active device should be stabilized for a wide range of frequencies.

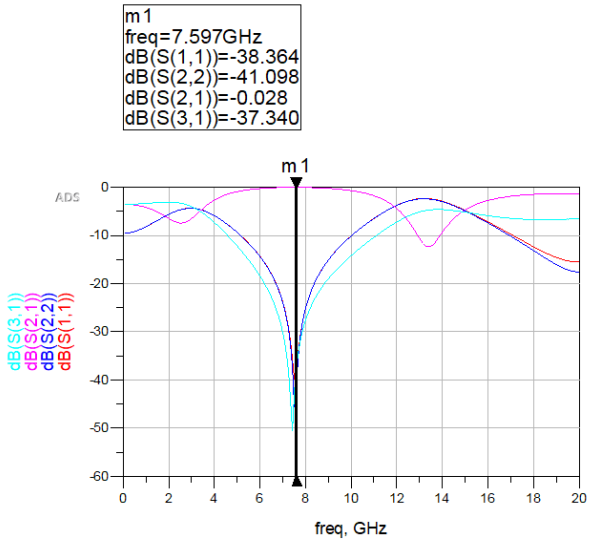

Figure 4.17: Bias Tee for Ku band

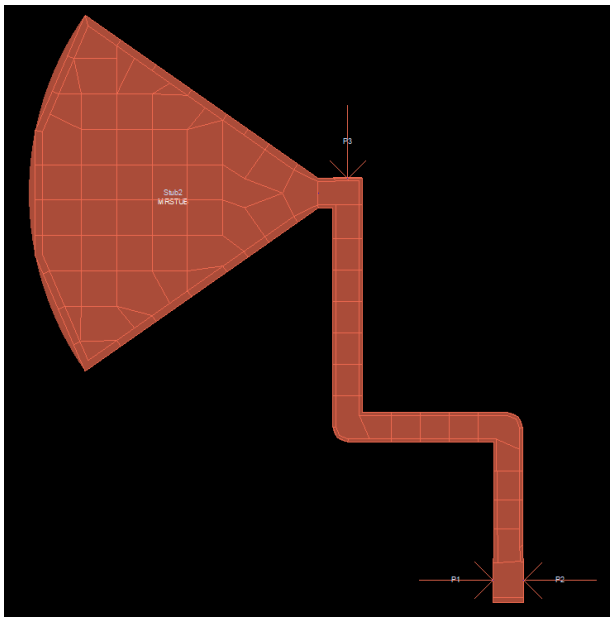

Figure 4.18: Bias Tee simulations

From Figure 4.19, simulation confirms that the same core as X band design can be used. Both Mu values are over 1 from DC to 20 GHz, thus, the transistor is unconditionally stable for Ku band.

Finally, last step is matching and, attending to X band case, Ku band transistor should be easily matched without modifying its stabilization.

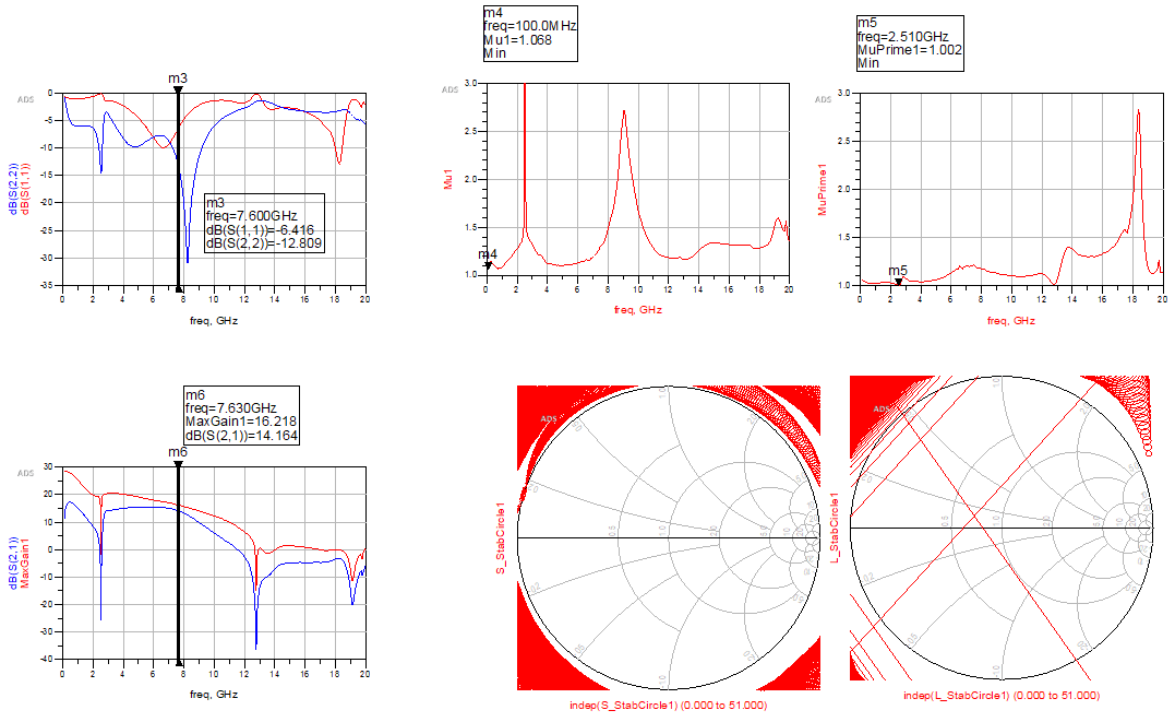

Figure 4.19: Ku band SiGe bipolar transistor before matching

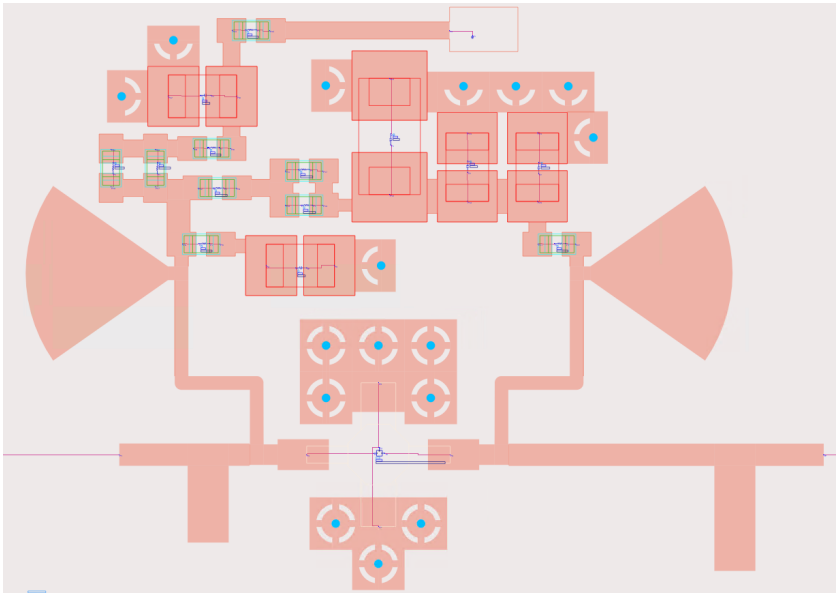

Figure 4.20: Ku band SiGe bipolar transistor Space Qualified matched

In conclusion, SiGe bipolar transistor for Ku has achieved a 15.88 dB gain, higher than the gain obtained for X band.

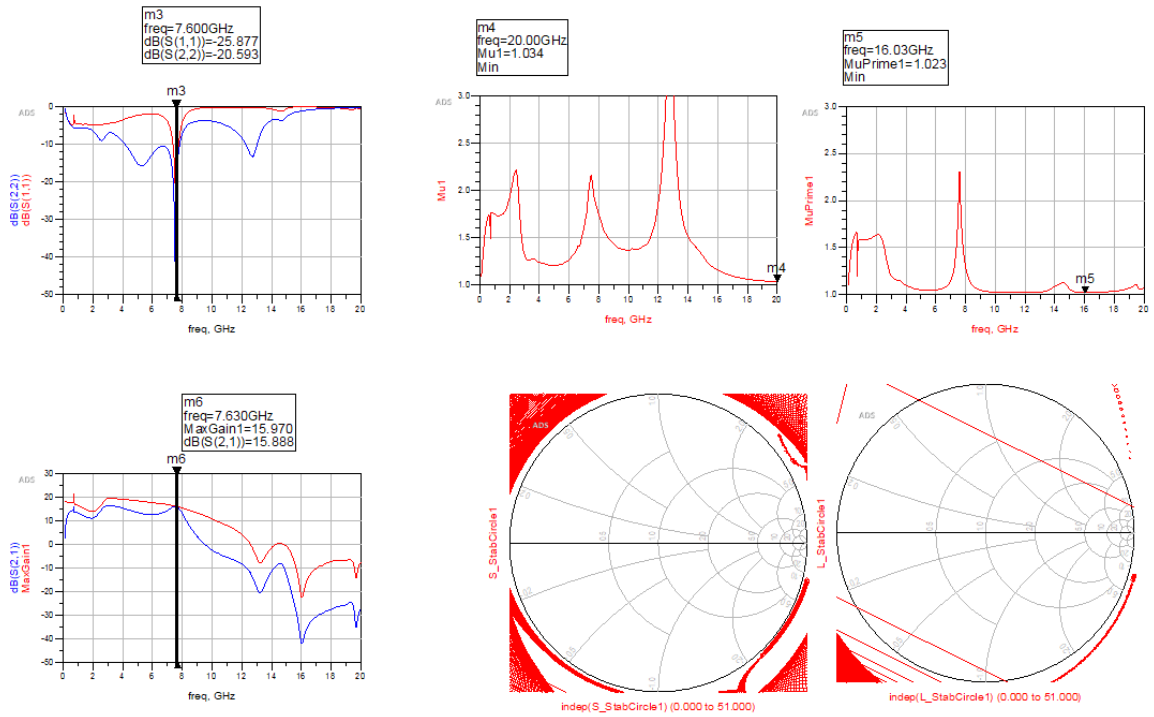

Figure 4.21: Ku band SiGe bipolar transistor Space Qualified simulation

4.3 Amplifier for Ka band

In the Ka band design, it is expected to have considerable changes in the transistor core since microstrip structures, as the Bias Tee, reduces its dimensions in large quantity.

Despite bias Tee dimensions have been reduced, this still does its functionality (Figure 4.22) and it can be easily added to transistor core. However, Ka band design cannot use the X band core since there is less space between Tees. As Figure 4.24 indicates, collector capacitance is located in a vertical position, resistors were redistributed and, some via holes for the transistor's emitter have been eliminated.

As Figure 4.25 indicates, both 50Ω resistors are still the key since the core is unconditionally stable just adding them in the right position. Additionally, it is a fact that the amplifier does not work properly for high frequencies. At first instance, it seems that the maximum available gain is 6.8 dB, which it is too much lower than X and Ku band specifications.
Finally, matching network needs to be designed to obtain this maximum gain.

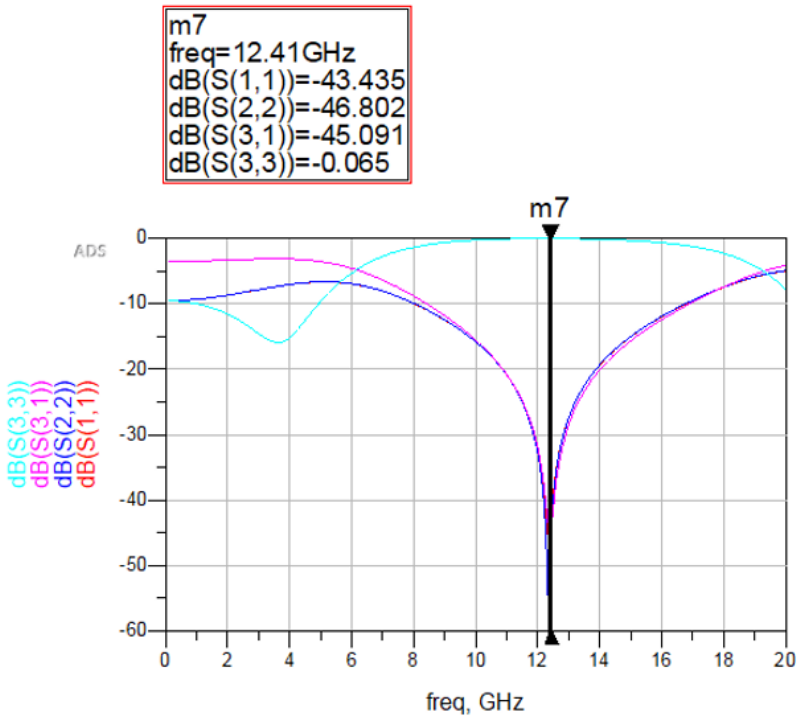

Figure 4.22: Bias Tee simulation for Ka band

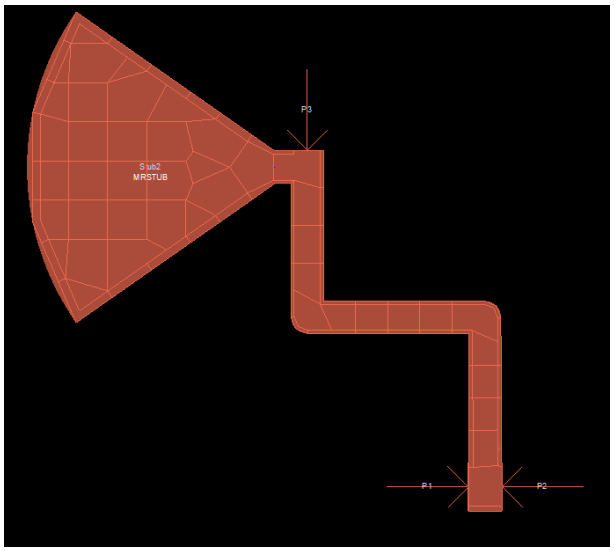

Figure 4.23: Bias Tee for Ka band

Once the matching network has been implemented, simulations for the active device at Ka band can be obtained.

In conclusion, from Figure 4.26 can be extracted that the transistor for Ka band has an extremely

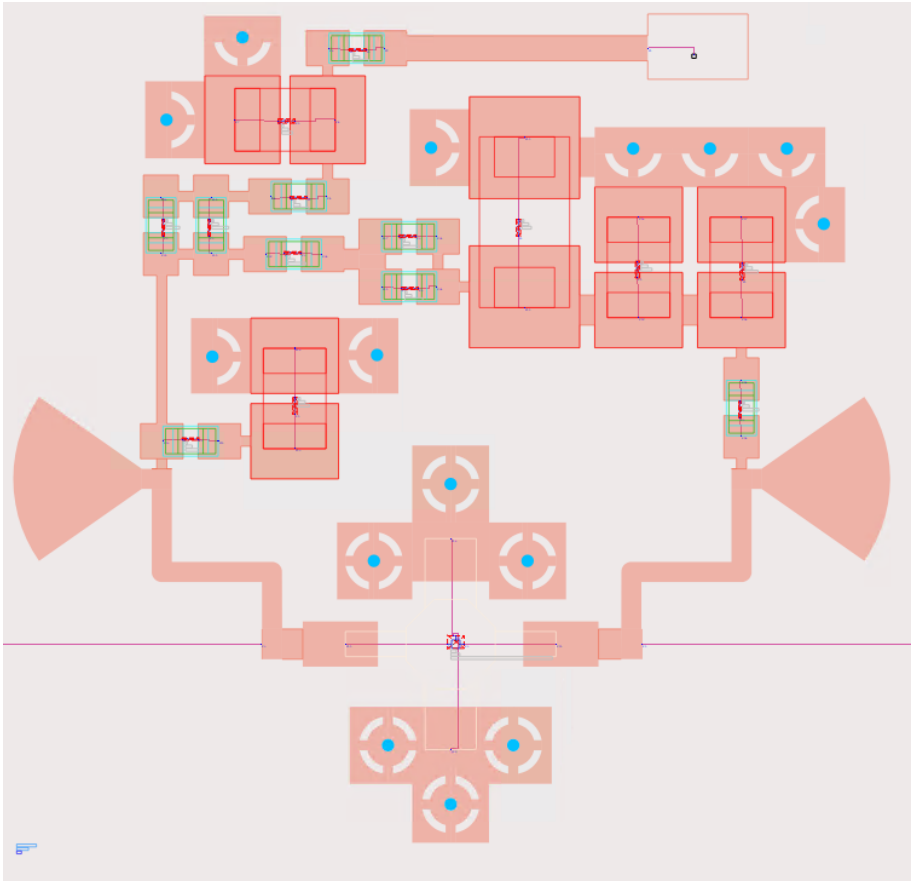

Figure 4.24: New transistor core for Ka band

low gain, thus, it could be a critical issue for the oscillator design. The obtained gain results to be 6.61 dB, therefore, a big effort needs to be done as it will be seen in next chapter.

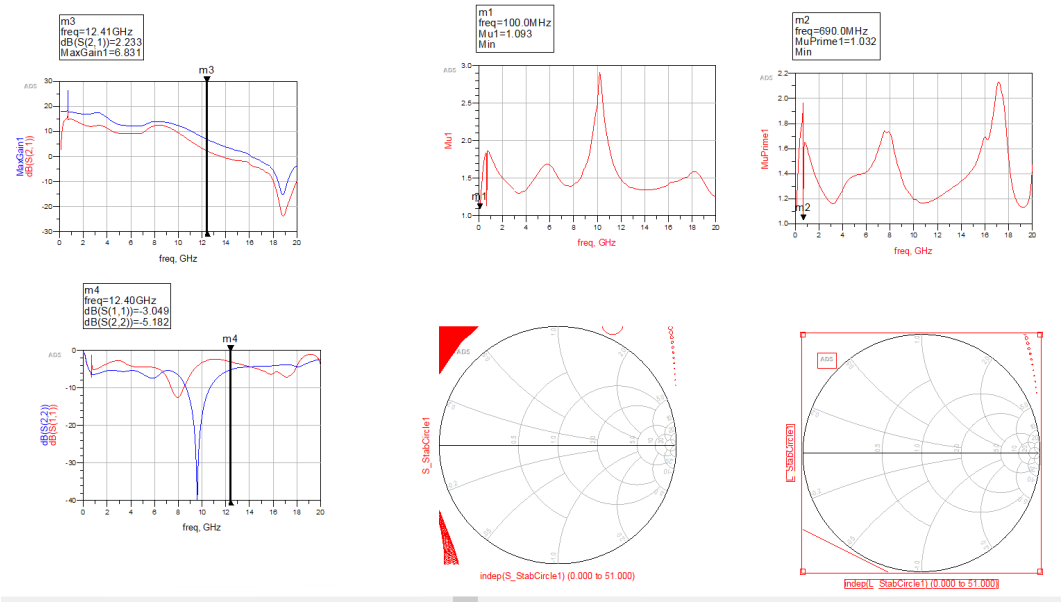

Figure 4.25: Amplifier's simulation before matching

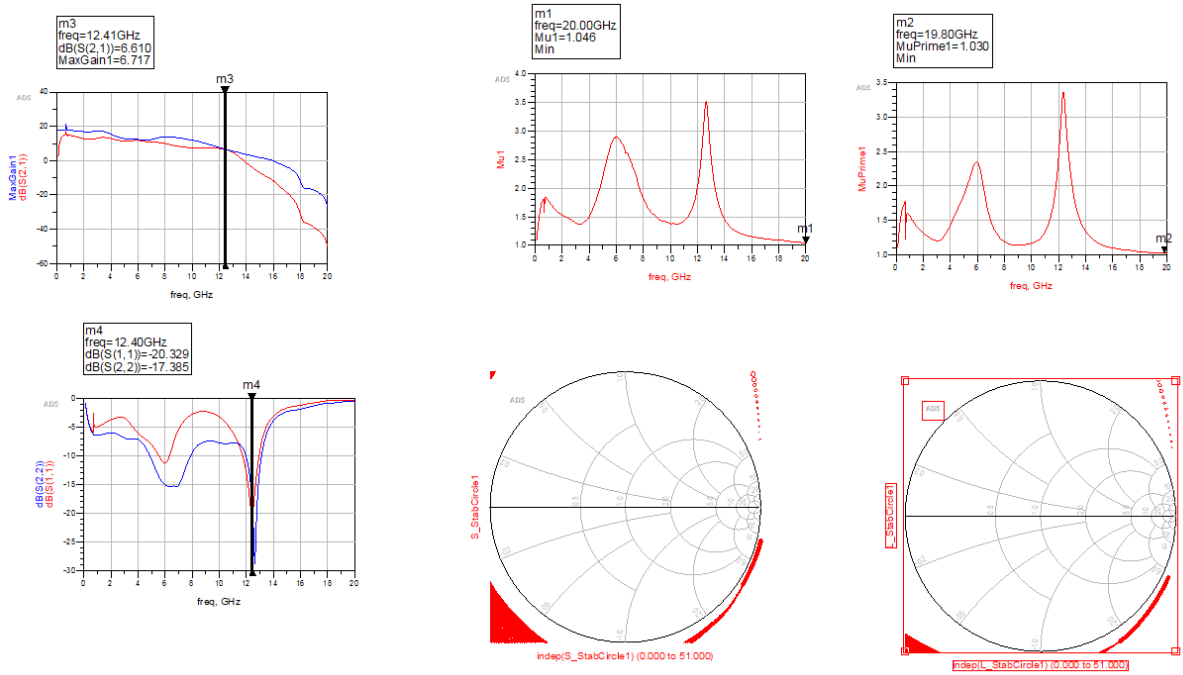

Figure 4.26: Amplifier for Ka band

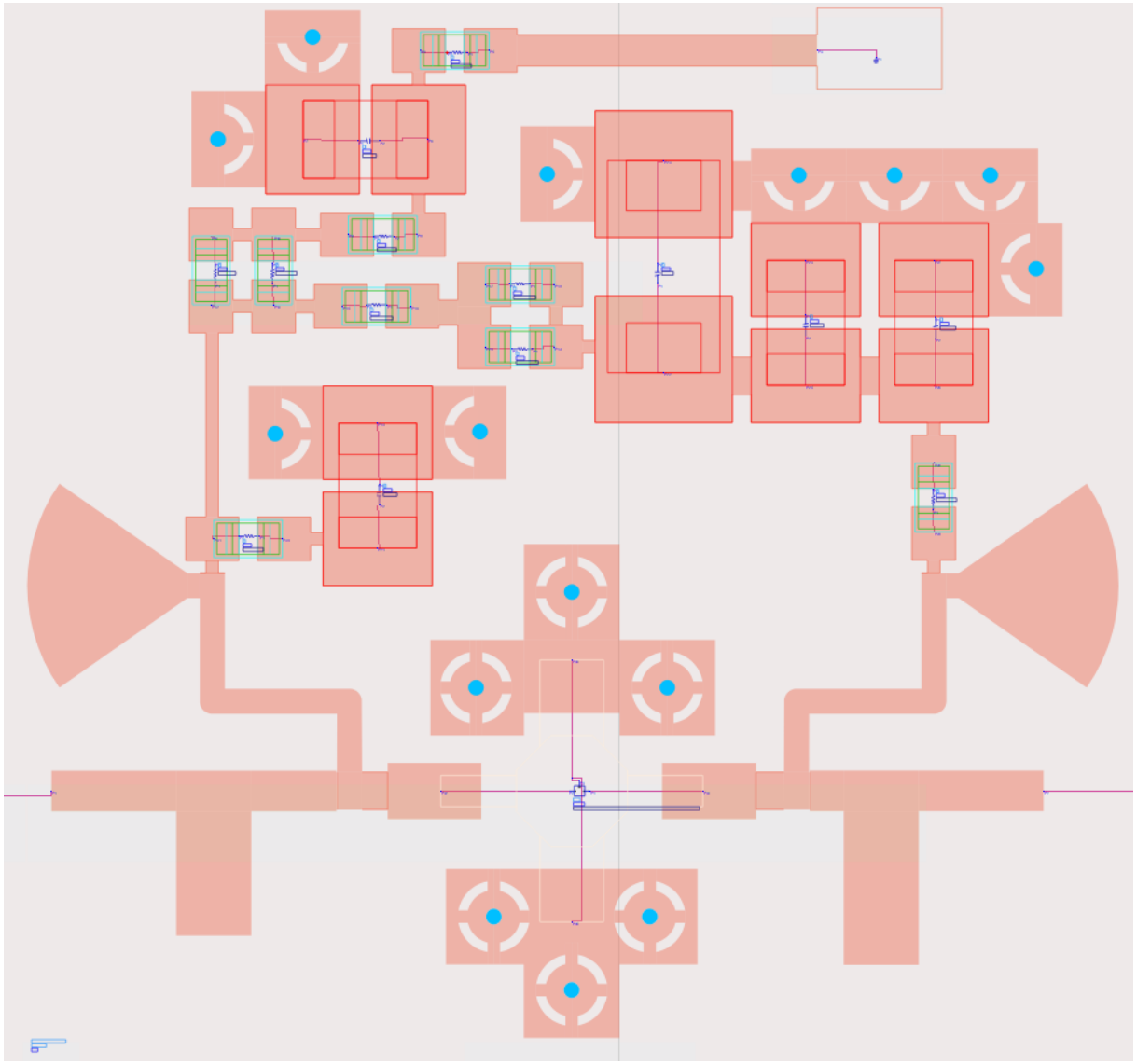

Figure 4.27: Transistor core for Ka band

Chapter 5

Simulation Results

Once the theoretical basis behind the oscillator has been explained, it is time to apply all the knowledge into closing the loop. As mentioned during the thesis, ADS and HFSS are the used software for designing. Specially, as ADS is a 2.5 dimension software, only the transistor core can be simulated. Resonator (plus tuning techniques) and phase pads will be designed using the Ansys software.
For this thesis, and before starting simulations, there is a set of initial assumptions that are needed:

- Designs are mounted over a 10 mils PCB of Duroid ($\epsilon_r = 2.94$)
- The feeding voltage at PCB has a value of 5V.

Therefore, as there are some components for designing, each of them needs to be analyzed separately, thus, this chapter is organized as follows:

1. Resonator: In this case, there are three different resonator designs, as each of them carry a different resonant frequency. Moreover, for each design, tuning techniques need to be applied.
2. Budget: It is essential for evaluating how the oscillator is working and if it accomplishes the defined specifications.

3. Passive device: Oscillator needs to be closed loop and it also needs to have an output for the next device. A passive structure as a Wilkinson or a Coupler could be a good choice.

5.1 Oscillator for Ku band (7.63 GHz)

The first band that is needed to be designed is the Ku band, at 7.63 GHz. At first instance, the Ku oscillator will not be a problem since the amplifier has a great gain for this band and the resonator dimensions are reasonable.

5.1.1 Puck simulations

Following the steps defined on Chapter 3, the first step to do is dimensioning the resonator height and diameter.

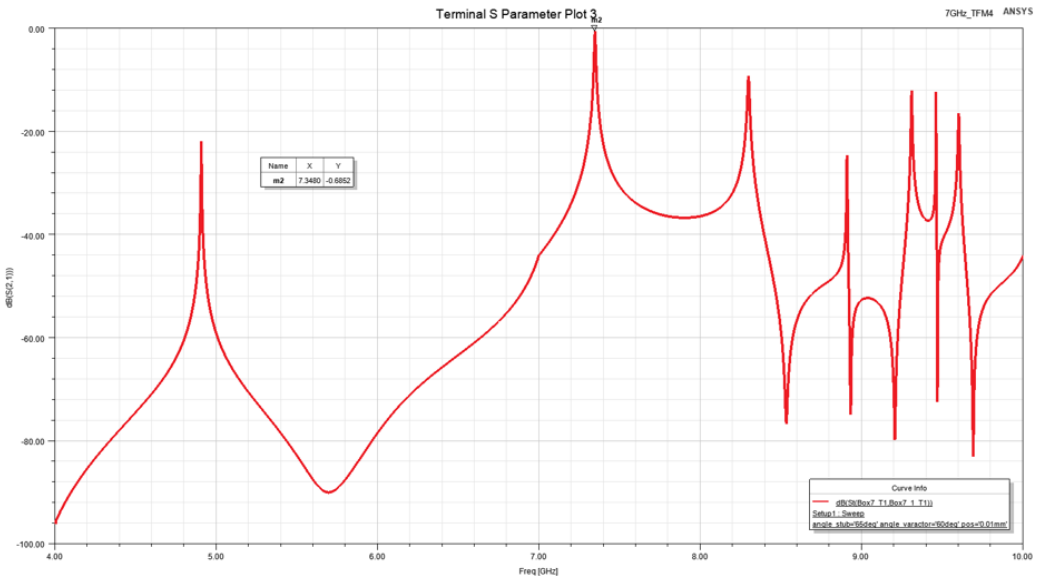

Figure 5.1: Early simulation

As Figure 5.1 shows, a first approximation has been obtained. In this case, puck has a diameter of 8.6 mm and 3.5 for height and, no tuning techniques have been applied. It can be checked that some modes are resonating due to the metallic cavity dimensions and properties. However, the most important result is obtained around 7.348 GHz, where places a -0.68 dB resonance

and, it could be a good beginning before shifting it.

Before continuing with simulations, it is important to appreciate in Figure 5.1 that the main resonance is located below the desired resonant frequency. If an above resonance is obtained, there are some troubles. In this case, puck should modify its own dimensions and, it is not the right path.

Once the dimensions are the definitive ones, it is time to look for some frequency shifting. Let's start with the metallic screw technique, which it provides a wider shifting, as previously explained. Here, the idea is to approximate a metallic disk until the desired frequency is the main resonance in oscillator.

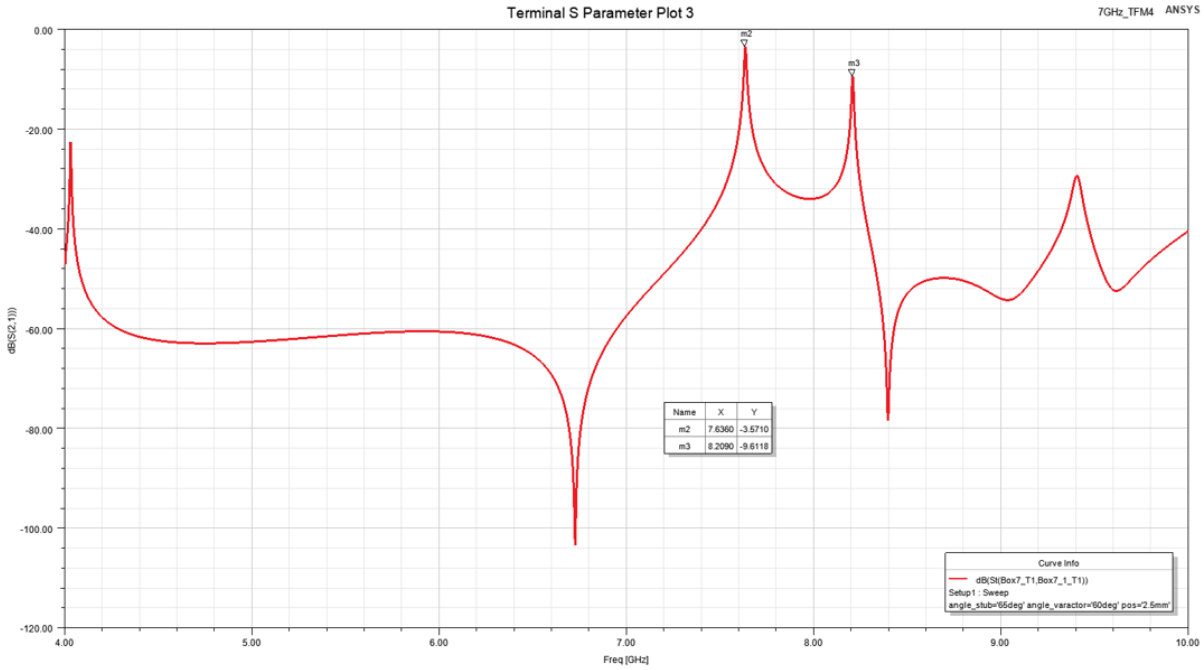

Figure 5.2: Puck simulation after metallic screw

The design rule for metallic screw is obtaining the desired frequency maintaining metallic screw at 1/3 of the gap between metallic cavity and resonator. As Figure 5.2 indicates, the new main resonance is located at 7.63 GHz (-3.57 dB) so, metallic screw becomes into a 300 MHz frequency shifting. Moreover, it can be checked that some cavity resonances have disappeared, not the 8.2 GHz (-9.61 dB). Cavity resonances could be a critical issue if the gap between both resonances is lower (below 500 MHz) but, in this case the cavity resonance will be easily eliminated by the active device.

Finally, an additional microstrip line is added between resonator and the output coupled line which achieves a finest tuning through a hyperabrupt varactor diode. As explained in Section 3.5.2, a shifting range around 5 MHz allows to exactly make it oscillate at the required frequency.

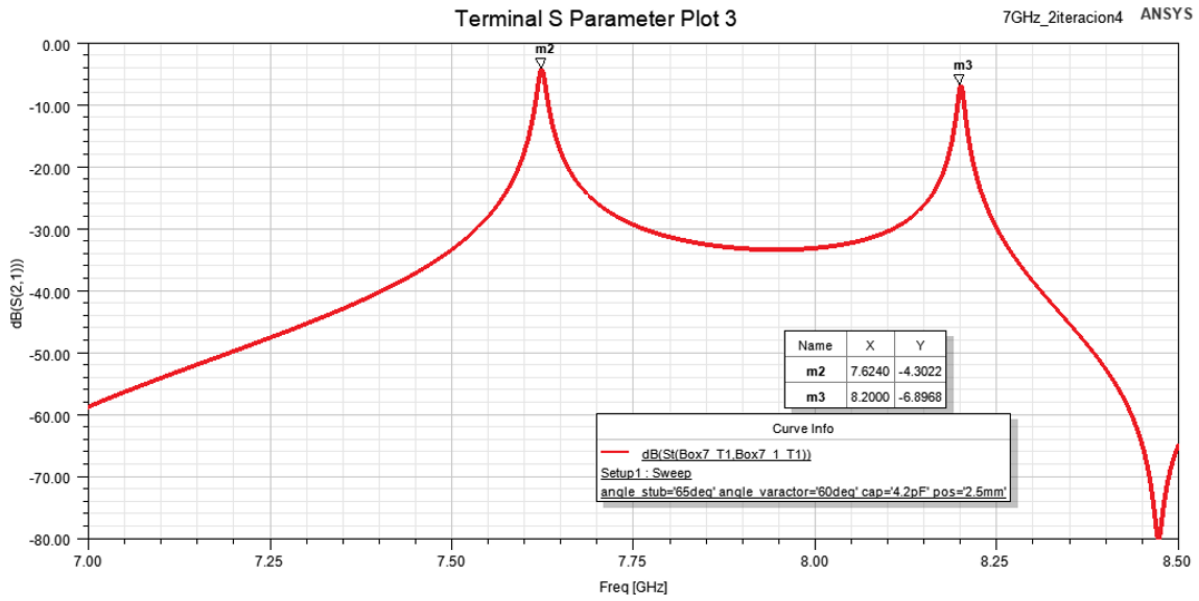

Figure 5.3: Puck simulation after varactor

In Figure 5.3, it can be checked the varactor's effect. In this case, frequency is slightly shifted down for a few of MHZ and losses increase around 1dB. Moreover, cavity's resonance still has a great impact but, it is far from main resonance.

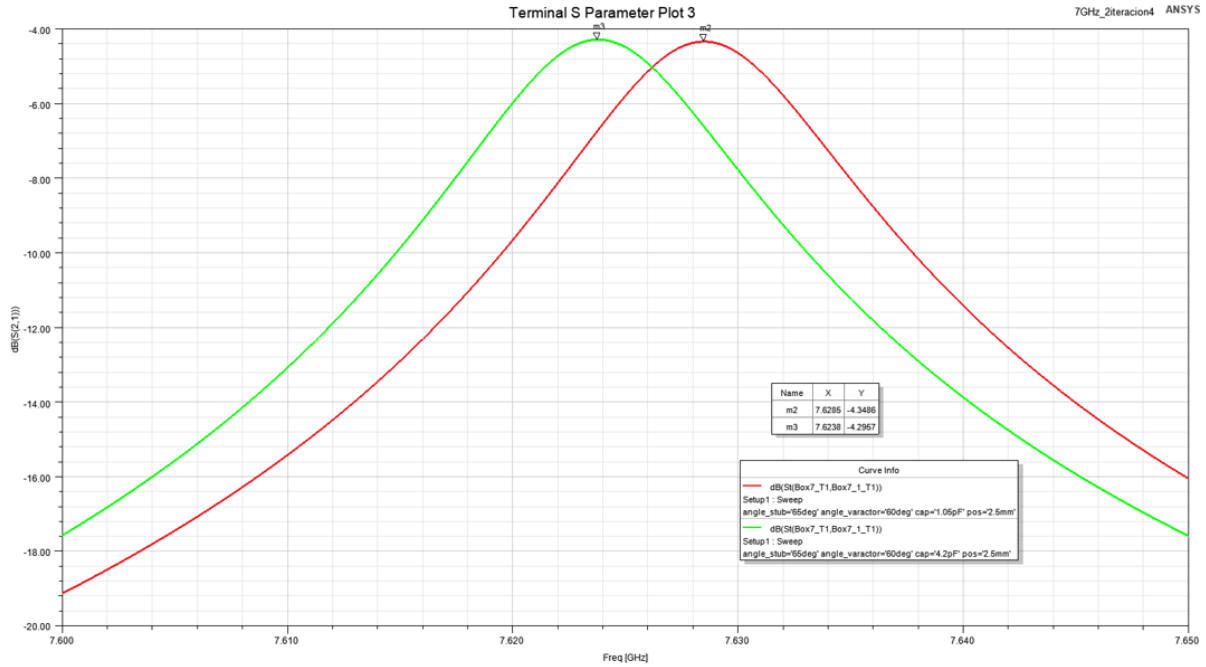

Figure 5.4: Fine tuning due to varactor

Finally, Figure 5.4 shows the frequency tuning due to varactor diode. In this case, green curve plots a 4.2 pF capacitance; otherwise, red line plots varactor capacitance feed by 5 V, 1.05 pF. As previously explained, a 5 MHz frequency tuning provides fine tuning.

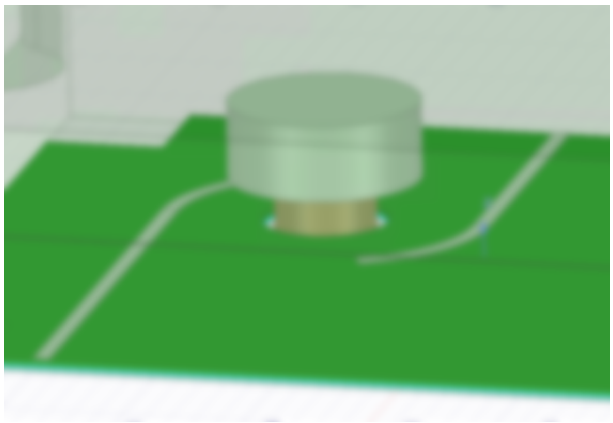

Figure 5.5: Early puck design

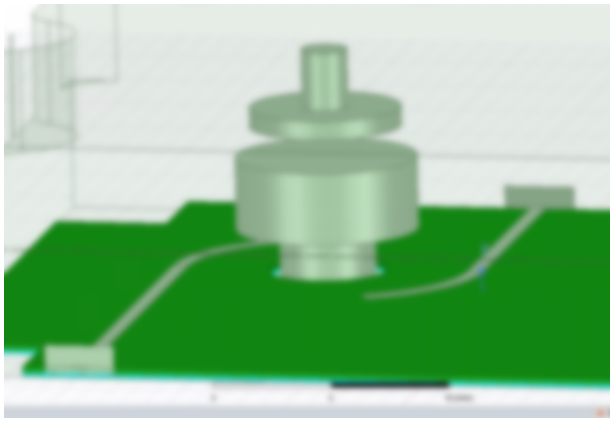

Figure 5.6: Puck plus metallic screw

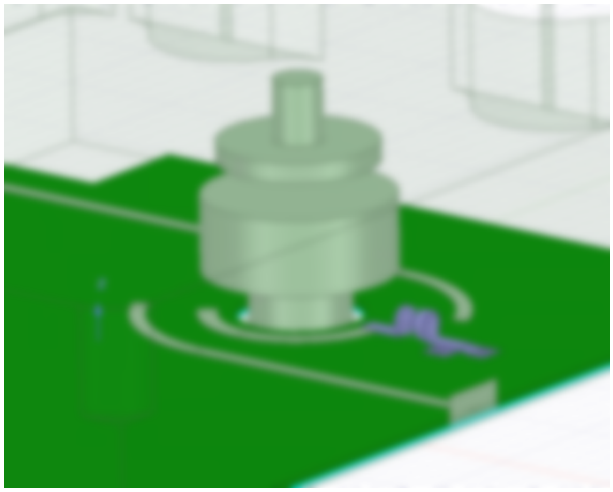

Figure 5.7: Puck plus varactor

5.1.2 System design

At that point, the use of a budget will help choosing which is the next step to do. Now, the Ku band oscillator contains a resonator for the desired frequency and active device matched for the same frequency as resonator. As a summary, the transistor for Ku band provides 15.8 dB of gain (Section 4.1) whereas the puck introduces a 4.3 dB loss.

As Figure 5.8 indicates, there is some microstrip path between the components which can be translated in ohmic losses (-0.7 dB). Finally, it is needed to design a passive element, such as a balanced Wilkinson (-3 dB) or a Coupler, for closing the oscillation loop and create an output for the next CIMR subsystem. Additionally, it can be checked that Figure 5.8 contains a 5.3 dB

	DRO Ku band (7,63 GHz)					
	Puck	Ohmic losses	Ampli	Ohmic losses	Hybrid	Att
					Wilkinson	Pi Attenuator
Gain (dB)	-4,3	-0,35	15,8	-0,35	-3	-5,3
					Loop Gain:	7,8

Figure 5.8: Budget before passive device

Pi Attenuator. The attenuator results from defining a 2.5 dB loop excess gain in linear region as a specification for the design. Thus, as the transistor provides a large quantity of gain, the design avoid a gain excess just locating a 5.3 dB attenuator before the active device.

As mentioned, for the 7.63 GHz oscillator, a balanced Wilkinson will be in charge of closing the main oscillation loop. It allows to divide oscillator's power equally and provides loss for the oscillator main loop.

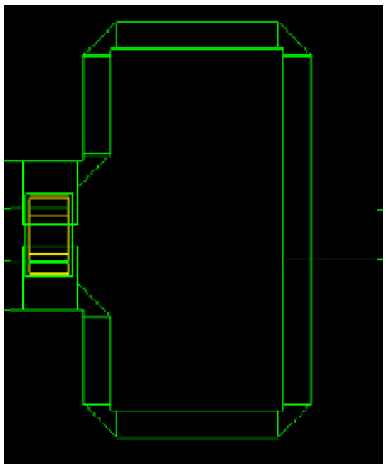

Figure 5.9: Balanced Wilkinson for Ku band

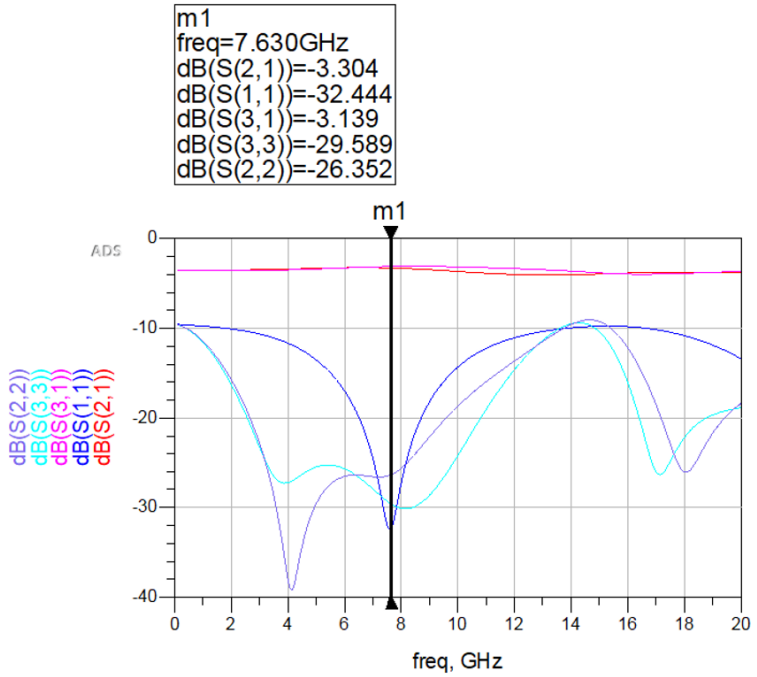

Figure 5.10: Wilkinson simulation

The Wilkinson proposed on Figure 5.9 follows the typical balanced Wilkinson structure. Moreover, simulation (Figure 5.10) indicates that it works properly. All three ports are well matched (around -30 dB) and there is a clear power division between ports 2 and 3.

Finally, budget needs to be updated with the Wilkinson's loss value. The final budget is the following one:

	DRO Ku band (7,63 GHz)					
	Puck	**Ohmic losses**	**Ampli**	**Ohmic losses**	**Hybrid**	**Att**
					Wilkinson	Pi Attenuator
Gain (dB)	-4,3	-0,35	15,8	-0,35	-3,13	**-5,17**
					Loop Gain:	7,67

Figure 5.11: Final oscillator budget

In conclusion, the final budget has a loop gain of 7.67 dB, much higher than the aim of 2.5dB so, a 5.17 dB Pi attenuator will be placed before the transistor. Therefore, at first instance the budget indicates that oscillating condition will be easily obtained for Ku band.

Finally, it is good mentioning that some additional parts have been added to final design for preventing and ensuring that the desired resonance is the one that resonates.

Figure 5.12: Ku band Oscillator Layout

1. Varactor also needs to be protected from DC spurious. As explained for amplifier, just after the DC input, a RC needs to be placed for filtering the DC flow. Moreover, it is followed by a bias Tee, which prevents RF flow to influence the DC input. Finally, just before the varactor's coupled line, a low value resistor is located to avoid diode's saturation.

2. As explained in budget, it is desired locating a Pi Attenuator just before the amplifier for accomplishing the 2.5 dB loop gain.

3. As explained in Section 2.2.3, oscillator also needs to achieve the phase criterion. For this reason, some additional pads are added around the oscillator loop to provide an extra

phase shifting.

4. An additional Pi Attenuator is located at the oscillator's output port for controlling the quantity of power that oscillator delivers for the next CIMR subsystem.

5.2 Oscillator for X band (8.63 GHz)

As Ku band oscillator, the X band oscillator (8.63 GHz) should be an straightforward design. In fact, Ku and X bands are only separated by a 1 GHz frequency gap, thus, designs will look very similar. Resonator will be practically the same since tuning techniques, as metallic screw, allows a 500 MHz frequency shifting. In addition, the transistor gain specifications are still good for not to worry about, just one or two dBs of difference in comparison to Ku band active device.

5.2.1 Puck simulations

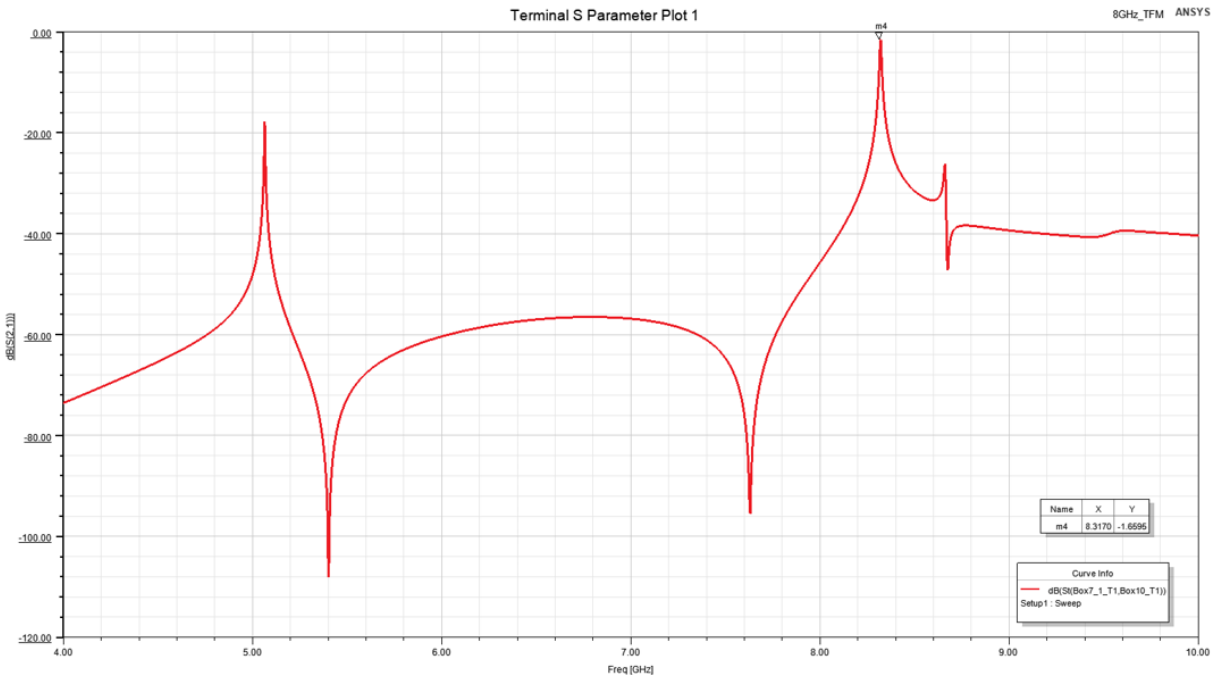

Figure 5.13: Early simulation

In this case, X band resonator is defined by 7.3 mm diameter and 3.25 mm for height. As mentioned above, Ku and X band resonator almost have the same dimensions but, as explained in Section 3.4, there is a clear trend to minimization as resonant frequency increases.

Attending to Figure 5.13, resonant frequency is located at 8.31 GHz (-1.65 dB), which it is a good starting point before applying any of the frequency tuning techniques. However, in this case, a resonance due to metallic cavity is located near the desired frequency, at 8.7 GHz. It is mandatory to eliminate it or just shifting it to maintain a wide frequency margin with respect to the main resonance.

Now, that the final puck dimensions are defined, it is time to apply the metallic screw tuning to reach the desired frequency with the main resonance.

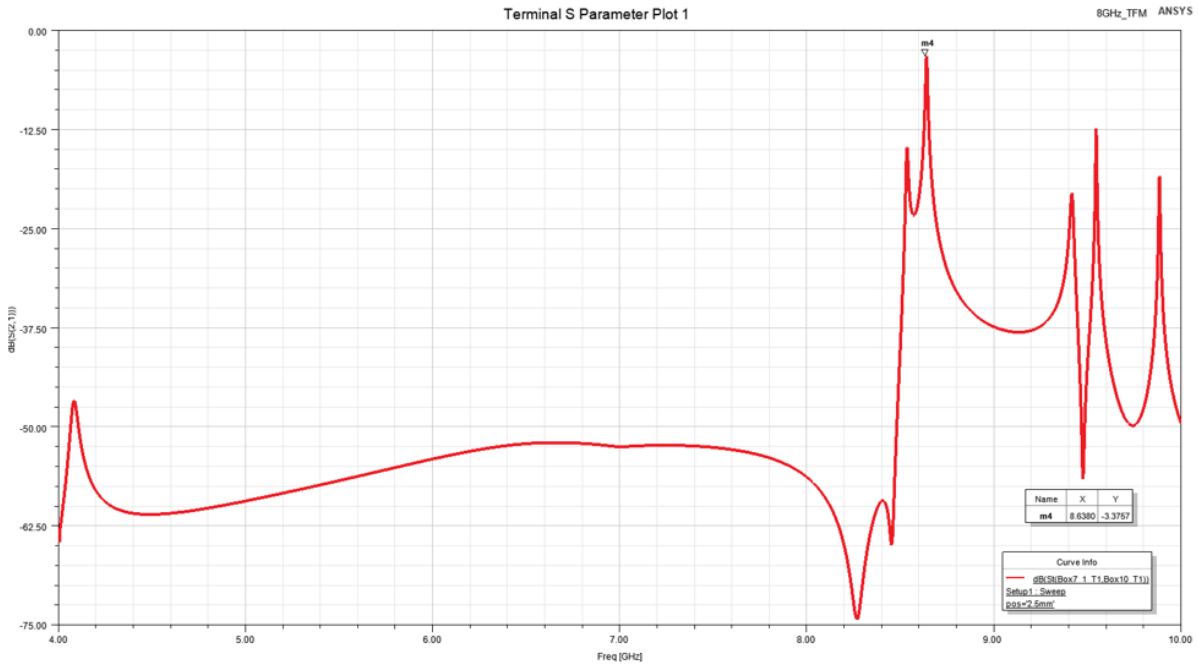

Figure 5.14: Puck simulation after metallic screw

Following the 1/3 rule for metallic screw, the desired resonant frequency was achieved. As Figure 5.14 indicates, main resonance is located at 8.63 GHz (-3.37 dB), which it is exactly the desired frequency for the design. However, cavity resonance still is in a critical frequency. The cavity resonance could become into a shifting of the resonant frequency.

Adding the varactor does not provides significant changes in the scenario. Varactor simulation (Figure 5.15) does not modify the cavity resonance near resonator, or modifies the rest of cavity

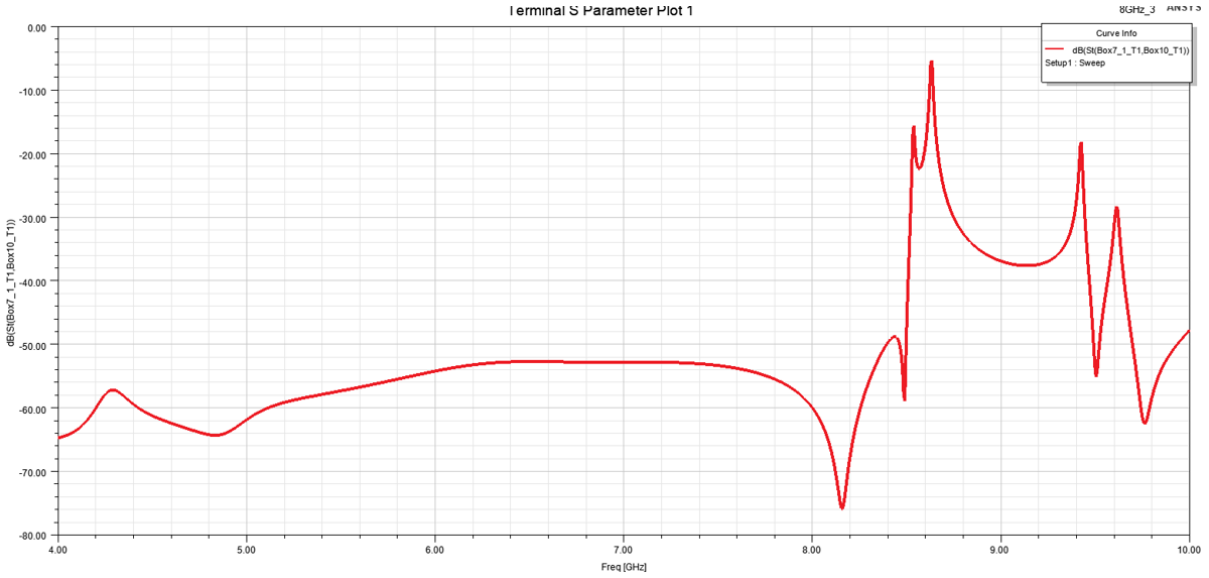

Figure 5.15: Puck simulation after varactor

resonances. However, varactor accomplishes the behavior which was selected for (Figure 5.16).

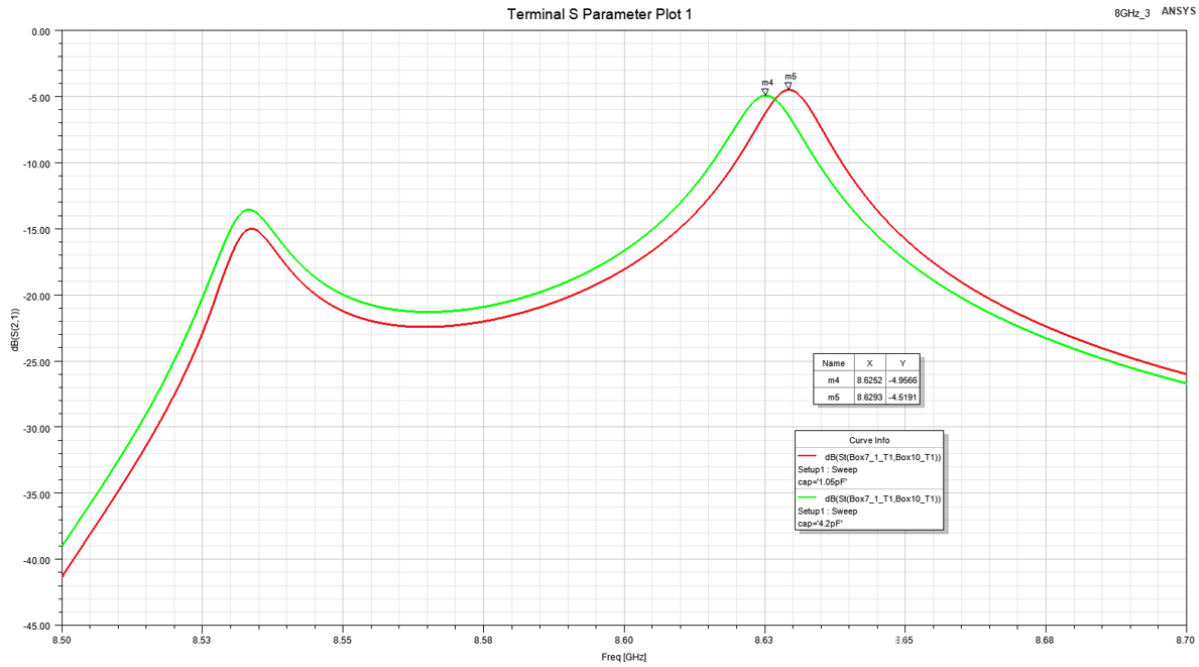

Figure 5.16: Varactor fine tuning

As desired, varactor provides a 4 MHz frequency tuning. Red curve on Figure 5.16 indicates the frequency response when varactor is being feed by 5V. In this case, the main resonance is located at 8.629 GHz with 4.51 dB of loss. Below that, at 8.625 GHz, the 0V varactor provides a resonance with 4.9 dB of loss.

Finally, as mentioned during X band resonator design, there is a metallic cavity resonance that could turn into a problematic issue. The solution here is locating a metallic pillar to modify the cavity volume, thus, only cavity resonance will be shifted.

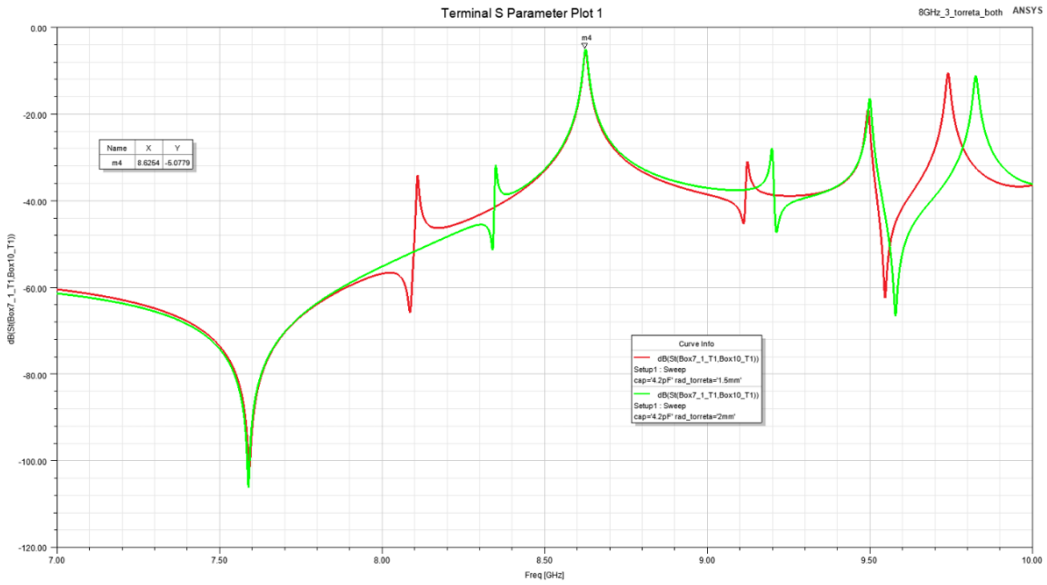

Figure 5.17: Metallic pilar tuning

As indicated in Figure 5.17, cavity resonances are now far from puck's resonance. In fact, there is correlation between pillar diameter and the frequency shifting. Red curve plots a 3 mm diameter pillar, whereas green curve indicates the frequency response for a 4 mm diameter pillar. Finally, due to mechanical reasons, a 4mm diameter pillar will be in the middle of the cavity, as Figure 5.18 shows.

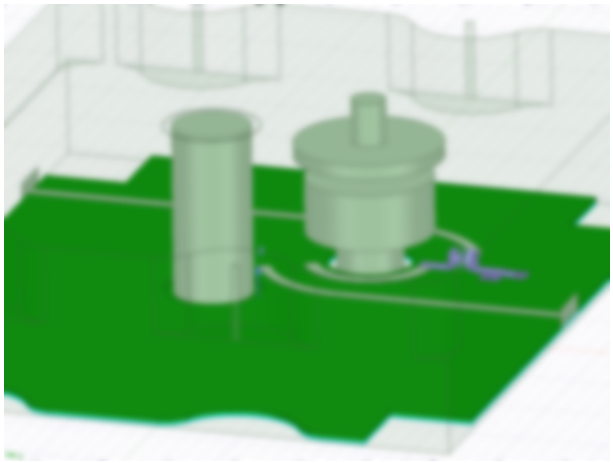

Figure 5.18: HFSS simulation view

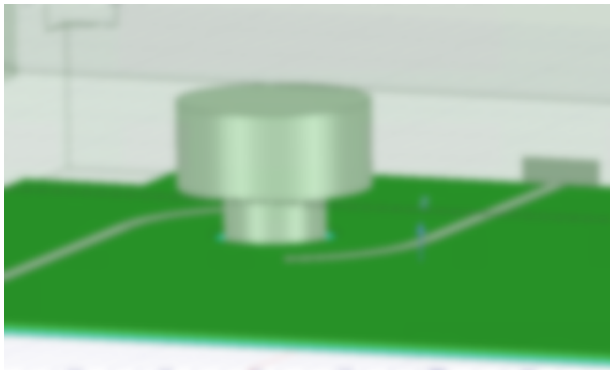

Figure 5.19: Early puck design

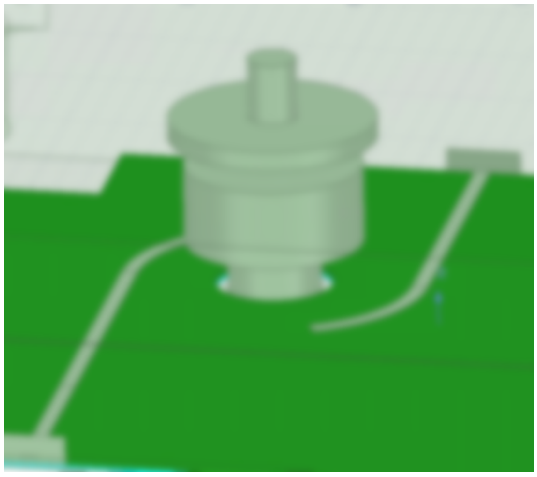

Figure 5.20: Puck plus metallic screw

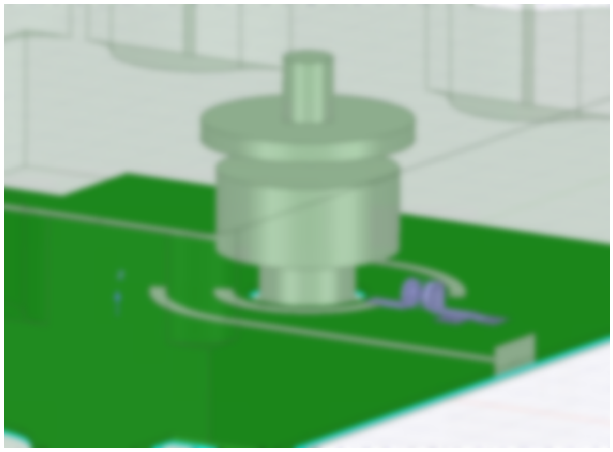

Figure 5.21: Puck plus varactor

5.2.2 System Design

At this point, oscillator for X band contains a puck with 5 dB of loss and a transistor core with 14.3 dB of gain. At first instance, and knowing the similarities with Ku oscillator, the X band oscillator can easily resonates at the desired frequency.

	DRO X band (8,63 GHz)					
	Puck	Ohmic losses	Ampli	Ohmic losses	Hybrid	Att
			BFY740		Wilkinson	Pi Attenuator
Gain (dB)	-5	-0,38	14,3	-0,38	-3	3,04

Figure 5.22: X band budget before passive device

From Figure 5.22, it can be observed that the transistor can easily cover all the losses coming from resonator and microstrip lines (0.76 dB of loss). As Ku band design, Balanced Wilkinson is the proposed choice to close the oscillation loop.

Finally, as Wilkinson simulation indicates (Figure 5.23), Wilkinson provides a 3 dB loss for the oscillation port, thus, loop budget from Figure 5.22 perfectly summarizes the X band oscillator design. Moreover, as indicated in the budget, a 3dB attenuator needs to be located just before the active device for achieving the 2.5dB gain excess in linear region criterion.
As summary, apart from puck dimensioning, tuning position, the main differences between Ku and X band oscillators are the microstrip structures as bias Tee, Wilkinson and phase pads, the SiGe bipolar transistor matching network and the cavity pilar.

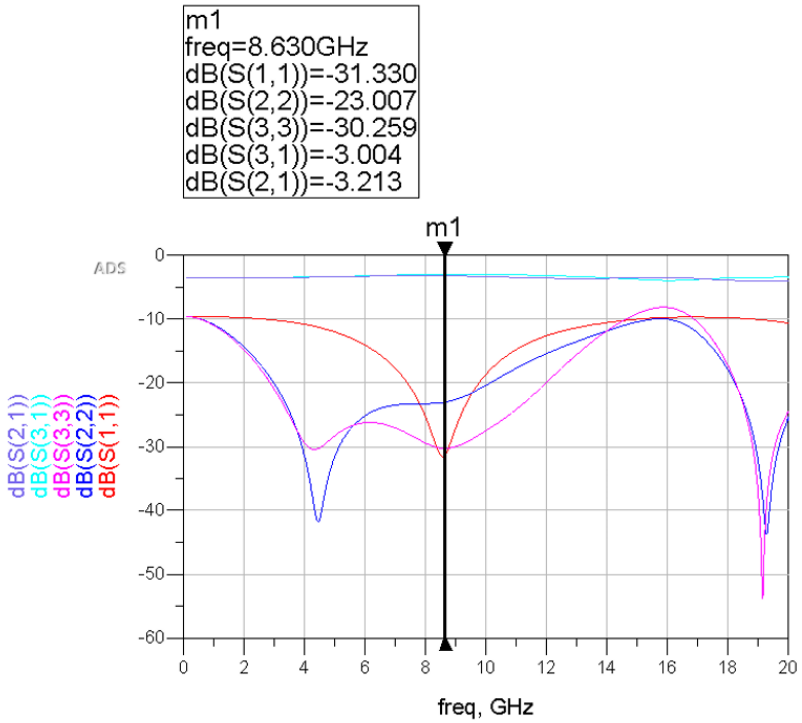

Figure 5.23: Balanced Wilkinson for X band

As Figure 5.24 indicates, oscillator for X band is similar to the Ku band. Distribution of the elements and its connections look alike.

5.3 Oscillator for Ka band (12.41 GHz)

The Ka band oscillator is the most difficult design so far. Basically, as it is desired the same puck material, resonator will be minimized in a considerable scale, thus, resonator will be more responsive with minimum changes in cavity and some non-desired resonances will be coupled. Moreover, as the amplifier has more gain for low frequencies, cavity resonances could become into the oscillator's main frequency.

Figure 5.24: X band Oscillator Layout

5.3.1 Puck simulations

Comparing Ka band resonator with X/Ku band resonators, the 12.41 GHz resonator is the smallest one. As explained in Chapter 3, the resonant frequency increases as puck dimensions becomes smaller.

In this case, puck's dimensions are 4.6 mm for diameter and 2.55 mm for height. As recently mentioned, Ka band resonator is around a 40% smaller than X band puck. However, resonator accomplishes the desired resonant frequency as Figure 5.25 indicates. It can be checked that main resonance is located 12.185 GHz, just a bit below from the aimed frequency, and it has an acceptable loss, 0.35 dB. In this case, design is looking for low loss since the transistor characteristics are not favorable for the higher frequencies. Additionally, the cavity resonance appears once again at 9 GHz. Ka oscillator needs to specially focus on this cavity resonance since active device will provide a much higher gain on it in comparison to Ka band frequency.

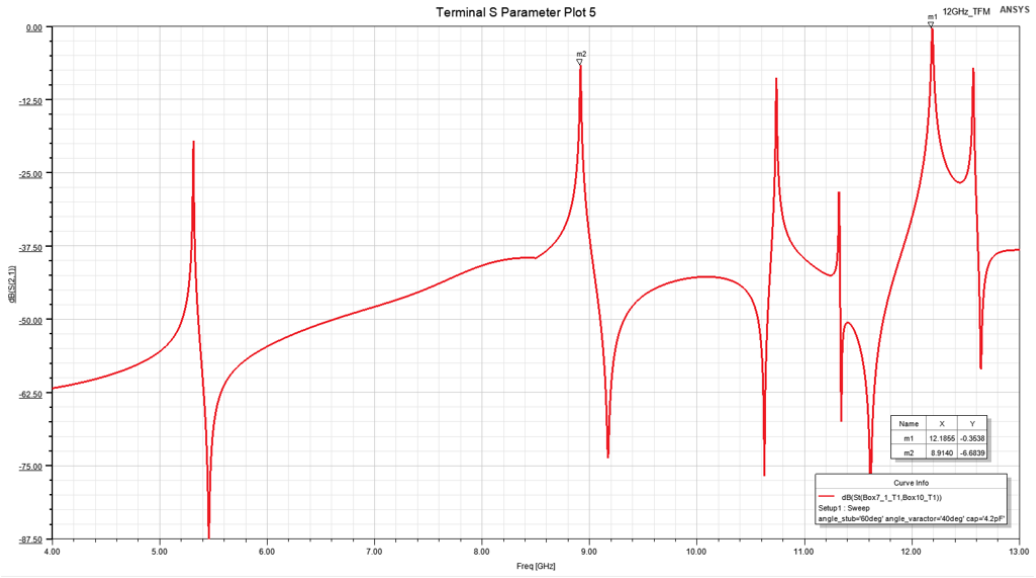

Figure 5.25: Early simulation

At this point, let's apply the metallic screw technique for bringing the resonator's resonance up to the required frequency (12.41 GHz).

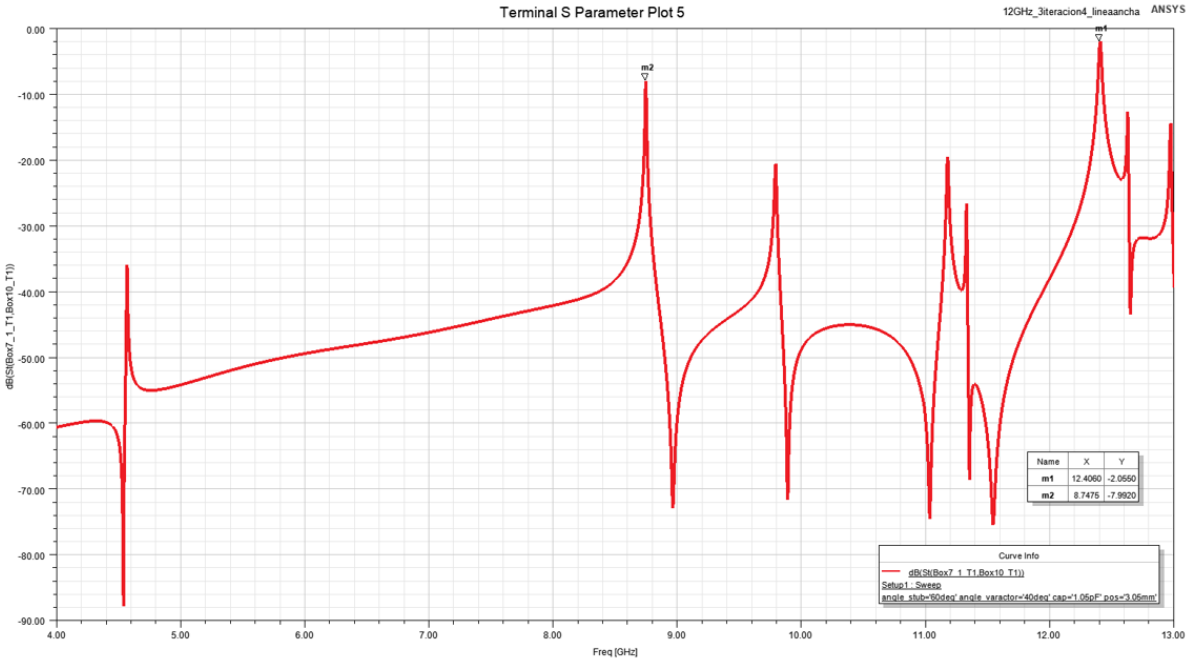

Figure 5.26: Puck simulation after metallic screw

Following the same metallic screw rule as the rest of resonators, the resonant frequency achieves 12.41 GHz with 2.05 dB due to coupling losses (Figure 5.26). The low losses level provides a

wider margin for designing the rest of the oscillator loop, which it is always good news. Now, the varactor diode will be coupled to obtain a finest frequency tuning.

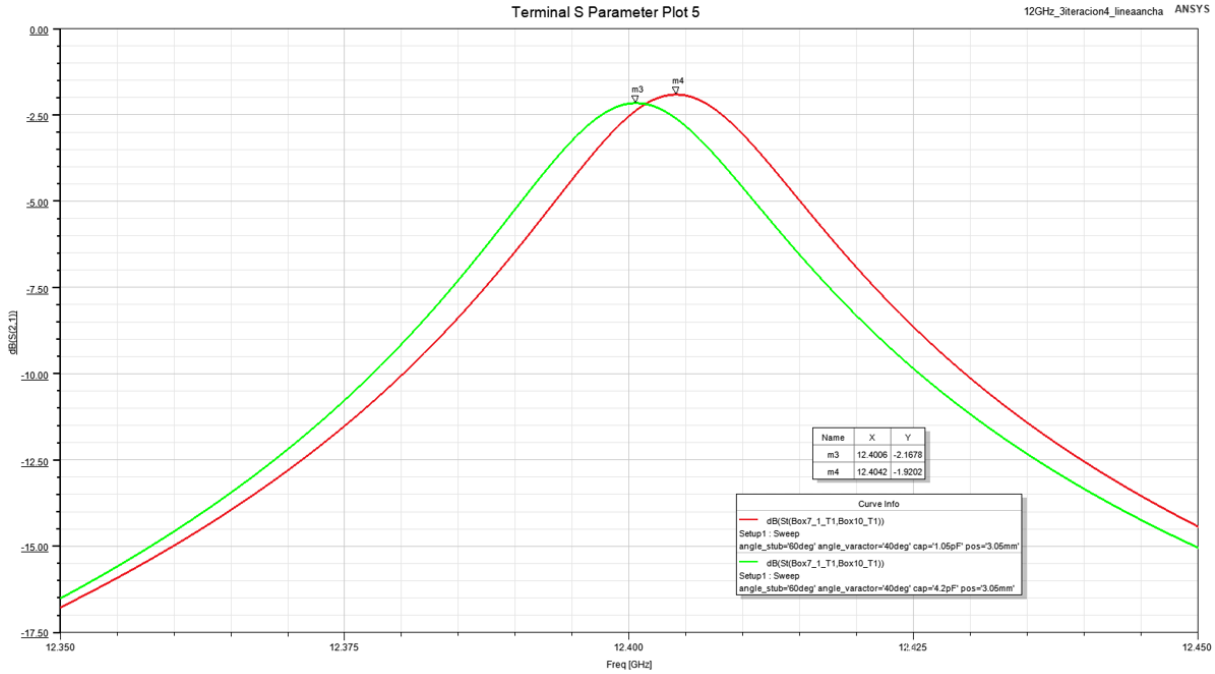

Figure 5.27: Puck simulation after varactor

As indicated in Figure 5.27, active device provides 4 MHz for frequency tuning. Moreover, coupling losses were not modified so, it is a good result for that tuning.

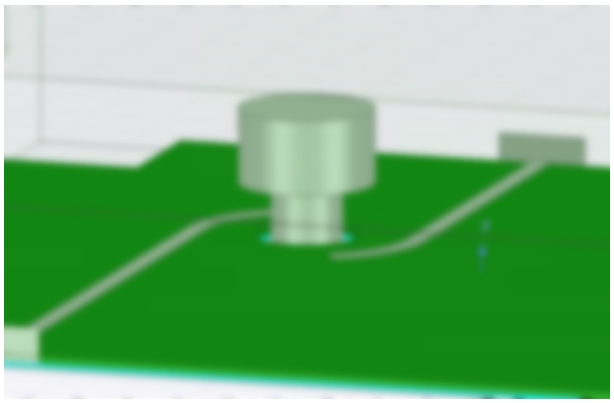

Figure 5.28: Early puck design

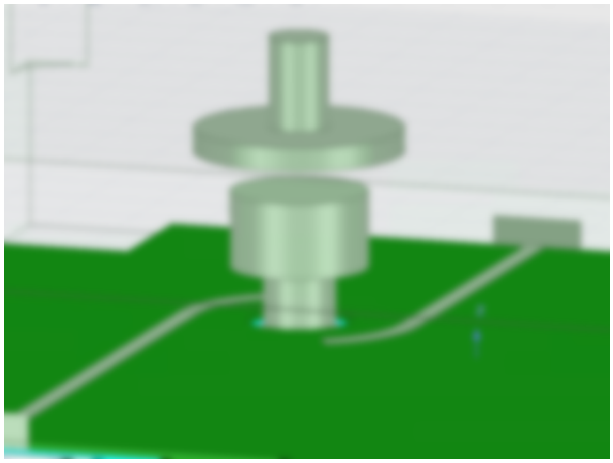

Figure 5.29: Puck plus metallic screw

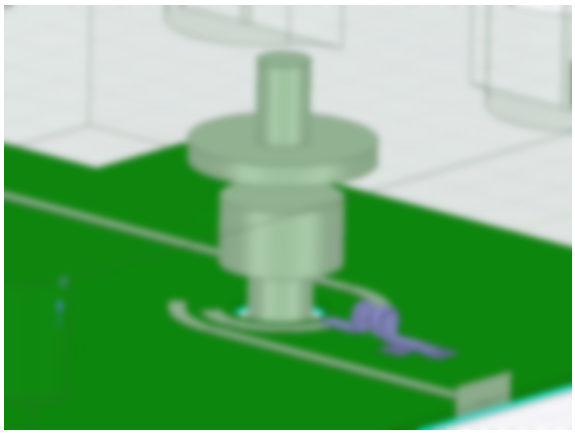

Figure 5.30: Puck plus varactor

5.3.2 System Design

At this point, oscillator for Ka band contains a puck with 2.2 dB of loss and a transistor core with 6.6 dB of gain. At first instance, it seems that by adding a balanced Wilkinson the 2.5 dB gain criterion for the oscillator will not be accomplished. Thus, other passive structure needs to be located to close the oscillation loop and providing and output port.

As indicated in Figure 5.31, Ka band design currently has a 3.73 dB loop gain. In that case, and as mentioned above, a balanced Wilkinson can not be used since the desired final behavior was defined around 2.5 dB for the excess loop gain. Thus, it is known that the typical microstrip coupler reduces its losses in big scale.

	DRO Ka band (12.41 GHz)					
	Puck	Ohmic losses	Ampli	Ohmic losses	Hybrid	Att
					Coupler	Pi Attenuator
Gain (dB)	-2,2	-0,335	6,6	-0,335	-0,587	-0,643
					Loop Gain:	3,143

Figure 5.31: Ka band budget before passive device

For Ka band oscillator, the desired device is a 13 dB coupler which provides the desired output signal and closes the loop. The next subsytem will need to cope with less received power due to the coupler's presence.

Figure 5.32: 13 dB Coupler for Ka band

As mentioned, the coupler follows the typical coupled lines configuration, where the upper line refers to the direct path. In this case, Figure 5.32 left port will be connected to active's device output and the other to resonator's input, thus, closing the oscillation loop. Below this line, there is a coupled port, which provides an input for the next subsystem in the CIMR chain and, an isolated port connected to a 50Ω resistor.

As Figure 5.33 presents, simulation looks very attractive since all ports are well matched to main RF line and, the obtained coupling (S(2,1)) is 13.3 dB, which it is valid for this frequency band. Moreover, it looks that loss in oscillator loop has been reduced since coupler's direct path loss is 0.463 dB (S(3,1)), far from 3 dB of loss introduced by a balanced Wilkinson.

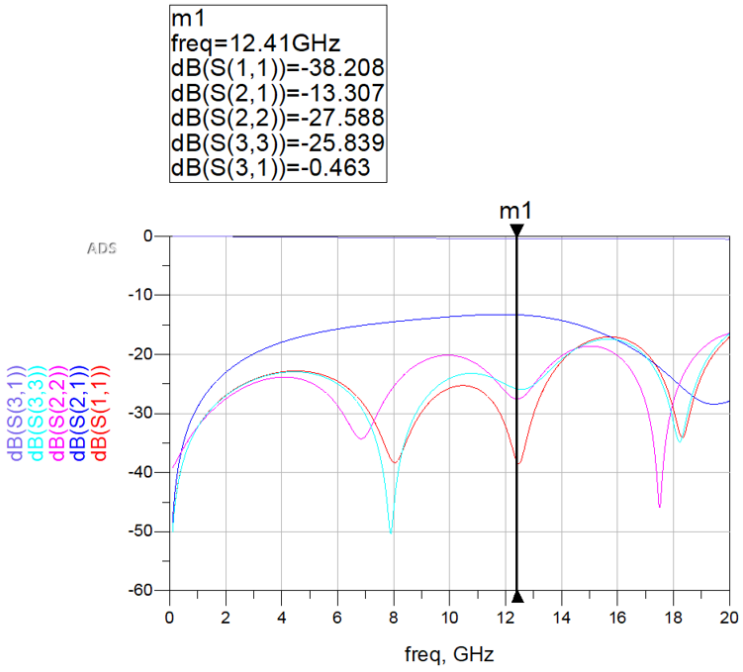

Figure 5.33: Coupler simulation for Ka band

	DRO Ka band (12.41 GHz)					
	Puck	Ohmic losses	Ampli	Ohmic losses	Hybrid	Att
					Coupler	Pi Attenuator
Gain (dB)	-2,2	-0,335	6,6	-0,335	-0,587	-0,643
					Loop Gain:	3,143

Figure 5.34: Budget for Ka band oscillator

Finally, Ka band oscillator obtains 3.26 dB for loop gain, which it is over the 2.5 dB of gain defined as objective. However, it has no sense placing a 0.7 dB attenuator since extremely low value resistor will be needed (Figure 5.34). Thus, Ka band oscillator will not have any Pi attenuator.

As a summary, final Ka band layout follows the same distribution as the other oscillators. However, Ka layout also has its own characteristics as the coupler or the new set of phase pads.

Figure 5.35: Ka band oscillator layout

Chapter 6

Conclusion

6.1 Summary of the work

As mentioned in the introduction, Chapter 2 shows that negative resistor method is a fundamental for the oscillator design. Resonator is the key device since it is the one who selects the resonant frequency. On the other hand, the active device allows the accomplishment of the Barkhausen criterion.

As the resonator is the most critical device, Chapter 3 summarizes a set of design rules. As mentioned, the resonator dimensioning is extremely important since it is difficult modifying its dimensions, the resonators tend to be custom pieces and the lead time is around a four months. As solution, the resonator is designed for a lower resonant frequency and, some tuning techniques are externally applied. The metallic screw technique provides a wide range of frequency shifting (around 500 MHz), while the varactor diode technique provides the final adjust, being a frequency shifting of 5 MHz.

In Chapter 4, the full procedure for designing an active device core is explained. Once the active device has been selected, it is mandatory to follow a set of rules for correctly feeding the device. In this thesis, the biasing network follows the collector feedback configuration since it is the most stable in temperature. Moreover, the generic core for all three design was indicated and it provides a good stabilization and matching.

Finally, simulations can be checked in Chapter 5. For the Ku and X band designs, the proce-

dure was straightforward and the results look very promissing. On the other hand, the Ka band oscillator contains some variations to compensate the worse frequency response of the selected active device.

6.2 Future work

As mentioned, the simulations look very promissing and, the next step is to check if these simulations are similar to the real measurements. Therefore, the future work is to firstly receive all the material for all three prototypes.

Firstly, it would be good to check if the oscillator's dimensions are the correct to obtain the desired resonant frequency or they need some corrections. As mentioned in this thesis, the oscillators have been designed always for a lower resonant frequency since metallic screw provides a certain margin of correction. However, if the resonator results to be over the resonant frequency, some supplier iterations would be needed. The supplier iterations could cause serious issues in terms of project schedule.

In case of approving the resonators response, it could be interesting to correlate the tuning provided by shifting techniques between the HFSS simulations and the real measurement. The metallic screw tuning seems to be reasonable, on the other hand, as HFSS does not simulate active devices, it could be interesting to check if the provided varactor model is valid. As mentioned in this thesis, the suppliers do not provide enough information about these devices.

Finally, it is also important to check if the phase pads were well-designed. As mentioned in this thesis, the Barkhausen's phase criterion is also critical to obtain the resonant scenario so, it is also desired to correlate the simulations with the real measures.

In conclusion, it is desired to check if the oscillators are well-integrated and the system's performance accomplishes the expected performance.

Bibliography

[1] "Stability and frequency compensation, howpublished = https://www.slideserve.com/seoras/stability-and-frequency-compensation, journal = Slideserve."

[2] D. M. Pozar, *Microwave engineering / David M. Pozar.* 2017.

[3] L. Kilic, C. Prigent, F. Aires, J. Boutin, G. Heygster, R. T. Tonboe, H. Roquet, C. Jimenez, and C. Donlon, "Expected performances of the copernicus imaging microwave radiometer (cimr) for an all-weather and high spatial resolution estimation of ocean and sea ice parameters," *Journal of Geophysical Research: Oceans*, vol. 123, 2018.

[4] "CIMR, howpublished = https://www.esa.int/esa_multimedia/images/2020/11/cimr, journal = ESA."

[5] P. J.-R. M. C. Gabarro, A.Turiel, "New methodology to estimate arctic sea ice concentration from smos combining brightness temperature differences in a maximum-likelihood estimator," *The Cryosphere*, vol. 11, 2017.

[6] F. Ulaby and D. Long, *Microwave Radar and Radiometric Remote Sensing*. 2014.

[7] A. Malki, L. E. Abdellaoui, J. Zbitou, A. Errkik, A. Tajmouati, and M. Latrach, "A novel design of voltage controlled oscillator by using the method of negative resistance," *International Journal of Electrical and Computer Engineering (IJECE)*, vol. 8, 2018.

[8] M. V. Kuliev, "Factors affecting the long-term stability of microwave oscillators for space electronic equipmen," *Electronic engineering Series 2 Semiconductor devices*, vol. 258, 2020.

[9] A. Soutehkeshan, N. Masoumi, and Y. Alekajbaf, "A 10 watts linear power amplifier using symmetric stub gando matching networks," pp. 1–6, 08 2020.

[10] O. Kizilbey, O. Palamutcuogullari, and B. S. Yarman, "Design of low phase noise 7.7 ghz dielectric resonator oscillator," 2013.

[11] S. J. Ha, Y. D. Lee, Y. H. Kim, J. J. Choi, and U. S. Hong, "Dielectric resonator oscillator with balanced low noise amplifier," *Electronics Letters*, vol. 38, 2002.

[12] T. H. Lee and A. Hajimiri, "Oscillator phase noise: A tutorial," *IEEE Journal of Solid-State Circuits*, vol. 35, 2000.

[13] A. Tadjalli, A. Sebak, and T. Denidni, "Resonance frequencies and far field patterns of elliptical dielectric resonator antenna: Analytical approach," *Progress in Electromagnetics Research*, vol. 64, 2006.

[14] P. G. D. Kajfez, "Dielectric resonator," *Noble Publishing Corparation*, 1998.

[15] G. B. A.N. Farr and D. Williams, "Novel techniques for tuning of dielectric resonators," *Proceedings of the 13th European Conference*, pp. 916–922, 1983.

[16] B. Virdee, "Investigation of different microstrip topologies for tuning dr te01d-mode resonant frequency," *Proceedings of the 1994 Asia-Pacific Conference*, 1994.

[17] "escc qualified parts list(qpl), howpublished = `https://escies.org/download/webdocumentfile?id=68847`, journal = ESCC."